PETROGRAPHIC INVESTIGATION OF SELECTED SAMPLES

FROM DRILL CORES EYREVILLE A AND EYREVILLE B:

CHESAPEAKE BAY IMPACT STRUCTURE, VIRGINIA

Except where reference is made to the work of others, the work described in this thesis is my own or was done in collaboration with my advisory committee. This thesis does not include proprietary or classified information.

_____

Jennifer Lynn Glidewell

Certificate of Approval:

_____

Mark G. Steltenpohl
Professor
Geology and Geography

_____

David T. King, Jr., Chair
Professor
Geology and Geography

_____

Willis E. Hames
Professor
Geology and Geography

_____

R. Scott Harris
Sr. Doctoral Candidate
Department of Geological Sciences
Brown University

_____

Joe F. Pittman
Interim Dean
Graduate School

PETROGRAPHIC INVESTIGATION OF SELECTED SAMPLES FROM DRILL CORES EYREVILLE A AND EYREVILLE B: CHESAPEAKE BAY IMPACT STRUCTURE, VIRGINIA

Jennifer Lynn Glidewell

A Thesis

Submitted to

the Graduate Faculty of

Auburn University

in Partial Fulfillment of the

Requirements for the

Degree of

Master of Science

Auburn, Alabama
May 10, 2008

PETROGRAPHIC INVESTIGATION OF SELECTED SAMPLES

FROM DRILL CORES EYREVILLE A AND EYREVILLE B:

CHESAPEAKE BAY IMPACT STRUCTURE, VIRGINIA

Jennifer Lynn Glidewell

_____

Signature of Author

May 10, 2008

Date of Graduation

THESIS ABSTRACT

PETROGRAPHIC INVESTIGATION OF SELECTED SAMPLES

FROM DRILL CORES EYREVILLE A AND EYREVILLE B:

CHESAPEAKE BAY IMPACT STRUCTURE, VIRGINIA

Jennifer Lynn Glidewell

Master of Science, May 10, 2008
(B. S., University of Houston, 2002)

143 Typed Pages

Directed by David T. King, Jr.

The meteoritic impact process is expressed uniquely in marine, sedimentary target impact structures versus hard, dry crystalline targets. Wet sediments accommodate extreme pressures and temperatures differently than crystalline rocks. The Chesapeake Bay impact event took place on the continental shelf of the passive Atlantic margin during late Eocene, enabling exceptional preservation of the feature. In 2005, the Eyreville A and B cores were drilled in the central zone of the Chesapeake Bay structure. These cores were acquired through the International Continental Drilling Program/United States Geological Survey Chesapeake Bay impact structure deep-drilling project. Fifty-two samples were allocated to the Auburn University research group in 2006.

The sample set was photographed as hand samples and most hand samples were then made into thin sections, which were studied and imaged. After a sample sheet was developed for petrographic analysis, the samples were analyzed including hand-sample description, thin-section investigation with a petrographic and universal-stage microscope, and, in rare instances, analysis of thin sections using an electron microprobe and scanning electron microscope. This work produced a modal analysis and inventory and description of shock-related features for each sample.

The stratigraphic assemblages of the Eyreville core established by the USGS were used in this study. The results of sample analysis were evaluated with respect to their stratigraphic position. Assemblage 1 is the basal section and includes broken pieces of schists and pegmatites that locally grade into granite. Assemblage 2 is a zone of lithic breccias, suevite, and impact melt rocks. A relatively thin layer of gravelly sand forms Assemblage 3. The mixed granites of Assemblage 4 are allochthonous blocks with variable textures and compositions. Assemblage 5 contains impactoclastic sands and breccias and sedimentary megablocks and boulders.

Shock features were noted within Assemblages 1, 2, 3, and 5, but traces of shock may also be present in the mixed granites of Assemblage 4. Shock features include kink-bands, mechanical microtwins, planar microstructures (PMs), toasted quartz, mosaicism in quartz, recrystallized minerals, and quenched silica glass. Diagnostic methods used to evaluate PMs yielded results consistent with previous work, which explained a variation of PM orientation with depth. Traces of L- or LL-chondrite meteorite material may have been found within altered melt from Assemblage 2; this section experienced the highest shock regime, more than 35 GPa locally, inferred from its greater volume of melt material.

ACKNOWLEDGEMENTS

The author was introduced to her Auburn University advisor by Dr. David Rajmon, who perhaps unknowingly gave her life a welcome change of direction. The author would like to thank her advisor for the opportunity to work on the Eyreville samples. Dr. King has worked diligently as an advisor and provided invaluable experiences that have greatly contributed the author's graduate student experience and life. The faculty and staff of the Department of Geology and Geography, including thesis committee members Dr. Willis E. Hames and Dr. Mark G. Steltenpohl, have made many efforts to enhance the author's education and future. R. Scott Harris has worked in a tireless, dedicated manor as a mentor to the author and this thesis is a better product because of his guidance.

Several scientists outside the Auburn University Department of Geology and Geography have helped with various aspects of data acquisition. Dr. Curtis Shannon (Department of Chemistry, Auburn University) as well as his graduate students provided use of microRaman analytical equipment. Chris Fleischer (Department of Geology, Univerisity of Georgia) provided training and supervision on the electron microprobe.

Words cannot express the gratitude for the immense love and support the author has always received from her family, especially the immediate members: William, Shirley Sowards, Edward, and Janeé LeBow Glidewell.

Journal style used:	Meteoritics and Planetary Science
Computer software used:	Adobe Acrobat® 7 Professional
	Corel DESIGNER®
	Corel PHOTO-PAINT®
	Microsoft® Office Professional Edition 2003: Word, Excel, PowerPoint
	Nikon® NIS-Elements D 2.30
	Renishaw® WiRE 2.0
	RockWare® LogPlot 3

TABLE OF CONTENTS

LIST OF TABLES

LIST OF FIGURES

INTRODUCTION

The fundamental process of meteorite impact cratering on Earth has been investigated rigorously only for about the last sixty years. During this era, impact studies have become recognized as a distinct branch of the geosciences. Scientists from around the world have laid the foundation for impact research, initially through the analysis of crystalline-target impact structures. Sedimentary impact targets, especially ones in marine environments, have distinct differences in the way the heat and pressure of this near-instantaneous event are accommodated. Marine impacts result in a unique shock response in target lithologies and their constituent minerals, as well as in different morphologies, depth-diameter ratios, and modifications of this type of impact structure (Grieve and Pilkington 1996). Such special features associated with marine, sedimentary-target impact structures have only just begun to be documented and explained at the time of this thesis research.

A meteorite impact into the outer shelf of the late Eocene Atlantic margin formed the Chesapeake Bay impact structure (CBIS). The CBIS is an 85 km-diameter, buried circular feature centered on the town of Cape Charles, which is located on the Delmarva Peninsula, Virginia (Fig. 1). The CBIS was subsequently covered by marine sediments

of the Atlantic Coastal passive margin and is now one of the best preserved, buried impact structures, as well as the seventh largest known impact feature on Earth.

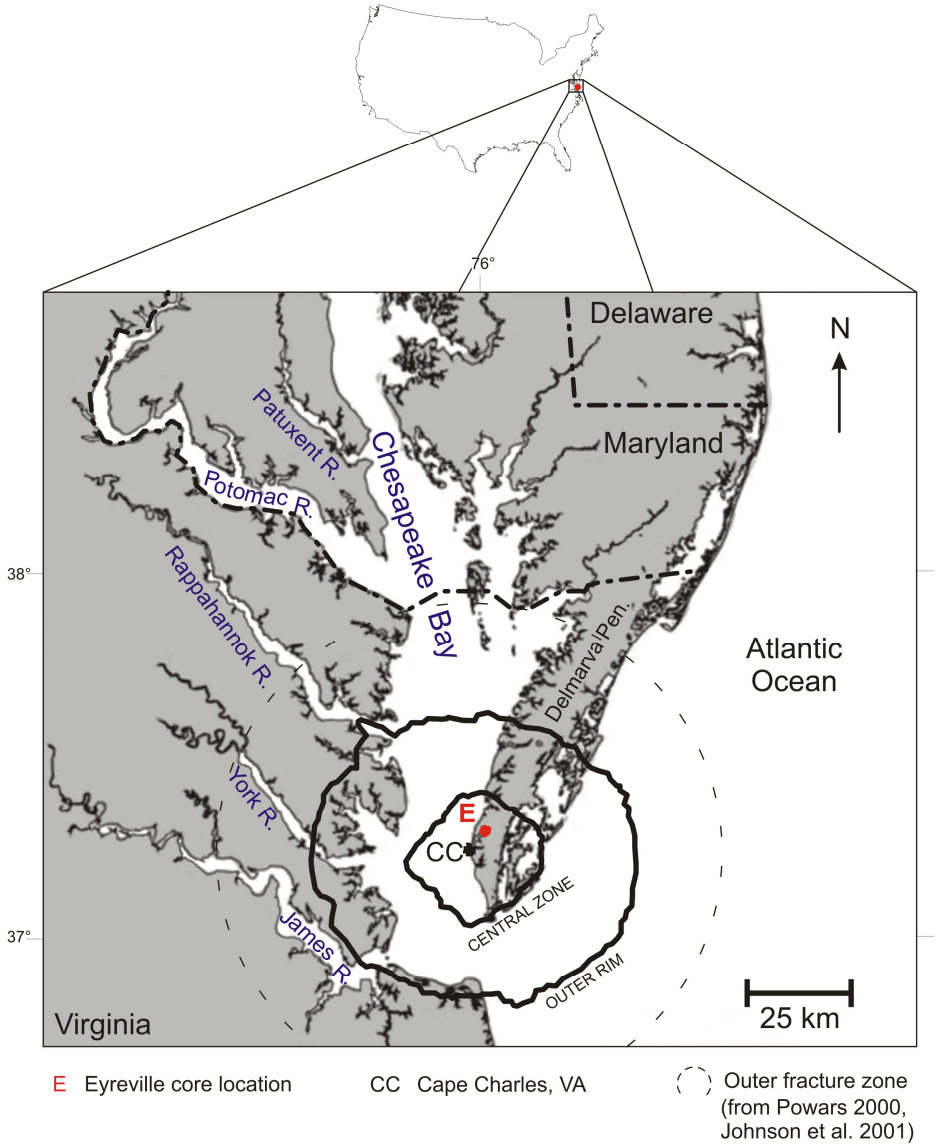

Fig. 1. Regional location map for the Chesapeake Bay impact structure (crater extent from Powars and Bruce 1999; base map from Hobbs 2004).

In 2005, the International Continental Drilling Program (ICDP) and the United States Geological Survey (USGS) sponsored the drilling and retrieval of deep core samples from the central zone of the CBIS. Three locations (A, B, and C) were drilled at the Eyreville site on the Buyrn family farm near the town of Cape Charles (Fig. 1). The Eyreville A core was drilled from a subsurface depth of 125.6 to 940.9 m (412.1 to 3086.9 ft), while Eyreville B was drilled between depths of 737.6 and 1766.32 m (2419.95 to 5795.0 ft). The C drill site retrieved samples from the post-impact sediments between the surface and a depth of approximately 140.2 m (459.97 ft). Core samples were competitively requested by the scientific community during 2003 and in March 2006 samples were marked for extraction from the drill cores. In response to an accepted proposal (King and Petruny 2003), fifty-two samples from sites A and B were marked, cut, and subsequently shipped to Auburn University during May and July of 2006. Eyreville A and B sites are represented by 17 and 35 samples, respectively (Appendix A). The samples, except for the uppermost one (KP 30, 443.83 m or 1456.13 ft), are from the impactite facies of the CBIS.

Because this thesis is associated with a larger-scale project, it adheres to scientific objectives outlined by the USGS (Edwards et al. 2004). The focus of this work is to present a petrographic analysis for each sample per the pre-drilling agreement among participating institutions (Edwards et al. 2004). A standard petrographic analysis of hand samples and/or thin sections was completed for all of the fifty-two samples (3 samples do not have thin sections, Appendix A). Shock effects were documented where present in the samples. As a result, the research helped to meet a USGS objective, which is the

description of impact breccias and shock deformation of constituent grains. The assessment of shock features, evaluated primarily from melted clasts and quartz microstructures, could contribute to subsequent research in order to better understand the behavior of impact-induced energy through porous sediments and underlying rocks. The analysis of the CBIS is in an early stage and research done for this thesis may be a foundation for understanding the formation and structure of the feature.

GEOLOGIC SETTING

The impact occurred on the outer continental shelf of the late Eocene Atlantic Ocean (Fig. 2). The water depth near the location of the impact event was between 40 and 260 m (131-853 ft; Horton et al. 2005a). The target of this impact event consisted of seawater, 1-1.5 km of deltaic and shallow-marine shelf sediments (Lower Cretaceous to upper Eocene), and crystalline metamorphic and igneous rocks that range in age from Proterozoic to Paleozoic (Fig. 3; Horton et al. 2005b; Poag et al. 2004).

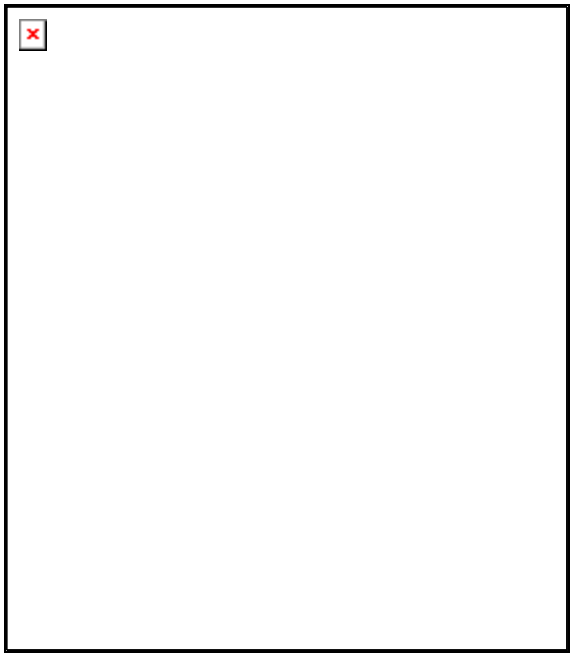

Fig. 2. General paleogeography for the Chesapeake Bay impact structure (CBIS) and present-day physiographic provinces. White dashed line approximates the Late Eocene shoreline and blue dashed line estimates the edge of the continental shelf (from of Poag et al. 2004; image from Halusa and NASA/GSFC/JPL MISR Science Team 2000).

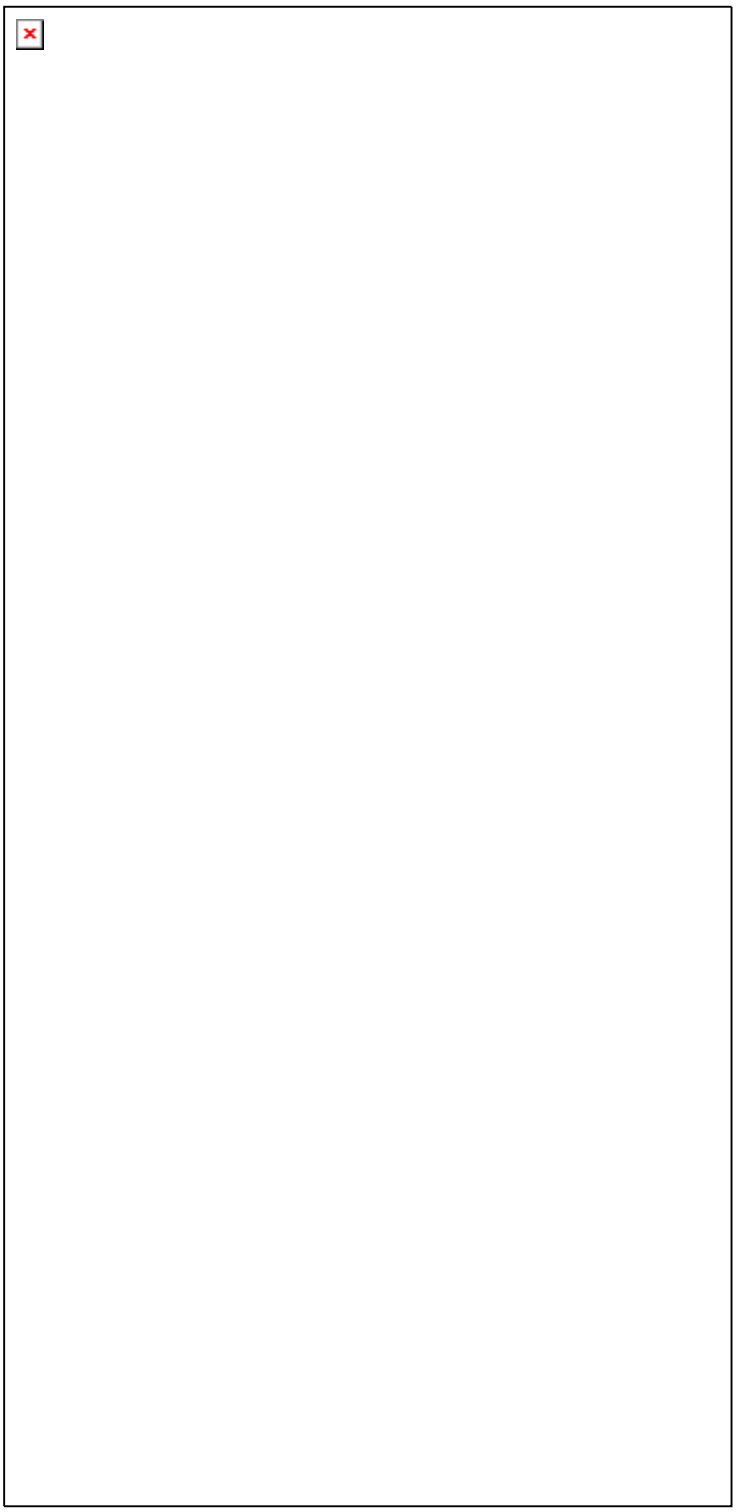

Fig. 3. Simplified cross-section and stratigraphic section of the CBIS. a) Cross section from west to east across the structure showing location of (b) and the Eyreville core location (Fig. 4) and b) Stratigraphic section showing pre- and post-impact deposits. Wavy lines are unconformities (modified from Poag et al. 2004).

In this passive-margin setting on the mid-Atlantic shelf, marine deposition was interrupted only briefly and continued immediately after the impact event. Thus, the crater was preserved as a large, near-pristine example of complex marine-target structure. Because of this good preservation and accessibility of the feature, it is ideal for the acquisition of core samples. The Chesapeake Bay structure and surrounding area has been cored in several places, but in 2004 a drilling initiative suggested another core location within the central zone (Edwards et al. 2004). After deliberation by the ICDP and USGS, the core-retrieval location was chosen to be on the Eyreville plantation, north of Cape Charles on the Delmarva Peninsula (Fig. 1).

Once drilled, the Eyreville cores provided a basis for the generalized stratigraphic sequence for the inner crater and post-impact units, which was soon after established by the USGS (Gohn et al. 2006). The relatively pristine impactite facies from 1766.3-443.9 m (5794.95-1456.36 ft) was separated into stratigraphic units by Gohn et al. (2006) and have been further subdivided (Fig. 4; Horton et al. 2007; Powars et al. 2007). Horton et al. (2007) subdivided the lower portion of the core into structure-filling units referred to as Assemblages 1 through 4. Assemblage 1 (1766.22-1560.24 m or 5794.69-5118.90 ft) includes schists and granite pegmatites that locally grade into granite (Fig. 4). Assemblage 2 (1560.24-1397.16 m or 5118.90-4583.86 ft) consists of a basal graphite-rich breccia, a middle section of lithic-clast-rich breccia, and an upper section with melt-rich suevite (Fig. 4). A mixed section of lithic blocks and sands from 1397.16-1371.11 m (4583.86-4498.39 ft) defines Assemblage 3 (Fig. 4). Assemblage 4 represents

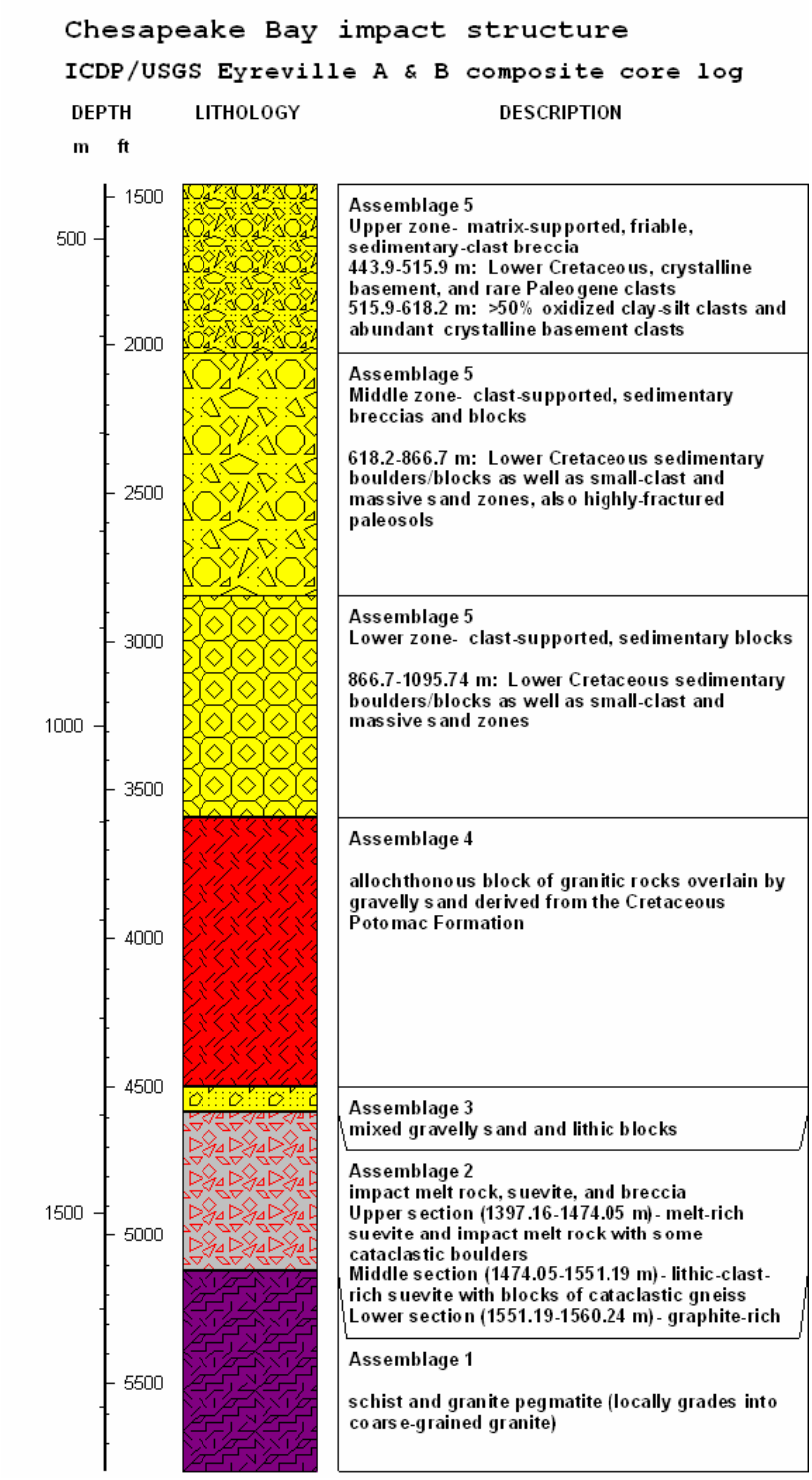

Fig. 4. Composite stratigraphic section for the Eyreville core (see location on cross section from Fig. 3a; stratigraphic descriptions from Gohn et al. 2006, Powars et al. 2007, and Horton et al. 2007).

allochthonous mixed granitic rocks that span between 1371.11 m or 4498.39 ft and 1095.74 m or 3594.95 ft (Fig. 4). The upper 652.8 m (2141.73 ft) of impactites include lithic breccias and sedimentary blocks. Powars et al. (2007) subdivide this interval into a lower section (1095.74-866.7 m or 3594.95-2843.50 ft) containing mainly sedimentary boulders and blocks, a middle section (866.7-618.2 m or 2843.50-2028.22 ft) of sedimentary blocks with abundant oxidized clay-silt clasts, and an upper section (618.2-443.9 m or 2028.22-1456.36 ft) of muddy glauconitic sands containing various fragments of crystalline basement lithologies (Fig. 4). This report refers to the three zones of Powars et al. (2007) as Assemblage 5.

In addition to structure-filling stratigraphy, the Eyreville core (core C) recovered a complete section of post-impact sediments. Post-impact marine, siliciclastic, silty and sandy sediments vary in thickness between 200 and 550 m (656.17 and 1804.46 ft) over the crater (Poag et al. 2004). Twenty one formations from Poag et al. (2004) are shown in Fig. 3 above the impactite facies. The post-impact sediments from Eyreville C are not part of this study.

Through extensive geological and geophysical investigation, the shallow, sedimentary section has been well-documented and is still being studied. However, the origin and orientation of basement rocks in the region around and beneath the Chesapeake Bay crater continues to be somewhat controversial. Faulting and fragmentation of basement blocks through orogenic processes and rifting has resulted in several possible interpretations of the existing geophysical data. Magmatic arc rocks of

the Late Proterozoic to Early Cambrian Carolinian terrane were emplaced on the Cambrian Laurentian margin during the Carolinian collisional event and extend to the present continental edge in this region (Glover et al. 1997). Subsequently, Alleghanian dextral transpressional shearing parallel to the orogen and Mesozoic extension deformed and fragmented the Carolinian plate (Bradley 1982; Gates et al. 1986; Gates et al. 1988; Glover 1989).

The faults and flexures of this thinned and heated crust represent the transitional zone between the continental and oceanic crust, whereas the present shelf marks the approximate edge of the oceanic crust (Fig. 2; Poag et al. 2004). The Baltimore Canyon trough was formed from rapid subsidence due to thermotectonic processes along this hinge zone and the maximum sediment thickness in the trough reaches as much as 12 km (Fig. 5; Poag et al. 2004). The East Coast Magnetic Anomaly was thought to be an 'edge effect' of the continent-ocean boundary, but recent ideas for the anomaly support the theory of magmatic underplating during breakup for higher velocity crust (White et al. 1987; Sheridan et al. 1993).

Seismic data was interpreted by Sheridan et al. (1993) to indicate a north-south-striking trace under the center of southern Chesapeake Bay. Wells on the Delmarva Peninsula have encountered low-grade metamorphic rocks correlated with the Carolina slate of the Avalonian terrane (i.e., Carolinia; Hibbard et al. 2007) and wells west of the Bay have penetrated high-grade gneiss correlated with the Goochland terrane (i.e., Grenville-age Laurentian crust; Sheridan et al. 1993). This detachment fault is probably

Fig. 5. Generalized basement structural features for Atlantic margin in the region of Chesapeake Bay. The extent of zones related to the Central Piedmont suture and Jurassic volcanic wedge is derived from available data. (base map from USGS 2008; structures and zones from Sheridan et al. 1993).

the Central Piedmont suture (Fig. 5; Sheridan et al. 1993). Furthermore, the age of the granites in the USGS Langley core (see Previous Work section) suggests the eastern and southern portions of the Chesapeake Bay basement comprise rocks of peri-Gondwanan magmatic arc terranes (Carolinia; Horton et al 2005b). Horton et al. (2005b) report $^{206}Pb/^{238}U$ analysis on zircon (SHRIMP) from granite in the USGS Langley well samples that yield an age of 612+/-10 Ma. This is younger than the Mesoproterozoic Laurentian crust, so the suture between Laurentia and the arc terranes likely has a north-south trend throughout most of Chesapeake Bay and may shift west-northwest near the mouth of the York River (Sheridan et al. 1999; Horton et al. 2005b). Scarcity of data currently prevents the determination of a precise location for the suture.

Adjustment of subsurface structure in response to sediment loading is a common geologic occurrence along Earth's continental margins. The impactor collided just west of the subsiding hinge zone and today the structure has an eastward tilt from approximately 36 million years of flexural subsidence (Poag et al. 2004). Cenozoic strata overlying the crater record sporadic differential movement around the buried rim (Johnson et al. 1998). Miocene strata in a graben under the York River are deformed above the rim and unconformities in Pliocene-Pleistocene strata strike parallel to the rim and dip very slightly away from the crater to indicate synchronous deposition and deformation (Johnson et al. 1998). Although four earthquakes were reported in southeastern Virginia less than 40 km from the crater rim, the seismicity is coincident with the low levels observed for this part of the coastal plain (Sibol et al. 1996, 1997). As a result of relatively minimal overburden, forces that contribute to fault slip are assumed to be minimal; however, structures reported by Johnson et al. (1998) coupled with the extensive faulting of Eocene to Miocene sediments over the crater suggest slip may be notable.

Coastal configuration and deposition of the present-day Chesapeake Bay region was likely strongly influenced by basement and crater structure throughout the early Pliocene (Ramsey 1992; Hobbs 2004). The modern morphology of the Bay area was evident in the early to middle Pleistocene (Mixon 1985). Escarpments of normal faults that mark the crater rim are noticeable today along the York River and on the Delmarva Peninsula in Virginia (Poag et al. 2004).

PREVIOUS WORK

Humans have been observing impact-crater morphologies on Earth for thousands of years and, with the help of telescopes, on other planetary surfaces for hundreds of years. It was not until the middle part of the twentieth century that a select few people connected these bowl-shaped features with meteoritic impact (Baldwin 1949; Dietz 1947). Baldwin (1949) made comparisons of lunar craters to structures on Earth. Robert Dietz (1947) began to associate certain lithologic features as diagnostic indicators of impact structures. The Apollo era in the 1960s and 1970s and subsequent launches of probes to explore our Solar System ushered in the realization that meteorite impact is indeed a subject of "universal importance" (Pati and Reimold 2007).

The early investigations ushered in the study of shock metamorphic effects on the target rocks. Such studies initially focused on several structures in American and Canadian, in Africa and Australia, and in Germany at the Ries structure (Barringer 1931; Dietz 1947, 1959, 1960a, 1960b; Shoemaker and Chao 1961; Shoemaker et al. 1963; Dietz 1964; Roddy 1966; Stöffler 1966; French 1967). Eugene Shoemaker (1963) noted that fragments of the impactor were present around Meteor (or Barringer) crater. He also noted shocked grains and high-pressure polymorphs of quartz at Barringer (Shoemaker et al. 1963). The first notable compilation of papers on shock metamorphism was French

and Short (1968). Thirty years later, French (1998) presented the quintessential handbook on the subject, *Traces of Catastrophe*, which is basically a source used ubiquitously by the impact geology and planetary science community. Melosh (1999) authored an inclusive book that details the many aspects of impact geology and physics. Other solid foundations to the analysis of the mineralogy and geochemistry of shock metamorphism such as Stöffler (1972) and for quartz, specifically, Engelhardt and Bertsch (1969), Stöffler and Langenhorst (1994), and Grieve et al. (1996), which are classic review papers.

Numerous scientists around the world have contributed to today's extensive body of knowledge regarding geophysics and geology of impact structures. However, despite this level of investigation, analyses pertaining to the uniqueness of structures created by the impact of a meteorite into marine, sedimentary targets have only just begun in the last two decades as of this report (e.g., Ormö and Lindström 2000). Conclusions that have been made about crystalline-target impacts simply do not apply well to those that occur in unconsolidated, wet materials. The most famous sedimentary-target impact structure that has been studied by many international scientists is Chicxulub. Sharpton et al. (1991) and Hildebrand et al. (1991) were some of the first to document Chicxulub and to suggest that this impact contributed to the K-T mass extinction.

Impact structures usually have an obvious appearance on the surface, but when they are in the subsurface, they are typically detected as some sort of anomaly (e.g., structural, magnetic, gravity, groundwater, etc.). The first known mention of an anomaly

associated with the Chesapeake Bay region was by USGS scientist Samuel Sanford (1913). He mentioned an "inland bulge" of saline water that was centered on the town of Cape Charles.

Dagfin J. Cederstrom, a USGS scientist, published various works regarding sedimentological and hydrological analyses in the region of the Chesapeake Bay over a 35 year period (1938-1972). Cederstrom (1945) referred to the region as a "fault zone" to account for the presence of the anomalous breccias. He later noted in a groundwater study that "in the vicinity of the Chesapeake Bay this water is somewhat brackish and in places contains more than 1,000 parts per million of chloride" (Cederstrom 1946). It is no surprise that in the 1940's Cederstrom did not conclude the anomalies were due to an impact structure, as there was no evidence to suggest anything other than salt water seepage along a fault.

In 1983, T. Scott Bruce was on a drilling team for a research well for the state of Virginia in Newport News, Virginia (Tennant 2001). This project produced core samples with older fossils on top of younger ones. In 1986, Bruce joined with David Powars (USGS- Reston) to drill core samples from what is known now as the Exmore site (Fig. 6). This work in turn yielded the first modern samples that were clearly impact breccias with what appeared to be melted particles in them (Powars et al. 1987, 1990, 1991, 1992). Soon thereafter, drilling results from Deep Sea Drilling Project (DSDP) Leg 95, site 612, (~220 km or 136.7 mi northeast of Cape Charles) produced evidence of impact ejecta in the mid-Atlantic region, which included impact indicators such as

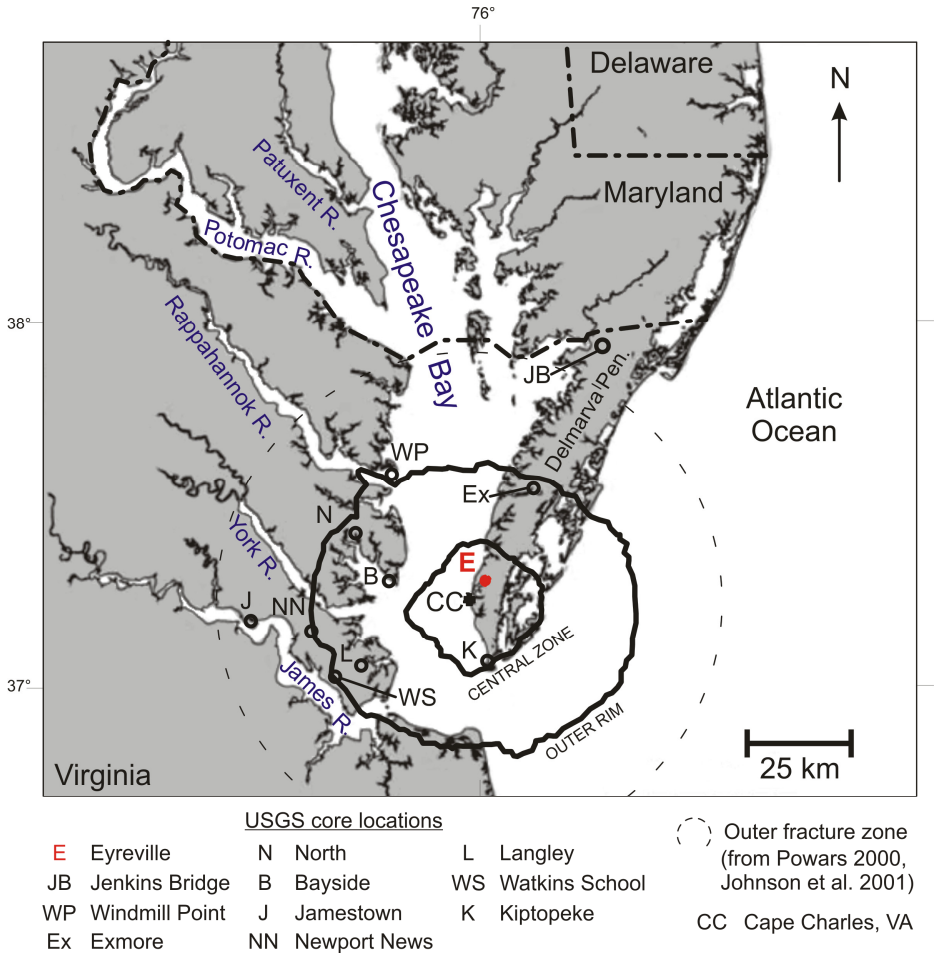

Fig. 6. Regional map of the Chesapeake Bay structure showing USGS core locations (crater extent from Powars and Bruce 1999; base map from Hobbs 2004).

coesite, shocked quartz, and impact-melted glass (Poag et al. 1987; Thein 1987). This led investigators Glass (1989) and Koeberl (1989) to the conclusion that a local impact event was the source of the North American Tektite Strewn Field. Glass (1989) and Koeberl (1989) also deduced that the impact structure must be a few hundred kilometers from Site 612 because of the increased thickness of the ejecta layer at this location. The work of many people, mainly USGS scientists, and a stockpile of seismic data compiled since 1975, pointed towards an impact explanation for the anomalous salinity and breccias in the subsurface of the Chesapeake Bay (Poag et al. 2004).

C. Wylie Poag (USGS), an experienced scientist with this region's geology who was aboard the significant DSDP site 612 cruise, made the interpretation that an apparent meteorite impact structure lay in the Chesapeake Bay area and this was indeed the source of the North American Strewn Field (Poag et al. 1992). Poag then jointly published with David Powars, Scott Bruce, and others who presented even more evidence that the subsurface anomaly was an impact structure (Poag et al. 1993). A formal affirmation of impact origin and correlation of the structure with the North American Strewn Field was made by Koeberl et al. (1996), citing geological and geophysical data and specific evidence of shock metamorphism in the rock samples. The circular subsurface feature was named the Chesapeake Bay impact structure.

In 2000, the Chesapeake Bay Crater Project was launched by the USGS, the Virginia Department of Environmental Quality, and NASA (Horton et al. 2005b). This joint effort produced core samples from four deep drill sites near the crater rim and in the

annular trough of the western portion of the structure between 2000 and 2002 (Fig. 6; Catchings et al. 2001; Gohn et al. 2001; Powars et al. 2001; Poag 2002; Poag et al. 2002; Edwards and Powars 2003; Sanford 2003; Self-Trail 2003; and Horton et al. 2005b).

A wide range of geological and geophysical data was compiled over 16 years, including data from 234 boreholes and of 2,018 km of seismic data gathered by over 10 different sources from the region in and around Chesapeake Bay (Poag et al. 2004). With this data set, Poag et al. (2004) published a comprehensive book on the Chesapeake Bay crater. This source includes a CD-ROM with 7 maps, 11 seismic profiles, and 29 figures. The book and CD-ROM are thorough sources for anyone interested in studying marine impacts in general, and Chesapeake Bay in particular.

In 2005, the Eyreville core samples were acquired as a result of the externally funded partnership between the USGS and the ICDP known as the Chesapeake Bay Impact Structure Deep Drilling Project. Gohn et al. (2006) was the first initial, generalized report from the project that synthesized data from three closely-spaced drill sites, A, B, and C, at Eyreville (Fig. 6). This location, in the central basin of the structure, had a total drilling depth of approximately 1766.3 m or 5794.95 ft (Gohn et al. 2006). This article delineated five major stratigraphic sections within the impactites as follows: schist and pegmatites from 1766.3-1550.0 m (5794.95-5085.30 ft), suevite and lithic breccia from 1550-1393 m (5085.30-4570.21 ft), sediment with lithic blocks from 1393-1371 m (4570.21-4498.03 ft), granite megablocks between 1371 and 1096 m

(4498.03-3595.80 ft), and sediment-clast breccia and megablocks from 1096 to 444 m or 3595.80 to 1456.69 ft (Gohn et al. 2006; see Fig. 4 in preceding section).

The Auburn University research group has published three abstracts (King et al. 2007; Glidewell et al. 2007; Glidewell et al. 2008) since the ICDP/USGS lifted the publication moratorium on Eyreville core data in October 2007. The stratigraphic results presented in these abstracts are summarized below.

The lowest section of the core (1766.3-1550 m or 5794.95-5085.3 ft) consists of blocks and megablocks of cataclastic and non-cataclastic schist, gneiss, and granite that contain suevite veins and are, in some cases, imbued with dark, carbon-rich material. It can be suggested that the lower part of this succession is the product of early mixing of wall-hugging suevites with comminuted and fractured basement breccias. The next interval (1550-1393 m or 5085.3-4570.21 ft) consists of layers of suevite and polymict breccia intercalated with blocks of gneiss underlying a sequence of very coarse sands (1393-1371 m or 4570.21-4498.03 ft). Coarse sands here contain weakly to unshocked sedimentary clasts and may represent initial resurge and collapse of the higher transient crater wall. Granite megablocks (1371 and 1096 m or 4498.03-3595.8 ft) likely foundered off the central peak. Above the granites (1096 to 818 m or 3595.8-2683.73 ft) are sands composed of slumped and partly disaggregated megablocks of the lower Cretaceous Potomac Formation, separated and intruded by dikes of impactoclastic sands. Between 818-527 m (1729.0-2683.73 ft) is mostly Potomac-sourced impactoclastic sands containing clay blocks and gravel layers, and 527-451 m (1729.0-1479.66 ft) consists of

impactoclastic breccias. The uppermost impact interval (451-443.9 m or 1456.37-1479.66 ft) comprises glauconitic sands terminating in a 0.5 m-thick zone of laminated, silty clays. Continued collapse and resurge is thought to have produced the sequence of sedimentary blocks and sands capped by washed-back fallout ejecta and fine-grained sediments that settled out of the water column.

Since the time that the Eyreville samples were obtained in 2005 and distributed internationally during 2006 and 2007, work has begun at many institutions on the analysis and interpretation of the entire Eyreville drill core. This thesis is a contribution to this joint research effort.

METHODOLOGY

The first phase in the investigation of fifty-two cut core samples from the Eyreville drill core was to take inventory and place them in stratigraphic order, create a sample spreadsheet (Appendix A), describe the core samples, and prepare them to be photographed. The samples were each placed on a lighted photography platform with a scale and images were captured with a digital camera. Several photos were taken of each sample to represent its attributes prior to cutting and other destructive analysis. These photos appear in Appendix B.

Thin sections were made by Idaho Petrographics and were left uncovered. Once the samples were received, point counting was completed on the uppermost 22 samples (KP17-KP 11, 444.38-1095.7 m or 1456.13-3594.85 ft), which represents the sedimentary part of the structure-filling section. A 200-point count for quartz, feldspar, rock fragments, glauconite, allochems, chlorite, muscovite, and matrix was done for each of these thin sections. In this process, the magnification on the Nikon LABPHOT2-POL petrographic microscope was 10X and the point counter used was a Swift, Model F, from Hacker Instruments, Inc.

Standard sample forms were developed to account for hand-sample description, a basic modal analysis of the thin section, description of shock features, and general notes. Analysis was done using a Nikon Eclipse 50iPOL petrographic microscope with reflected light capabilities at magnifications ranging from 2X to 40X. This microscope was connected to a Nikon DS-Fi1 U2 imaging system that used Nikon NIS-Elements D 2.30 software. Modal analyses were completed with this equipment to determine framework grain composition, percent matrix and cement, apparent grain rounding (after Powers 1953), type of grain contacts to qualitatively describe grain to grain relations (Pettijohn et al. 1987), and grain size (Udden 1898; Wentworth 1922).

Planar deformation features (PDFs) in quartz are a unique shock effect that is one of the main criteria for establishing that craters were formed by meteorite impact (Fig. 7; papers in French and Short 1968; Engelhardt and Bertsch 1969; Stöffler and Langenhorst 1994; Grieve et al. 1996). Even though Chesapeake Bay is a formally-acknowledged impact structure, it is still necessary to attempt to quantify shock values in order to try to understand the shock regime in the target rocks. It is also necessary to take precautions to delineate between true PDFs and planar features that can be caused by other processes. Standard methods presented by Phillips (1971) were used on a 5-axis Leitz Wetzlar petrographic microscope custom-fitted with a 5 axis Zeiss Universal stage. Once measuring the orientation of the pole to the planar features and the optic axis of the quartz grain is finished, one can then plot the data on a stereonet. This allows the polar angle to be determined. When two or more sets of planar features were present, the methods of Engelhardt and Bertsch (1969) were used to index the orientation of the planes.

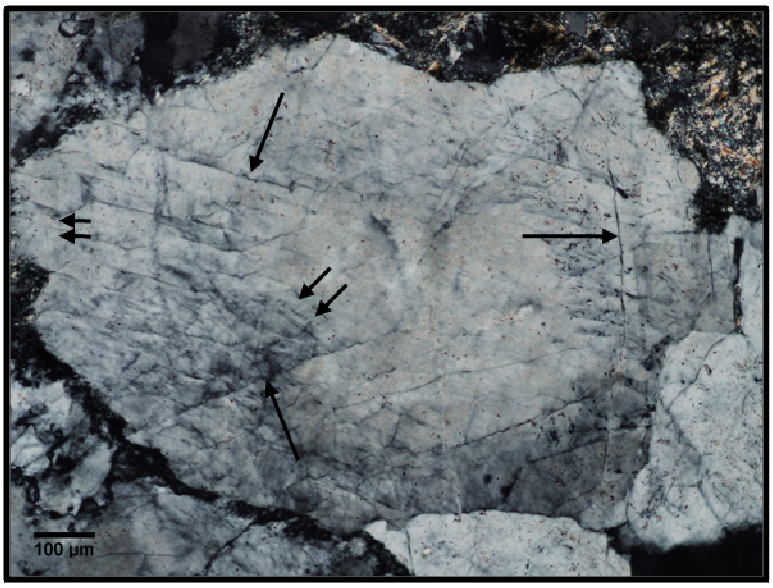

Fig. 7. Planar features (PFs; indicated by single arrows) and planar deformation features (PDFs; double arrows) in quartz in sample KP5 (4499.00-4499.10 ft or 1371.17-1371.20 m; XPL).

For some zones in thin sections that are too obscured by shock effects to describe compositionally or for grains that were too small to resolve using standard microscope optical methods, the author and R. Scott Harris employed other means of quantitative analysis. First an electron microprobe with energy-dispersive spectrometer (EDS) was used at the University of Georgia's Department of Geology for supplemental investigations. Second, very fine grains were analyzed with an environmental SEM in the Auburn University Materials Engineering Lab. Finally, a Renishaw inVia Raman Micro with a Leica microscope in a Renishaw RE02 enclosure was used at the Auburn University's Department of Chemistry to help determine molecular structure and thus composition of puzzling materials in a few thin sections. A 785-nm wavelength laser was used. This micro Raman spectroscopy data was observed in Wire 2.0 software.

PETROGRAPHY

The results of the petrographic analysis conducted on fifty-two samples selected by the Auburn University research group are presented in this section. A complete list of sample information including core of origin (i.e., Eyreville A or B), core box number, depths in meters and feet, and whether or not the sample is available in thin section are provided in Appendix A. Appendix B contains a cumulative collection of images for each sample, including hand sample photographs and photomicrographs as well as electron backscatter images from electron microprobe energy-dispersive spectrometer (EDS) when available (core box photos courtesy of David Powars, USGS- Reston). A composite core log of Eyreville locations A and B is presented in Appendix C. The log includes a gamma ray log (courtesy of the USGS), stratigraphic divisions and sub-divisions with depth, and lithologic features and descriptions (Horton et al. 2007; Powars et al. 2007). Appendices B and C are each in digital format on the DVD included with this work.

There are several points to keep in mind for this report of the sample set petrography. First, not all samples were made into thin sections, so three are simply described as core samples (Appendix A). Second, samples and their descriptions may be grouped according to stratigraphic section (Appendix C). Finally, oriented sample

pictures are noted in the image captions (i.e., samples were oriented vertically during core processing where the top of the sample is up).

The sample information is listed from the base of the core upwards in stratigraphic order according to USGS descriptions (Horton et al. 2007; Powars et al. 2007). For the sake of consistency in this joint research effort, the same style and descriptive names of stratigraphic sections from Horton et al. (2007) and Powars et al. (2007) are used. Where further subdividing intervals from what these authors established, the term "subsection" is employed. Each analysis is presented with sample depth information, pre- and post-impact petrographic classifications, a modal analysis, a report of impact-related features, an explanation or interpretation of these features and, where feasible, selected images of core samples and/or photomicrographs (in plane-polarized light-PPL or cross-polarized light-XPL).

A sample's "pre-impact" classification is an estimation of the protolith classification before impact deformation; the "post-impact" classification gives the present state of the rock, including appropriate impactite terminology (see Table 1). General petrographic terms for impactites and shock features are defined in Table 1. Classification terms proposed by Stöffler and Grieve (1994) as standard shock metamorphic descriptors are also defined in Table 1. The modal analyses include data associated with constituent particle compositions, orientations, sizes, and types of interstitial material. Grain/clast rounding and contact types usually used for sedimentary rock classifications are used here for descriptive purposes. The presentation of impact-

Table 1. General nomenclature for impactites and shock features: definitions of specific petrographic terms.

Term:	Definition:
Impactoclastic breccias or sands	Deposits of consolidated or unconsolidated sediment formed by ballistic transport and deposition of rocks during impact events; may contain melt particles[1]
Lithic breccia	Polymict impact breccias with a clastic matrix and shocked and unshocked mineral and lithic clasts, but without cogenetic impact melt bodies[1]
Suevite	Polymict impact breccias with a clastic matrix and shocked and unshocked mineral and lithic clasts with cogenetic glassy or crystalline impact melt particles[1]
Impact melt rock	Glassy, hypocrystalline, and holocrystalline rock solidified from impact melt containing variable amounts of clastic debris (e.g., clast-rich, clast-poor, clast-free)[1]
Planar microstructures (PMs)	Collective term comprising what may be shock induced planar fractures and planar deformation features[1]
Planar fractures (PFs)	Fractures occurring as sets of planar fissures (with >15 μm spacing[2]) parallel to rational crystallographic planes which in some cases are not be observed as cleavage planes under normal geological conditions[1]
Planar deformation features (PDFs)	Submicroscopic, amorphous lamellae (<2-3 μm thick[2]) occurring in shocked minerals as sets of planar features parallel to rational crystallographic planes that are indicative of shock metamorphism[1]
Decorated planar deformation features	Planar deformation features that have been annealed and contain "discontinuously aligned vugs and inclusions formed during the recrystallization of originally amorphous lamellae" [1]

[1]Stöffler and Grieve (1994).
[2]Stöffler and Langenhorst (1994).

related features for each sample in most cases uses terms from Tables 1 and 2. Specialized terminology relevant to this discussion of shock metamorphic or deformation features in the sample set is summarized in Table 2. The concluding sample discussions may estimate or interpret shock-related features and infer how certain features formed or what meaning they have in the context of localized shock metamorphism. The subsequent chapter to this petrography section is an elaboration of the sample discussions in that shock features and their vertical variation throughout the length of the core are considered.

Table 2. Nomenclature and definitions for shock features relevant to this study.

Term:	Definition:
Linear inclusion/vug trails (LITs)	General term used by thesis author for features mainly in quartz where PDFs may have been annealed, leaving only linear 'trails' of vugs and/or inclusions discernable with a petrographic microscope (essentially relict PDFs); not formally indicative of impact
Kink bands	Mechanical deformation features; observed in micas of various pressure histories, but commonly kinks of static origin are more symmetrical than kinking produced by shock[1,2]; Shocked biotites tend to be more intensely kinked, which results in smaller kink bandwidths than those that occur statically[1]; ~1GPa is thought to be the lower pressure limit for their formation under shock conditions[3]
Ladder texture	Short, closely spaced PDFs combined with twin lamellae to produce a ladder-like configuration[3]
Mosaic quartz	An irregular, 'mottled' optical extinction pattern in quartz with PDFs[5]
Toasted quartz	Displays medium to dark brown to orange brown colors in plane-polarized light and anomalous brown in cross-polarized light[4]; a post-shock feature that develops in response to exsolution of water from glass, especially along PDFs[6]; probably results from rapid recrystallization of PDF glass where sub-micron sized inclusions are in higher concentrations than that of decorated PDFs[6]
Lechatelierite	Silica glass formed from quartz at temperatures above 1713° C (3115.4° F)[5]
Schlieren	Bands/streaks of silica glass (lechatelierite) of locally laminar flow-banded melt; clear streaks are notable when lechatelierite mixes incompletely with other melt[5]
Ballen	Curved, crackled texture of curved fractures in lechatelierite produced from thermal stress and recrystallization (i.e., a devitrification feature)[5]
Microspherules	Fresh to altered, ≤mm-sized, melted spherules[5]

[1]Horz F. (1970).
[2]Schneider (1972).
[3]Horz F. (1969).
[4]Stöffler and Langenhorst (1994).
[5]French (1998).
[6]Whitehead et al. (2002).

Assemblage 1

Schist and granite pegmatite that locally grade into granites are present in Assemblage 1. The seven samples below are within this section that spans from 1766.22-1560.24 m or 5794.69-5118.90 ft (Fig. 8 and Fig. 9).

The pre-impact classification in Assemblage 1 includes mixed metamorphic and igneous lithologies, such as schist and granite. The post-impact classification is that the seven samples in Assemblage 1 include granite, cataclasite, schist, and pegmatite.

Sample number: KP 50	Depth: 5795.10-5795.25 ft	(1766.17-1766.21 m)
Sample number: KP 51	Depth: 5508.70-5508.80 ft	(1679.05-1679.08 m)
Sample number: KP 49	Depth: 5464.30-5464.75 ft	(1665.43-1665.56 m)
Sample number: KP 48	Depth: 5385.90-5386.00 ft	(1641.56-1641.59 m)
Sample number: KP 2	Depth: 5278.30-5278.40 ft	(1608.83-1608.86 m)
Sample number: KP 1	Depth: 5271.30-5271.40 ft	(1606.69-1606.72 m)
Sample number: KP 47	Depth: 5221.40-5221.50 ft	(1591.48-1591.51 m)

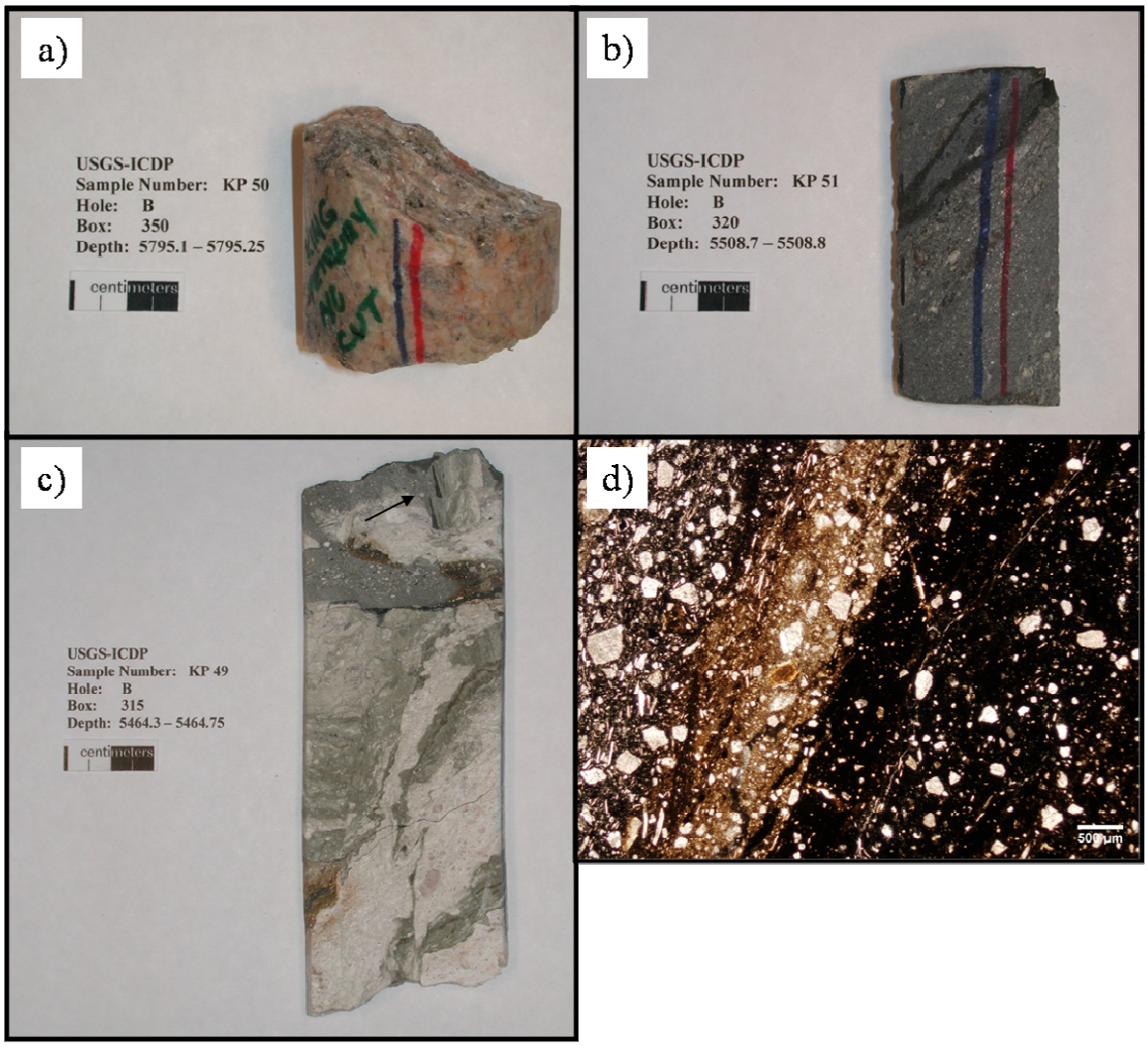

Fig. 8. Oriented core samples a) KP 50, b) KP 51, c) KP 49 (arrow points to split clast) and d) photomicrograph of KP 51 (oriented; plane-polarized light [PPL]).

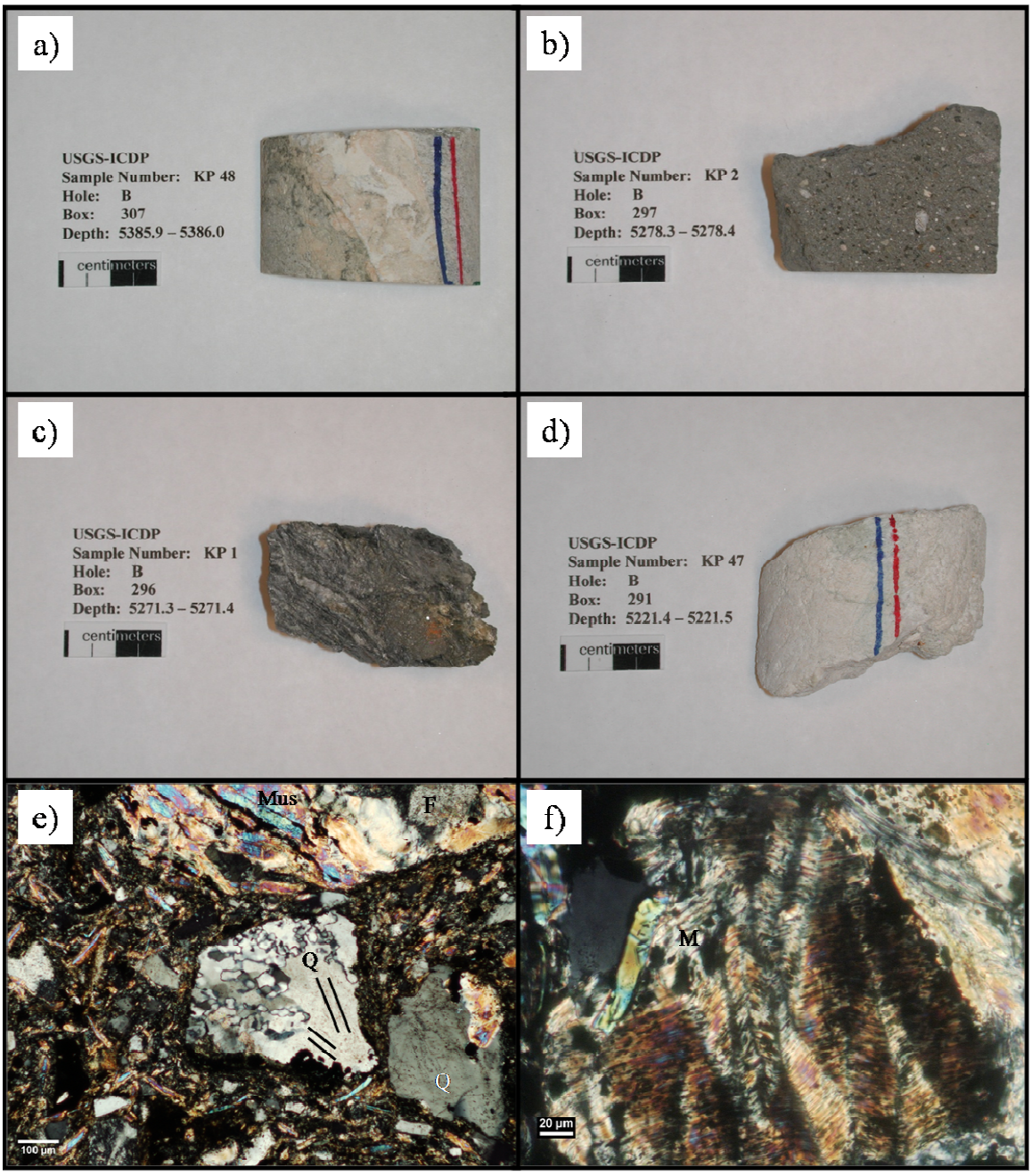

Fig. 9. Oriented core samples a) KP 48, b) KP 2, c) KP 1, d) KP 47, e) Photomicrograph of KP 2 (partially recrystallized quartz with planar deformation features (PDFs) at center, oriented; cross-polarized light [XPL]), and f) Photomicrograph of KP 1 (kink bands; XPL); Q=quartz, F=feldspar, Mus=muscovite.

Modal Analysis

Sample KP 50 (thin section) is a reddish, medium- to coarse-grained, granite with grains in an allotriomorphic texture (Fig. 8a). Approximately 43% of the sample is feldspar (mostly potassium feldspar and albite), 30% is muscovite, 25% is quartz, and up to 2% of KP 50 consists of opaque minerals. The thin section is greater than standard thickness (>30 μm).

Sample of KP 51 (hand sample) is banded with a black band surrounded by gray, foliated material with variable grain sizes. From the 'base' of the oriented sample, there is gray, very fine-grained schist that transitions up to gray, fine- to medium-grained schist with a sharp transition to the dark/opaque band with included quartz and feldspar grains, which is topped by a gray, slightly schistose breccia (Fig. 8b). The thin section reveals a gray, locally matrix-supported, graphite-rich, aphanitic to medium-grained, schist that transitions to foliated breccia (Fig. 8d). Sample KP 51 consists in large part (50%) of matrix, which is dominated by opaque material (likely graphite) with minor clays. Approximately 20% of KP 51 is lithic fragments (schist), 5% each is quartz and feldspar, 10% is muscovite, 5% contains more opaque minerals and possibly fibrolite, and up to 5% is silica cement.

Sample KP 49 (hand sample) may be a mylonitized cataclasite, or rock formed from fracturing and frictional sliding. This sample is pale pink, pale green, and light gray, fine- to very coarse-grained with small dark gray blebs surrounded by reddish haloes (Fig. 8c). Features of both brittle (micro-fractures/faults) and ductile (flow

banding or micro-folds) deformation are present. A clast near the top of the slab is split apart and the fault appears to be parallel to the surface of the core sample slice (Fig. 8c).

Sample KP 48 contains three banded/laminated zones visible in hand sample and thin section (Fig. 9a). On one edge of the thin section, quartzite covers approximately 30% of the sample, the middle zone of marble is 40% of KP 48, and the third zone (30%) on the other edge of the thin section is a green to brown, glassy area with quartz, feldspar, opaque minerals, titanite, rutile, zircon, apatite, olivine, and garnet interspersed. Sparry calcite is also interstitial and calcite is common as fracture fill. Cement consists of calcite and silica. The sample is pale pink to pale gray-green, matrix-supported, muscovite-rich, fine- to very coarse-grained, mylonitic and cataclastic schist.

Sample KP 2 is a medium gray, matrix-supported, polymict, clay- to sand-sized, lithic breccia (Fig. 9b). Lithic fragments (quartzite, schist, and amoeboid opaque particles) represent 33% of the sample, 30% is clastic matrix, 15% is muscovite and very minor biotite, 10% is feldspar, 5% quartz, 5% silica cement and calcite fracture fill, and 2% calcite or marble. Sand grains and larger clasts have floating contacts and their rounding ranges from very angular to well-rounded.

Sample KP 1 is a faulted, folded, gray, muscovite-biotite-graphite, clay- to granule-sized, schist with quartz, feldspar, and graphite lenses (Fig. 9c). Muscovite (80%), chlorite (9%), biotite (5%), titanite (2%), tourmaline (2%), and zircon (2%) dominate the sample with a total percentage of 55%. Opaque minerals are 20%, quartz is

14%, and feldspar is 11% of the total volume of KP 1. Grains and clasts are very angular to rounded and have mostly point and line contacts.

Sample KP 47 (hand sample) is a pale pink to white, pegmatite. It consists of albite with calcite-lined microfaults (Fig. 9d).

Impact-related features

Assemblage 1 includes kink bands, microtwins, PFs, and PDFs as possible evidence of shock in the seven samples.

Kink bands in muscovite are relatively common in KP 50. Albite has microtwins and PFs and what may be PDFs are present in quartz in KP 50. Sample KP 51 contains only bent mica grains are common and most of the sample is partially to totally opaque due to graphite content.

It is impossible to tell from the hand sample alone if the dark gray blebs in KP 49 are melt particles, or if they may be primary pyrite with surrounding reddish zones of oxidation. The mixed and deformed pale pink and green zones in the sample could be cataclastic.

Melt is present in KP 48 in a zone containing flow banding in green-brown glassy material. Quartz and feldspar appear to have been recrystallized in some areas. Linear

inclusion trails are common in quartz, twins are prominent in calcite, and a few mica grains are kink banded.

Bent and kinked muscovite grains are common, microfaults are noted in quartz and feldspar, and PDFs are common in quartz grains in KP 2 (Fig. 8e). A biotite grain, with "bird's eye," grainy to mottled extinction preserved, contains what appear to be PDFs and also has a zircon grain included that is surrounded by a pleochroic halo. A reddish-green-brown zone surrounds opaque possible melt particles that appear plastically deformed and have entrained quartz, feldspar, and mica grains.

A normal fault cuts through the entire sample and thin section and other faults and folds are present in KP 1. Kink bands are present in mica and deformation bands are common in quartz (Fig. 9f). There are several grains with PFs in a second direction in addition to the deformation bands.

Discussion

A general consensus among most scientists working on the Eyreville core samples is that shock deformation did not affect or only very slightly affected the base of the core where KP 50 is located (W. U. Reimold, personal communication, 2008). Twins, kink bands, and potential PMs seen together in one thin section may suggest otherwise, but further analysis with transmission electron microscopy (TEM) is necessary to determine if PDFs truly exist in KP 50. Sample KP 51 does not display notable evidence of shock, but the banded nature of the rock could imply that the bands/layers were emplaced by the

impact event. The mylonitic-cataclastic appearance of most of KP 49 could be a result of deformation associated with the impact event, but thin section analysis would be imperative for verifying this hypothesis. Sample KP 48 includes what could be bands of both cataclastic and mylonitic material. Anomalous green-brown material in KP 48 that could be altered melt because it displays characteristic flow banding. If the opaque material in KP 2 is melted material, then the sample is a suevite; otherwise, KP 2 is a shocked lithic breccia. Kink bands in KP 1 are probably a pre-impact feature, but folding and faulting cross-cuts the deformation-banded lenses of quartz, so folds and faults could be syn- or post-impact features.

Assemblage 2: Middle and Lower sections

Assemblage 2 consists of breccias, suevites, and impact melt rocks that range in depth from 1560.24-1397.16 m or 5118.90-4583.86 ft. Samples listed here are between 1560.24 and 1474.05 m or 5118.90 and 4836.12 ft (Fig. 10).

The pre-impact classification of rocks in Assemblage 2, middle and lower sections, includes many lithic fragments (within breccias) could have been sourced from the Lower Cretaceous non-marine deposits (quartz arenite and mudstone) as well as the numerous basement blocks of metamorphic and igneous varieties (schist, slate, , quartzite, and gneiss). The post-impact classification is that the seven samples in this middle section of Assemblage 2 range from lithic breccias to impact melt rocks.

Sample number: KP 3	Depth: 5103.60-5103.70 ft	(1555.58-1555.61 m)
Sample number: KP 46	Depth: 5089.70-5089.80 ft	(1551.34-1551.37 m)
Sample number: KP 4	Depth: 5082.05-5082.15 ft	(1549.01-1549.04 m)
Sample number: KP 45	Depth: 5013.30-5013.40 ft	(1528.05-1528.08 m)
Sample number: KP 6	Depth: 4998.60-4998.70 ft	(1523.70-1523.73 m)
Sample number: KP 44	Depth: 4937.00-4937.10 ft	(1504.80-1504.83 m)
Sample number: KP 43	Depth: 4862.80-4862.90 ft	(1482.18-1482.21 m)

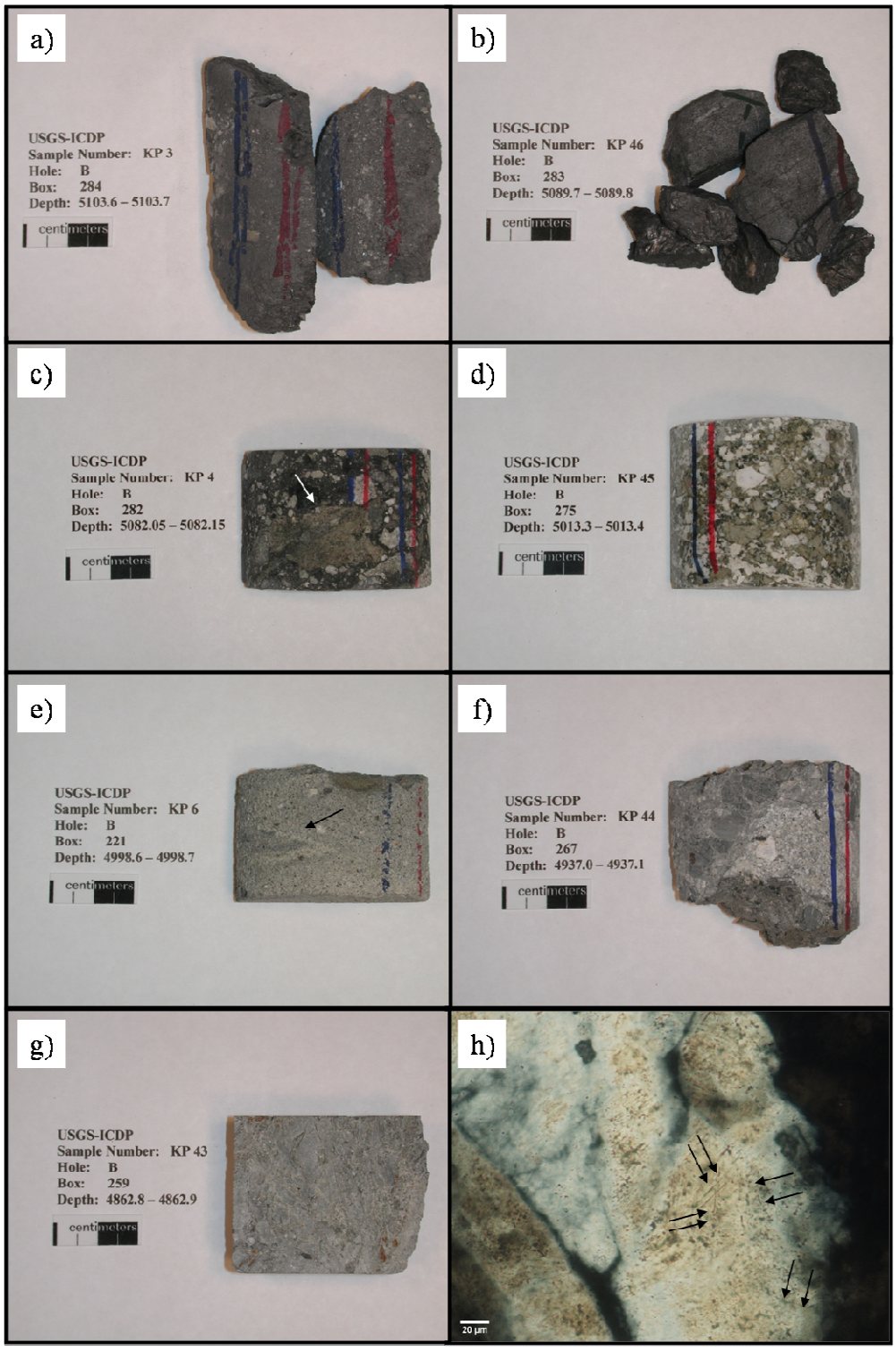

Fig. 10. Oriented core samples a) KP 3, b) KP 46, c) KP 4 (arrow points to altered melt in matrix), d) KP 45, e) KP 6 (arrow points to mixed sediments), f) KP 44, g) KP 43 and h) Photomicrograph of KP 4 (note slightly toasted appearance; arrows point to four sets of PDFs; XPL).

Modal Analysis

Sample KP 3 (thin section) is a dark gray, matrix-supported, competent, graphite-rich, polymict, clay- to pebble-sized, lithic breccia (Fig. 10a). Approximately 95% of the lithic fragments (40% of sample volume) are metamorphic (chlorite-muscovite schist, slate, quartzite, and gneiss), whereas 5% is likely sedimentary rip-up clasts of mudstone. Quartz and feldspar each represent 10% of the mode of KP 3, mostly graphite and traces of calcite make up 12%, and muscovite is 3% of the sample. The clastic matrix (20%) consists of graphite, clays, and micas, and silica cement is approximately 5% of KP 3. Grains and clasts in KP 3 are very angular to subangular and they have floating, point, and line contacts.

In the thin section of KP 46, a subtle schistose texture is present, but the core sample (Fig. 10b) is classified as a graphitic breccia by Horton et al. (2007). The thin section represents a dark gray, faulted, veined, graphite-rich, fine-grained schist. Sample KP 46 is void of lithic fragments. Approximately 35% of KP 46 is quartz, 25% is feldspar, 20% includes opaque minerals (including graphite) and calcite (mainly as fracture fill), and 15% consists of equal amounts of chlorite and muscovite. The matrix and cement are minor components and together may compose up to 5% of the sample. Grains and clasts in KP 46 are very angular to subangular and they have point, line, and concavo-convex contacts. Part of an opaque breccia dike or vein is near a thin section edge. Very fine-grained muscovite, quartz, and feldspar are ‘entrained’ in this feature.

Sample KP 4 is a dark gray, matrix-supported, competent, graphite-rich, polymict, clay- to pebble-sized, suevite and, at least locally, is an impact melt rock (Fig. 10c). The core sample of KP 4 contains obvious altered melt particles, especially in a 2.5 cm-wide zone of melt in the matrix which 'swept' around other grains. This sample is 60% lithic fragments, such as altered melt clasts, quartzite, schist, slate, gneiss, and mudstone, but 10% of KP 7 consists of matrix (graphite, clays, micas, and altered melt material). Approximately 12% of the sample is quartz, 7% is feldspar, and the remainder of KP 4 contains 4% muscovite and chlorite, with minor amounts of calcite as fracture fill, and opaque minerals (2%) and silica cement (5%). Grains and clasts have floating, point, and line contacts and range from very angular to subrounded.

Sample KP 45 (thin section) is a green, tan, and white, clast-supported, competent, polymict, clay- to pebble-sized, lithic breccia or a suevite, based on what could be traces of altered melt along grain boundaries, fractures, and cleavage (Fig. 10d). Thirty-five percent of KP 45 is feldspar, 30% is quartz, and 15% consists of lithic fragments of quartzite and schist. The clastic matrix and silica cement comprise approximately 10% of KP 45. Silicates in KP 45 such as muscovite, orthopyroxene, biotite, chlorite, and zircon are 8% total and less than 2% of the sample is an opaque mineral(s). There is a very minor amount of calcite as fracture fill (<1%). Grains and clasts in KP 45 are very angular to subangular and they have point, line, concavo-convex contacts, and sutured ones.

Sample KP 6 (thin section) is a tan to light gray, clast-supported, slightly friable, polymict, clay- to sand-sized, lithic breccia (Fig. 10e). Approximately 48% of sample is quartz, 30% is feldspar, 10% is a clastic matrix, 5% each of lithic fragments (quartzite, mudstone) and weak silica cement, and minor (2%) amounts of muscovite, orthopyroxene, and opaque minerals. Grain/clast rounding ranges from very angular to subrounded and contacts are floating, point, and line.

The thin section of sample KP 44 contains melt, although altered melt particles were not obvious in hand sample. As a result, this sample is a light gray, matrix-supported, competent, polymict, clay- to pebble-sized, suevite (Fig. 10f). Approximately 90% of the lithic fragments (40% of sample volume) are metamorphic (schist, slate, quartzite, and altered melt clasts), whereas 10% is likely a sedimentary clast of mudstone with graded bedding. Quartz and feldspar each represent 15% of KP 44, muscovite and biotite make up 7%, and calcite and opaque minerals are 3% of the sample. The clastic matrix (5%) consists of graphite, clays, and micas and silica cement is approximately 5% of KP 3. Grain and clast rounding in KP 44 is very angular to rounded, and the particles have floating and point contacts.

Sample KP 43 (thin section) is a light gray, clast-supported, competent, polymict, clay- to pebble-sized, lithic breccia (Fig. 10g). Approximately 28% of KP 43 is equal amounts of quartz and feldspar and other silicates are 45% of the thin section (50% muscovite, 50% fine-grained chlorite or serpentinite). Lithic fragments account for 20% of KP 43, 5% is clastic matrix and silica cement, and 2% is calcite and opaque minerals.

All types of grain or clast contacts are present and rounding ranges from very angular to subrounded.

Impact-related features

Because melted material is amorphous and isotropic in thin section, the graphite (an opaque mineral) content in KP 3 may obscure isotropic material. LITs and PDFs are prevalent in quartzite clasts within KP 3.

Sample KP 46 contains common slightly toasted quartz grains, as well as PDFs and LITs in fine-grained quartz. Deformation bands throughout the quartz vein are prominent (approximately one mm thick). Some calcite grains are microtwinned. The opaque dike or vein could be melt material (or carbon), but further tests are required to confidently determine its makeup.

In KP 4, schlieren in altered melt material are evident in the hand sample (Fig. 10c). Other shock features include mosaicism in a quartz clast, toasted quartz, as well as pervasive PFs in quartz with PDFs (Fig. 10h).

Sample KP 45 has a set of PDFs in nearly every quartz grain. Planar fractures are also very common. The thoroughly shocked specimen in thin section perhaps could have been inferred from the core sample, which has common bright white grains typical of the appearance of extremely shocked minerals (Whitehead et al. 2002; Fig. 10d). The kink bands are seen in muscovite. PMs are noted in feldspars. There are excellent examples

of ladder structures in feldspar and quartz. Many clasts are partially isotropic, with what could be melt along grain boundaries and fractures/cleavage, but grain boundaries are commonly preserved in KP 45.

Sample KP 6 includes approximately 68 quartz grains that contain LITs, but PDFs are rare and are found only in fine-grained quartz. There are at least two slightly toasted quartz grains. One feldspar grain has a microfault that off-sets twin lamellae.

In KP 44, most of the thin section is partially opaque to isotropic due in part to probable graphite in the matrix and altered melt. Several clasts are melted, and some grains have preserved grain boundaries. Schlieren are present as well as ballen texture and recrystallized quartz or feldspar. There is a minor amount of toasting in quartz grains and PFs are common. Approximately 23 quartz grains in KP 44 have one set of PDFs, 17 grains have two sets, three grains have two sets, one grain has four sets, and another grain has six sets.

Sample KP 43 has a few partially isotropic zones, some near opaque grains, and there is also some possibly recrystallized material. Due to the isotropic and opaque material, it is sometimes challenging to determine if a material is recrystallized or was initially microcrystalline. There are bent muscovite and chlorite grains. Some grains of quartz are very toasted, LITs are common, and PDFs, if present, are mostly one set (one quartz grain has two sets).

Discussion

Sample KP 3 displays subtle examples of shock features. Sample KP 46 includes some probable shock features, such as toasting and PDFS, but deformation bands in quartz may be a pre-impact feature. High shock pressures were likely experienced by certain constituents of KP 4, considering the extent of toasting, mosaicism, PMs in quartz, and the melt content of this sample (Fig. 10h). Sample KP 45 may have very minor amounts of altered melt material, but it is essentially a highly shocked lithic breccia. Sample KP 6 contains only subtle evidence of shock, but in hand sample the swirled/mixed gray and tan material is an obvious sign that the constituent grains experienced turbulence. The interspersed altered melt particles and prevalence of PMs in quartz document shock experienced by KP 44, a suevite. Lithic breccia sample KP 43 displays only a low to moderate amount of shock-related features.

Assemblage 2: Upper section

The samples in the upper section of Assemblage 2 (1474.05-1397.16 m or 4836.12-4583.86 ft) are classified as melt-rich suevite and contain the seven samples listed below (Fig 11).

The pre-impact classification of rocks in Assemblage 2, upper zone, includes many lithic fragments (within breccias) that could have been sourced from the Lower Cretaceous non-marine deposits (quartz arenite and mudstone) as well as the numerous basement blocks of metamorphic and igneous varieties (schist, pegmatite, and granite). The post-impact classification is that the diverse constituent grains and clasts of the target were mixed and/or melted and produced this particularly melt-rich breccia zone of suevites and impact melt rock. Sample 42, however, is a lithic breccia with extreme shock features, but with very little (if any) altered melt material.

Sample number: KP 52	Depth: 4582.50-4582.60 ft	(1396.73-1396.76 m)
Sample number: KP 7	Depth: 4590.20-4590.30 ft	(1399.09-1399.12 m)
Sample number: KP 32	Depth: 4591.30-4591.45 ft	(1399.41-1399.46 m)
Sample number: KP 39	Depth: 4611.90-4612.00 ft	(1405.71-1405.74 m)
Sample number: KP 40	Depth: 4632.85-4632.95 ft	(1412.03-1412.06 m)
Sample number: KP 41	Depth: 4641.40-4641.50 ft	(1414.70-1414.73 m)
Sample number: KP 42	Depth: 4779.25-4779.40 ft	(1456.72-1456.76 m)

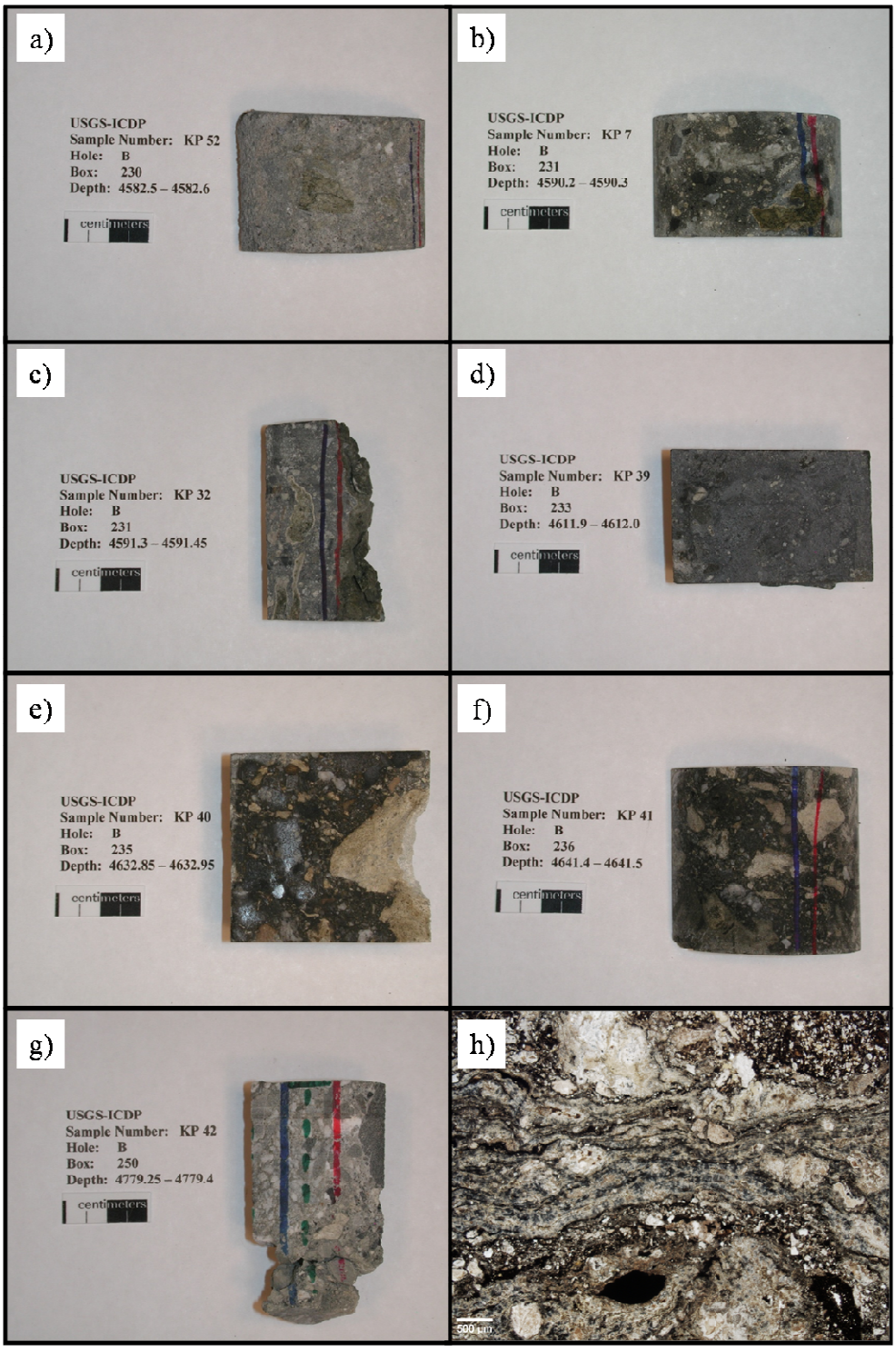

Fig. 11. Core samples a) KP 52 (oriented), b) KP 7 (oriented), c) KP 32 (oriented), d) KP 39, e) KP 40, f) KP 41 (oriented), g) KP 42 (oriented) and h) Photomicrograph of KP 39 showing relict melted matrix (PPL).

Modal Analysis

Sample KP 52 is a medium gray, matrix-supported, competent, polymict, clay- to pebble-sized, suevite (Fig. 11a). At least six probable altered glass/melt clasts were visible in the hand sample. Approximately 30% of KP 52 consists of lithic fragments (mudstone, quartzite, schist, altered melt), 25% of the sample is quartz, 10% is feldspar, whereas chlorite and muscovite represent 8%. A minor 2% of the sample is opaque minerals as well as apatite, garnet, and zircon. Sample KP 52 is 5% cement and the matrix (20%) is made up of clay minerals and some partially isotropic material. Grains and clasts are very angular to rounded in shape and only have floating contacts.

Sample KP 7 has altered melt particles visible in the hand sample and is a gray, matrix-supported, competent, polymict, clay- to pebble-sized, suevite (Fig. 11b). This sample is 50% lithic fragments, such as melt clasts, quartzite, schist, slate, and mudstone, but approximately 25% of KP 7 consists of matrix (graphite, clays, micas, and possible altered melt) material. Ten percent of the sample is quartz, 3% is feldspar, and the remainder of KP 7 contains 5% muscovite, biotite, and chlorite, with minor amounts of opaque minerals (2%) and silica cement (5%). Grains and clasts have floating contacts and range from very angular to subrounded.

Sample KP 32 (thin section) is another example of a medium to dark gray, matrix-supported, competent, polymict, clay- to pebble-sized, impact melt rock with altered melt particles visible in hand sample (Fig. 11c). Approximately 45% of the sample is composed of lithic fragments (altered melt particles, schist, graphite and quartzite), 15%

is quartz, 12% is feldspar, with minor components of muscovite and opaque minerals (3%) and silica cement (5%). The matrix (20%) is composed of clays, micas, and what may be altered glassy zones. Grains and clasts range from very angular to well-rounded and have floating to diffuse contacts.

In KP 39 (thin section), altered glass is present in the matrix that is 45% of the thin section (Fig. 11h). This sample is a dark gray, matrix-supported, competent, polymict, clay- to pebble-sized, impact melt rock with 5% silica cement (Fig. 11d). Sample KP 39 is approximately 30% lithic fragments (altered melt clasts, gneiss, and quartzite), 10% is quartz, 9% is feldspar, and 1% is opaque minerals. Grain and clast rounding spans from subrounded to well-rounded and there are floating grain contacts.

In KP 40 (thin section), the type of matrix, cement, and grain/clast contacts are very similar to KP 39 and it is also a gray, matrix-supported, competent, polymict, clay- to pebble-sized, suevite (Fig. 11e). Sample KP 40 contains more and larger lithic fragments (63%) including altered melt particles, gneiss, schist, and quartzite and 20% clastic matrix. Quartz and feldspar each account for approximately 5% of the sample and silica cement (4%) muscovite (2%) and opaque minerals (1%) are minor components. Grains and clasts range from angular to well-rounded in shape.

Sample KP 41 (thin section) is extremely similar to KP 40 (Fig. 11f). The only differences include mudstone (with graded bedding) as an additional type of lithic

fragment, clasts and grains range in shape from very angular to rounded. There is approximately 10% volume of opaque material in KP 41.

Sample KP 42 is an highly shocked, light grayish tan, clast-supported, competent, polymict, clay- to pebble-sized, lithic breccia with a minor amount of isotropic material in the matrix (Fig. 11g). Approximately 70% of sample KP 42 is composed of lithic fragments (mudstone, schist, quartzite, and granite), 10% of quartz and feldspar (each), 5% of muscovite, and a minor 1% of KP 42 is opaque minerals. The matrix (carbonate, micas, clays, and probable altered glass) and cement (silica and carbonate) are very minor components (approximately 4%). Grains and clasts have floating, point, and line contacts and their shapes are from subrounded to rounded.

Impact-related features

The mottled matrix of KP 52 is isotropic in some areas and contains approximately nine altered melt bodies (an estimated 15% of sample is melt). Melt features include schlieren, ballen, vesicles, and recrystallized quartz. One of these melt bodies is mixed and swirled into the matrix. Several plucked areas in the thin section appear to have contained altered melt as well. Probable PDFs (1 set) are in at least five quartz grains and are in three to four different directions in two other grains. Some fractures and LITs, which are common in quartz in KP 52, appear bent. Fractures along cleavage planes in feldspars are common.

Sample KP 7 contains common toasted quartz and LITs or PDFs in quartz in one direction or one set. One quartz grain contains three sets of PDFs, and at least four other grains contain two sets. A twinned feldspar grain contains microfaults. Considering the graphite in the matrix and at least 10 altered melt clasts, most of the thin section is at least partially isotropic to opaque. Schlieren are extensive in the altered melt clasts and recrystallized feldspar or quartz is 'floating' in the matrix and is also located within a flow-banded, altered melt clast.

Most everything in KP 32 appears to have been partially melted, thoroughly melted and amorphous, or recrystallized to a fine-grained fabric and most of the thin section is at least partially isotropic. Schlieren are extensive in this sample and there are also examples of ballen, vesicles, and what could be recrystallized quartz and/or feldspar without original grain boundaries preserved. This indistinct recrystallized material is occasionally entrained in flow-banded or schlieren-rich zones as well as clasts or grains that were stretched along flow bands. Toasted quartz grains are present and three grains display two sets of PDFs, one grain has three sets, and one grain has at least five sets. Microfaults offset twins in feldspar and a grain of muscovite is kink banded.

Samples KP 39, KP 40, and KP 41 contain a matrix that is dominated by isotropic material and is interpreted from textural characteristics to be altered melt (Fig. 11h). For example, ballen quartz and schlieren are plentiful, whereas vesicles and recrystallized quartz and/or feldspar are also in KP 39 and KP 40. Sample KP 41 displays flow banding

or schlieren, ballen quartz, vesicles, and toasted quartz grains. Melt clasts are present in blebs or amoeboid shapes in KP 39, KP 40, and KP 41.

While investigating KP 41 altered melt with an electron microprobe and scanning electron microscope (SEM), compositions of very fine-grained spinels were attained. The resulting data yielded anomalously high Ni and Cr levels (Fig. 12a and b).

In KP 42, quartz grains within a granite fragment commonly show toasting and PMs. A ladder structure is well-preserved in a feldspar grain within a granite clast. There are also bent twin planes in a feldspar grain. Another area contains what is interpreted, without quantitative compositional data, as a recrystallized feldspar grain. The grain, with original boundaries preserved, is slightly isotropic and has an almost microcrystalline fabric. There is likely some altered melt material or other type of isotropic matter 'swirled' in the matrix.

Discussion

This upper section of Assemblage 2 most likely experienced the highest temperatures and pressures of the stratigraphic section judging from the increase in glassy material as clasts and in the matrix of the samples. Numerous examples of textures such as schlieren and ballen of quenched silica glass can be found in this zone. A zone of silica melt in KP 41 contains a few very fine-grained spinels and is discussed below (Fig. 12a).

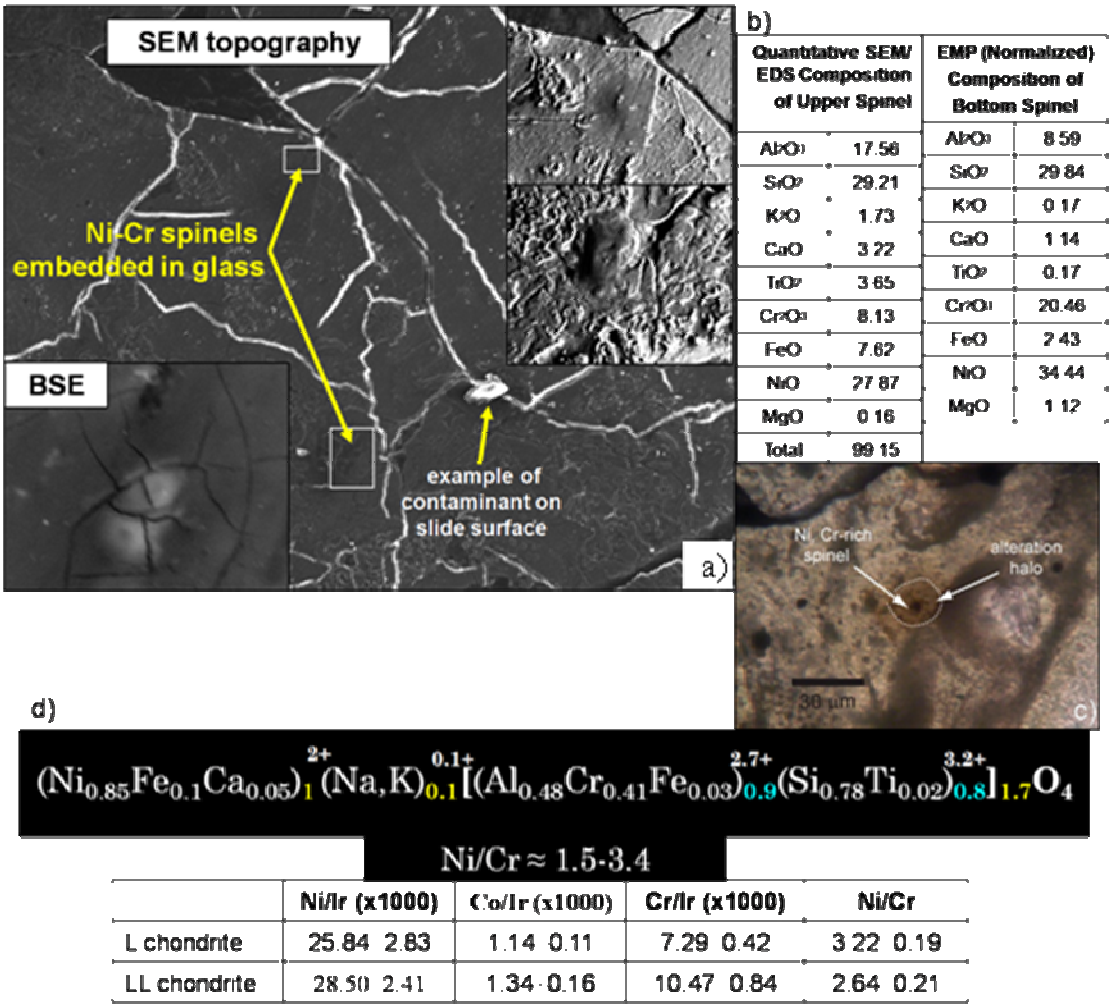

	Ni/Ir (x1000)	Co/Ir (x1000)	Cr/Ir (x1000)	Ni/Cr
L chondrite	25.84 2.83	1.14 0.11	7.29 0.42	3.22 0.19
LL chondrite	28.50 2.41	1.34 0.16	10.47 0.84	2.64 0.21

Fig. 12. Various images showing Ni-Cr spinels in KP 41 (1414.7 m). a) SEM and BSE images displaying raised hard grains surrounded by corrosion "moat" in glass results in low microprobe totals (grains also may have spots slightly below surface), b) Tables of SEM and EMP compositions for spinel grains shown in a). The Si-rich compositions indicate extreme disequilibrium, c) Photomicrograph of KP 41 showing alteration halo around a spinel grain (PPL), and d) Resulting stoichiometry and Ni/Cr ratio for spinels and comparison table or chondrite composition (R. Tagle, personal communication, 2007, 2008; Glidewell et al. 2007, 2008).

Composition of fine-grained spinels in altered melt

Fine-grained spinels in KP 41 occupy depressions in altered melt and display alteration haloes (Fig. 12a and c). Compositional data shown in Fig. 12b are anomalously high in Ni and Cr. The ratios of Ni to Cr in KP 41 range from 1.5-3.4 and are very similar to bulk compositions of L- or LL-type chondritic meteorites (Fig. 12d; R. Tagle, personal communication, 2007, 2008; Glidewell et al. 2007, 2008). The ratio range matches those of the type of impactor that created the Eocene Popagai structure in Russia. The author interprets the spinels in KP 41 to be the first report of the impactor type for the Chesapeake Bay structure (Glidewell et al. 2007, 2008).

Assemblage 3

Assemblage 3 has mixed gravelly sands and lithic blocks in the depth span of 1397.16-1371.11 m or 4583.86-4498.39 ft. Six samples fit into this zone and are described in Subsections 1 and 2 below. The description of KP 8 (Fig. 13) is singled out in Subsection 1 from the overlying samples in Assemblage 3 because it is a sandy breccia that contains a suevite clast, whereas the other five samples are mixed sands and lithic blocks and are grouped in the subsequent description (Subsection 2).

Subsection 1

The pre-impact classification of rocks in Assemblage 3, subsection 1, includes clastic sediments that came from Lower Cretaceous non-marine deposits (quartz arenite and mudstone). The post-impact classification is that Lower Cretaceous sediments were mixed to form the gravelly sands of this interval.

Sample number: KP 8 Depth: 4570.20-4570.40 ft (1393.00-1393.06 m)

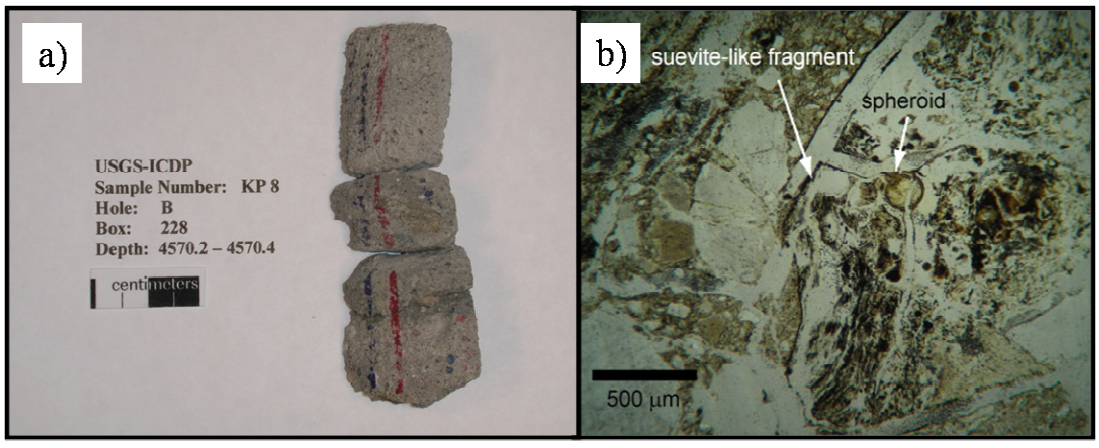

Fig. 13. Sample KP 8. a) Core sample (oriented), and b) photomicrograph (PPL).

Modal Analysis

Sample KP 8 (thin section) is a grayish beige, matrix-supported, clay- to pebble-sized, suevite that is weakly silica-cemented (Fig. 13a). Approximately 40% of the sample is quartz, 17% is feldspar, 10% consists of lithic fragments (suevite clast, mudstone, and chert), and other constituent grains include muscovite and garnet (5%), and opaque minerals (5%). Sample KP 8 consists of 20% matrix of clays and micas and 3% silica cement. Grain rounding ranges from very angular to subrounded and grain contact types include floating and point. The upper third and bottom sixth areas of the thin section are slightly darker zones of matrix.

Impact-related features

Features that could be related to the impact event are as follows: most quartz grains contain LITs; decorated PDFs are in a few quartz grains; there is one well-toasted quartz grain with PFs; and one suevite clast (Fig. 13b). The suevite clast includes microspherules, schlieren, vesicles, and probable ballen (Fig. 13b).

Discussion

The suevite clast in KP 8 near the base of the gravelly sand layer could have been entrained in the material as it slid in over the suevites. The sandy material is likely sourced from the Cretaceous Potomac Formation due to the dominant percentage of quartz and lack of glauconite and fossil fragments.

Subsection 2

The pre-impact classification of rocks in Assemblage 3, subsection 1, includes clastic sediments that came from Lower Cretaceous non-marine deposits (quartz arenite and mudstone). The post-impact classification is that Lower Cretaceous sediments were mixed to form the gravelly sands of this interval (Fig. 14).

Sample number: KP 33	Depth: 4559.70-4559.80 ft	(1389.80-1389.83 m)
Sample number: KP 31	Depth: 4515.50-4515.60 ft	(1376.32-1376.35 m)
Sample number: KP 34	Depth: 4512.23-4512.33 ft	(1375.33-1375.36 m)
Sample number: KP 9	Depth: 4508.00-4508.10 ft	(1373.97-1374.00 m)
Sample number: KP 5	Depth: 4499.00-4499.10 ft	(1371.17-1371.20 m)

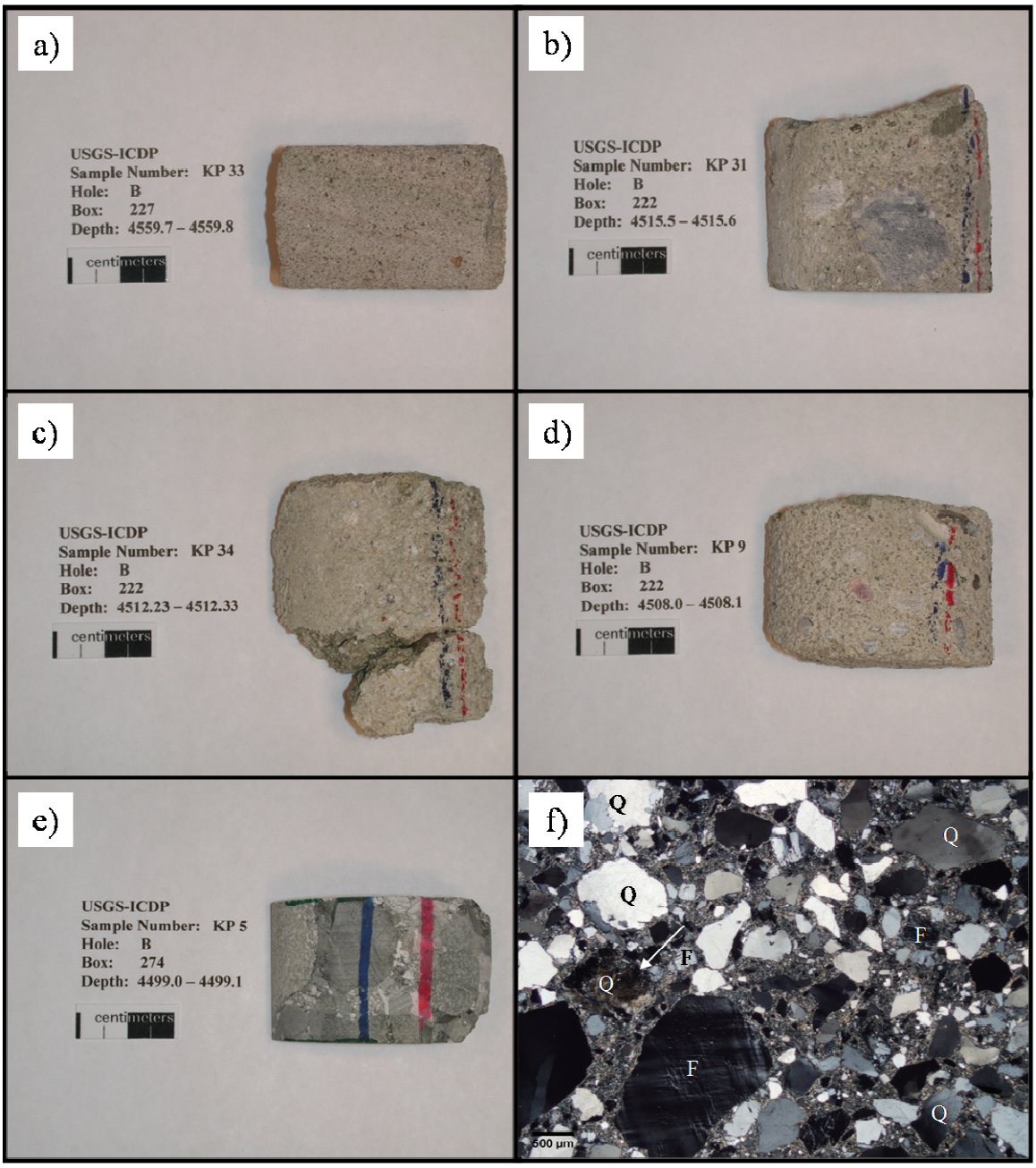

Fig. 14. Oriented core samples a) KP 33, b) KP 31, c) KP 34, d) KP 9, e) KP 5, and f) Photomicrograph of KP 33 (oriented; XPL); Q=quartz, F=feldspar.

Modal Analysis

Samples KP 34, KP 31, KP 33, and KP 9 (thin sections) are similar beige to tan, clast-supported, friable, clay- to pebble-sized, lithic breccias (Fig. 14a-d). In these samples, there is approximately 46% volume of quartz and 30% feldspar, with minor muscovite, lithic fragments, and opaque minerals (<10% volume combined). There is 15% volume of matrix comprising mica and clay minerals. Grain rounding is very angular to subrounded. Sample KP 33 has 4% volume more lithic fragments, approximately 10% opaque minerals, garnet (some relatively euhedral), and rare mafic minerals (clinopyroxene and olivine), and floating, point, and line grain contacts. Samples KP 34 and KP 31 are very similar to KP 33, but they have only floating and point grain contacts. Mafic minerals were not observed in KP 9, but otherwise it is very similar to KP 33.

Sample KP 5 (thin section) is a light gray to tan, mottled, clast-supported, moderately friable (weakly silica-cemented), clay- to granule-sized, lithic breccia (Fig. 14e). It contains over 90% volume of lithic fragments, including mudstone, schist, quartzite, and granite. The matrix (approximately 5% volume) consists mainly of clays, micas, and chlorite. Grain contacts in KP 5 are floating, line, point, and concavo-convex and the grain rounding ranges from very angular to rounded. Veins in metamorphic rock fragments contain quartz and very fine-grained material with radial extinction that is likely serpentine-group minerals.

Impact-related features

Sample KP 33 has common LITs and decorated PDFs in one direction in 22 quartz grains, and in 11 grains as two or three sets (Fig. 14f). Quartz LITs are ubiquitous in KP 31 and KP 34, and the frequency of these features in these samples suggests that any PDFs that were present in these samples were annealed. Linear inclusion trails, in some cases, may be relict PDFs. Nearly every quartz grain in KP 9 contains a LIT, one quartz grain has three directions of decorated PDFs, microfaults are in quartz and microcline, and there are several toasted quartz grains. Almost every grain/clast in KP 5 is either fractured, toasted, contains PDFs, exhibits mosaicism or has all four traits. Probable PDFs are common in KP 5 (usually as two sets), occurring in nearly every quartz grain.

Discussion

Quartz grains contain obvious ample evidence of shock deformation in Assemblage 3. Planar microstructures are common and other features such as microfaulting as well as mosaicism and toasting in quartz are in this interval.

Assemblage 4

Samples KP 10 and KP 12 are part of the allochthonous block of granitic rocks referred to as Assemblage 4 (Fig. 15). This section ranges from 1371.11 m or 4498.39 ft to 1095.74 m or 3594.95 ft.

The pre-impact classification of rocks in Assemblage 4 includes blocks of granites with variable composition and crystal size, which are thought to be detached from the basement of the impact target. The post-impact classification is that the blocks are a mixed assortment of granites, and KP 10 and KP 12 range from fine- to coarse-grained.

Sample number: KP 10	Depth: 4441.35-4441.45 ft	(1353.66-1353.69 m)
Sample number: KP 12	Depth: 3595.50-3595.80 ft	(1095.89-1095.98 m)

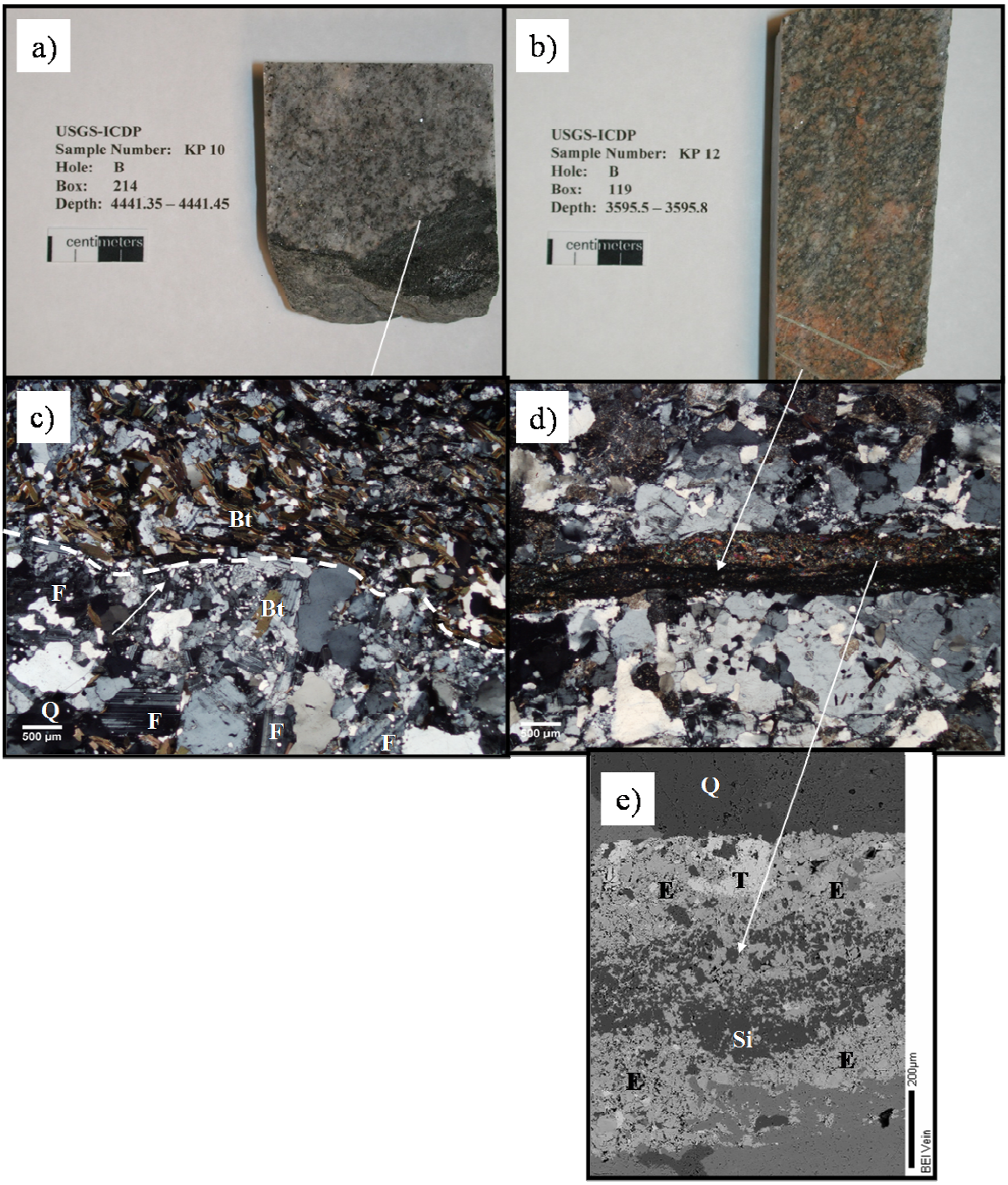

Fig. 15. Core samples a) KP 10 and b) KP 12, and photomicrographs c) KP 10 (oriented; XPL), d) KP 12 (XPL), and e) Electron backscatter image of lower vein in KP 12; Q=quartz, F=feldspar, Bt=biotite, Si=silica, E=epidote, T=titanite.

Modal Analysis

Sample KP 10 (thin section) is light gray and comprises approximately one-third biotite-chorite schist and two-thirds biotite-rich, fine- to medium-grained granite (Fig. 15a). Allotriomorphic granular fabric dominates the granite portion, while the remaining part of KP 10 is schistose. Other textures include perthitic and poikilitically enclosed mica in quartz and feldspar. Grains range in shape from anhedral to subhedral. The transition between the schist and granite is distinct and there is a grain size reduction along this boundary with both fine, dynamically recrystallized quartz, and subhedral biotite and chlorite grains (Fig. 15c). The sample is mostly quartz (30%), feldspar (35%), chlorite, biotite, and zircon (30% total), and minor opaque minerals (5%) are present. There has been alteration of feldspars to clay and no euhedral quartz or feldspars as well as no mafic minerals were observed.

Sample KP 12 (thin section) is a reddish, fine- to medium-grained, foliated meta-granite with allotriomorphic granular fabric (Fig. 15b). The upper part of the core sample (sample is oriented) displays a strong metamorphic foliation defined by mica grains and flattened, stretched quartz and feldspars (Fig. 15b). Perthite and mermykite are present and quartz is locally poikilitically enclosed in feldspar. Grains range in shape from anhedral (angular to well-rounded) to subhedral. This sample consists of approximately 85% quartz and feldspar in roughly equal amounts, minor muscovite, biotite, chlorite, and zircon (10% total), and opaque minerals (5%). Sample KP 12 is altered along veins, especially from feldspars to clay (not pictured, in several patches only clay appears to remain). Inclusions in feldspar are common and twinning in feldspar is the only other

distinct intragranular feature left. Grain boundary bulges and new grains indicate that quartz is dynamically recrystallized, particularly along fractures and grain boundaries.

Two sub-parallel veins are present in KP 12 (Fig. 15b, d, e). The 'top' vein is approximately 0.3 mm thick and quartz-filled, with slightly larger grains in the upper part of the feature and crystal size reduces downward. The 'bottom' vein or dike is isotropic to near-opaque and has a similar thickness. This vein is hypocrystalline and has a silica groundmass material that displays fluidal texture and migrates sinusoidally from the vein center to the walls among fine- to medium-grained epidote, titanite, and magnetite (Fig. 15e).

Impact-related features

Any features that may be impact-related are difficult to discern due to alteration. Sample KP 12 displays what could be PDFs.

Discussion

The alteration and veining are likely pre-impact features. The epidote-filled lower vein is a typical hydrothermal feature in granites in the region (M. G. Steltenpohl and W. E. Hames, personal communication, 2008).

Assemblage 5: Lower zone

Assemblage 5 is the uppermost section and contains sedimentary-clast breccias and sediment blocks. This portion of the Eyreville core is from 1095.74-443.9 m or 3594.95-1456.36 ft and the Lower zone of clast-supported sedimentary blocks/boulders includes seven samples and spans from 1095.74-866.7 m or 3594.95-2843.5 ft. Gravelly sands (i.e., samples KP 11 and KP 35) just above the granite blocks are grouped in Subsection 1 due to their percent matrix and lack of glauconite and fossils (Fig. 16). The remaining five sandy breccias are described in Subsection 2.

Subsection 1

The pre-impact classification of rocks in Assemblage 5, subsection 1, includes clastic sediments that came from Lower Cretaceous non-marine deposits (quartz arenite and mudstone). The post-impact classification is that Lower Cretaceous sediments were mixed to form the gravelly sands of this interval.

Sample number: KP 11	Depth: 3594.85-3594.95 ft	(1095.70-1095.73 m)
Sample number: KP 35	Depth: 3593.75-3593.85 ft	(1095.37-1095.40 m)

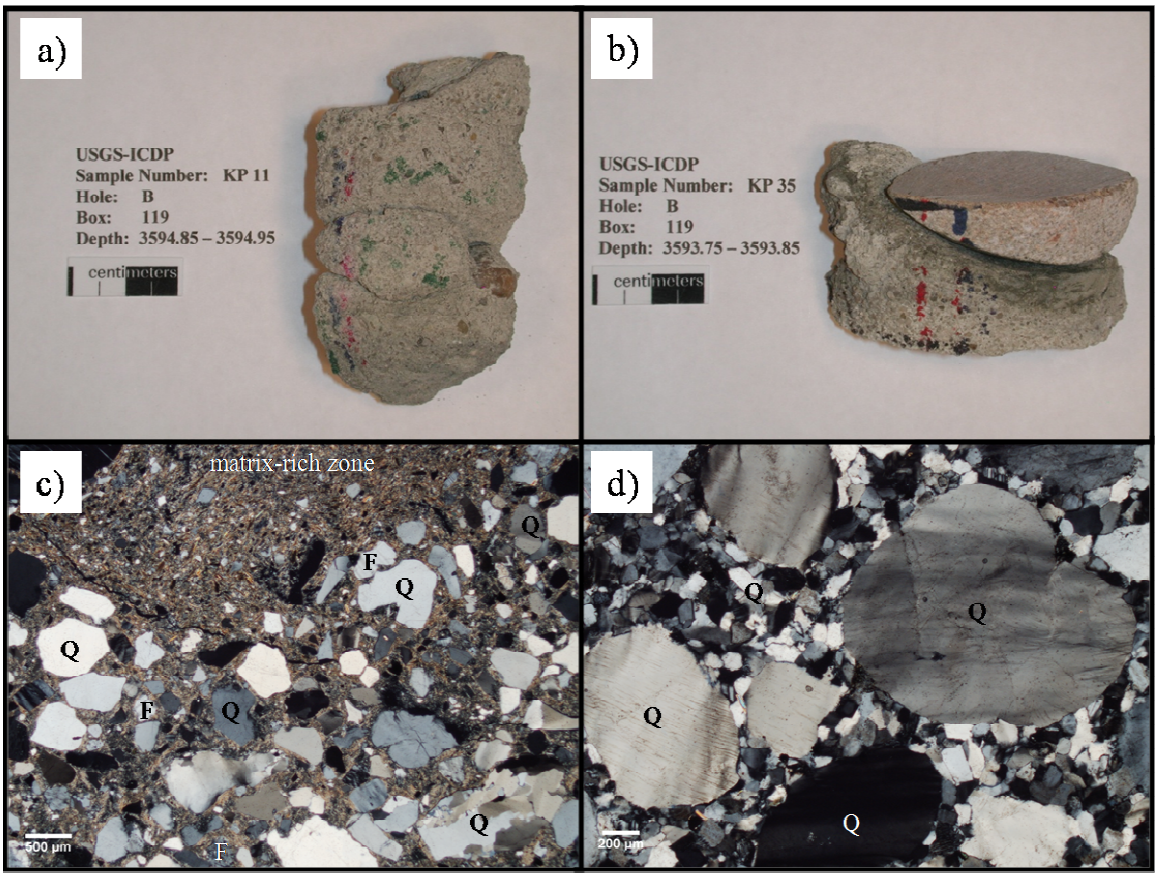

Fig. 16. Core samples a) KP 11 (oriented) and b) KP 35, and photomicrographs c) KP 11 (showing matrix-rich zone in sandy breccia, oriented; XPL), and d) KP 35 (showing PFs in grains of quartzite pebble; XPL); Q=quartz, F=feldspar.

Modal Analysis

Sample KP 11 is a beige, clay- to pebble-sized lithic breccia with very angular to subrounded grains (Fig. 16a). Eleven percent of KP 11 is muscovite, garnet, and opaque minerals. There is a zone in KP 11 of matrix-like material without distinct grain boundaries where muscovite grains sweep around the grains that bound this zone. Both KP 11 and KP 35 (thin sections) lack fossils and glauconite, contain 15-20% volume matrix, are clast-supported, contain 30-35% quartz, approximately 20% feldspar, are weakly silica-cemented, and have floating and point type grain contacts. Sample KP 35 is a gray, silt- to pebble-sized lithic breccia with very angular to rounded grains (Fig. 16b). A minor 4% of KP 35 contains opaque minerals, muscovite, olivine, garnet, zoisite, titanite, and zircon. A quartzite clast in hand sample was pebble-sized and it rested on the breccia separated from the matrix by a light green slaty material. A clast of matrix-like material is also present in KP 35.

Impact-related features

At least one toasted grain is present in KP 11 with approximately 38 quartz grains with LITs and two grains with PFs. Sample KP 35 contains 55 grains with LITs (both in the quartzite granule and smaller grains floating in the matrix) and six grains with PFs (Fig. 16d).

Discussion

The two samples in this gravelly sand do not include melt particles or preserved PDFs, so evidence of shock is somewhat circumstantial from the presence of LITs and

PFs (Fig. 16d). The matrix-like body in KP 11 appears to be injected material based on the intergranular relations of the micas that surround this zone (Fig. 16c).

Subsection 2

The pre-impact classification of rocks in Assemblage 5, subsection 1, includes clastic sediments that came from Lower Cretaceous non-marine deposits (quartz arenite and mudstone). The post-impact classification is that Lower Cretaceous sediments were mixed to form the sandy breccias of this interval (Fig. 17).

Sample number: KP 36	Depth: 3561.40-3561.50 ft	(1085.51-1085.55 m)
Sample number: KP 15	Depth: 3544.50-3544.60 ft	(1079.75-1079.78 m)
Sample number: KP 13	Depth: 3394.50-3394.60 ft	(1034.64-1034.67 m)
Sample number: KP 14	Depth: 3172.70-3172.80 ft	(967.04-967.07 m)
Sample number: KP 37	Depth: 2866.00-2866.10 ft	(873.50-873.53 m)

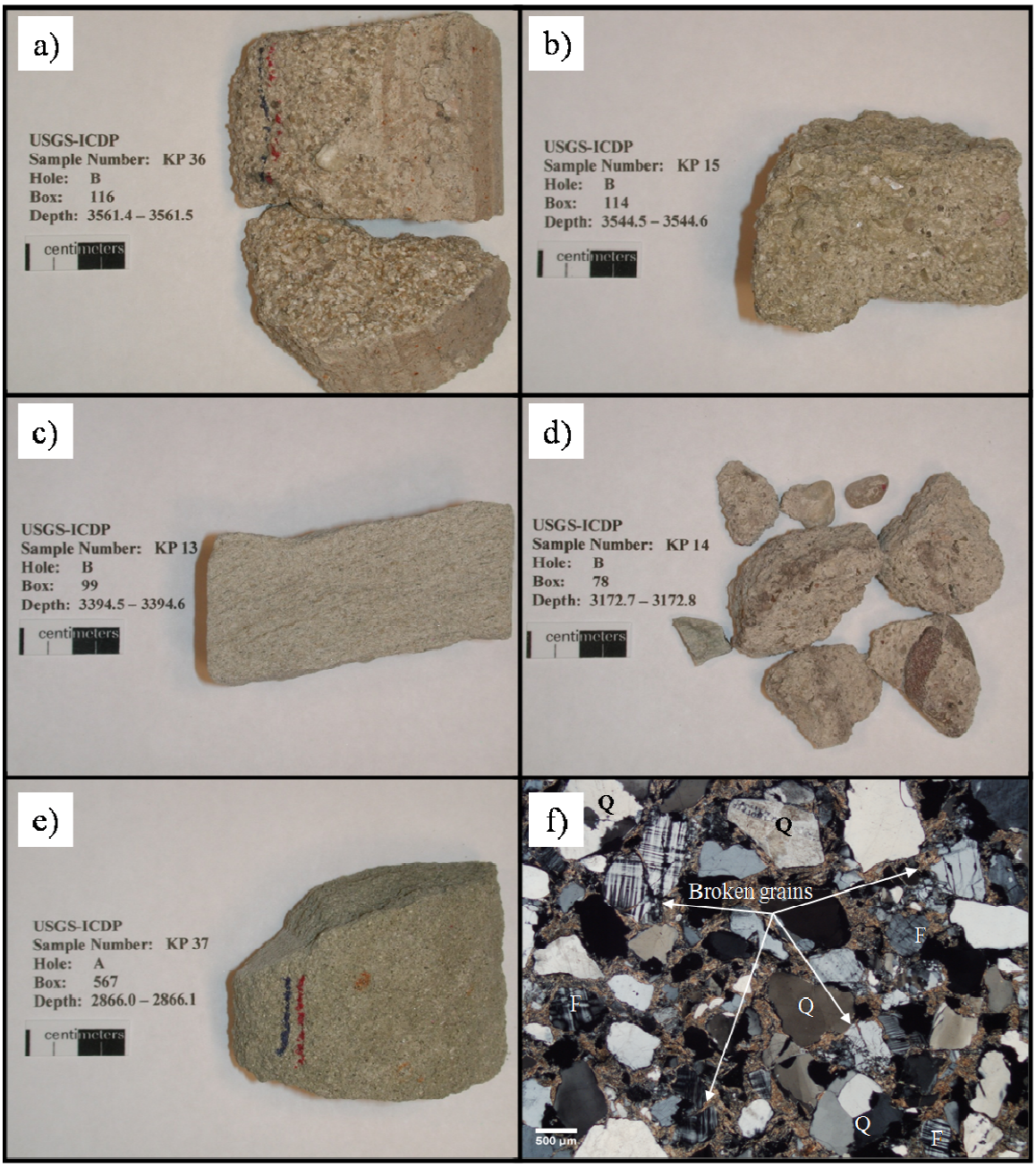

Fig. 17. Core samples a) KP 36 (oriented), b) KP 15 (oriented), c) KP 13 (oriented), d) KP 14, e) KP 37 (oriented), and f) Photomicrograph of KP 15 (showing broken grains, oriented; XPL); Q=quartz, F=feldspar.

Modal Analysis

Sample KP 36 to KP 37 represents the interval from 1085.51-873.53 m or 3561.40-2866.10 ft and is essentially void of glauconite and fossils and has 3% volume or less of rock fragments. There is no thin section sample for KP 14, so it is only grouped here from its hand sample description. The samples are all beige and friable, clay- to sand-sized, sandy impactoclastic breccias, have between 25 and 15% volume of matrix, and contain very angular to subrounded grains (Fig. 16a-e).

Sample KP 36 (thin section) has approximately 40% quartz, 30% feldspar, and 5% muscovite, zoisite, garnet, opaque minerals, and minor carbonate cement. Sample KP 36 has floating, point, and line grain contacts and ranges in grain size from silt to pebble.

In KP 15 (thin section), grain size generally ranges from silt to sand and grains have floating and point type contacts. Sample KP 15 has approximately 40% quartz, 30% feldspar, and 5% muscovite, zoisite, garnet, opaque minerals, and minor carbonate cement.

Sample KP 13 (thin section) has floating and point type grain or clast contacts and silt- to sand-sized grains. There does not appear to be carbonate cement in KP 13 and it contains 30% quartz, 20% feldspar, 15% of KP 13 is muscovite, garnet, orthopyroxene, and titanite, 5% opaque minerals, and 5% silica cement.

Sample KP 14 (core sample) ranges in grain size from silt to pebble and does not contain carbonate cement.

In KP 37 (thin section), there is 35% quartz, 30% feldspar, approximately 7% consists of muscovite, zircon, garnet, and titanite, 4% silica cement, and 3% opaque minerals. Sample KP 37 has floating, point, and line grain contacts and silt- to sand-sized grains.

Sample KP 36 contains several broken quartz and feldspar grains. Sample KP 15 is similar to KP 36, but has more pulverized quartz and feldspar grains (resembling a jigsaw puzzle; Fig. 17f). Sample KP 13 has zones of mica-rich matrix, some zones are rich in silica, and many muscovite grains are bent around non-mica grains.

Impact-related features

Samples KP 36 and KP 15 contain approximately 50 quartz grains with LITs, very rare PFs, and a noticeable amount of broken quartz and feldspar grains (although KP 15 has more broken material, Fig. 17f). Sample KP 13 is quite different in that it contains only slightly bent muscovite, no observed PFs, and only occasional LITs. In KP 37, there are approximately 70 quartz grains with LITs, two grains with PFs, and several bent muscovite grains.

Discussion

Sample KP 15 could have been very near to/along a fault and KP 36 somewhat near to a fault due to the presence of such prevalent fractured grains. The drastic difference in the shattered grains observed within samples 15 and 36 suggests a source of brittle deformation that was nearby to their final site of deposition. These samples are likely close to the base of the resurge deposit and constituent grains could have been fractured during this mass movement process.

Assemblage 5: Middle zone

Clast-supported sedimentary breccias and blocks dominate the middle zone of Assemblage 5 (866.7-618.2 m or 2843.5-2028.22 ft). Seven samples are described below (Fig. 18).

The pre-impact classification of rocks in Assemblage 5, middle zone, includes clastic sediments (quartz arenite, mudstone) that came from Lower Cretaceous non-marine deposits, with minor components of thin, Upper Cretaceous and Lower Paleogene marine deposits. The post-impact classification includes clastic sediments (quartz arenite, mudstone), which represent Lower Cretaceous sedimentary blocks that were transported by the impact and re-deposited. The sample set from this middle zone mainly consists of impactoclastic megablocks and associated sandy sediments.

Sample number: KP 16	Depth: 2843.50-2843.60 ft	(866.70-866.73 m)
Sample number: KP 38	Depth: 2838.65-2838.75 ft	(865.22-865.25 m)
Sample number: KP 19	Depth: 2835.95-2836.05 ft	(864.40-864.43 m)
Sample number: KP 20	Depth: 2829.40-2829.50 ft	(862.37-862.40 m)
Sample number: KP 21	Depth: 2787.80-2787.90 ft	(849.72-849.75 m)
Sample number: KP 22	Depth: 2650.15-2650.25 ft	(807.77-807.80 m)
Sample number: KP 23	Depth: 2183.70-2183.80 ft	(665.59-665.62 m)

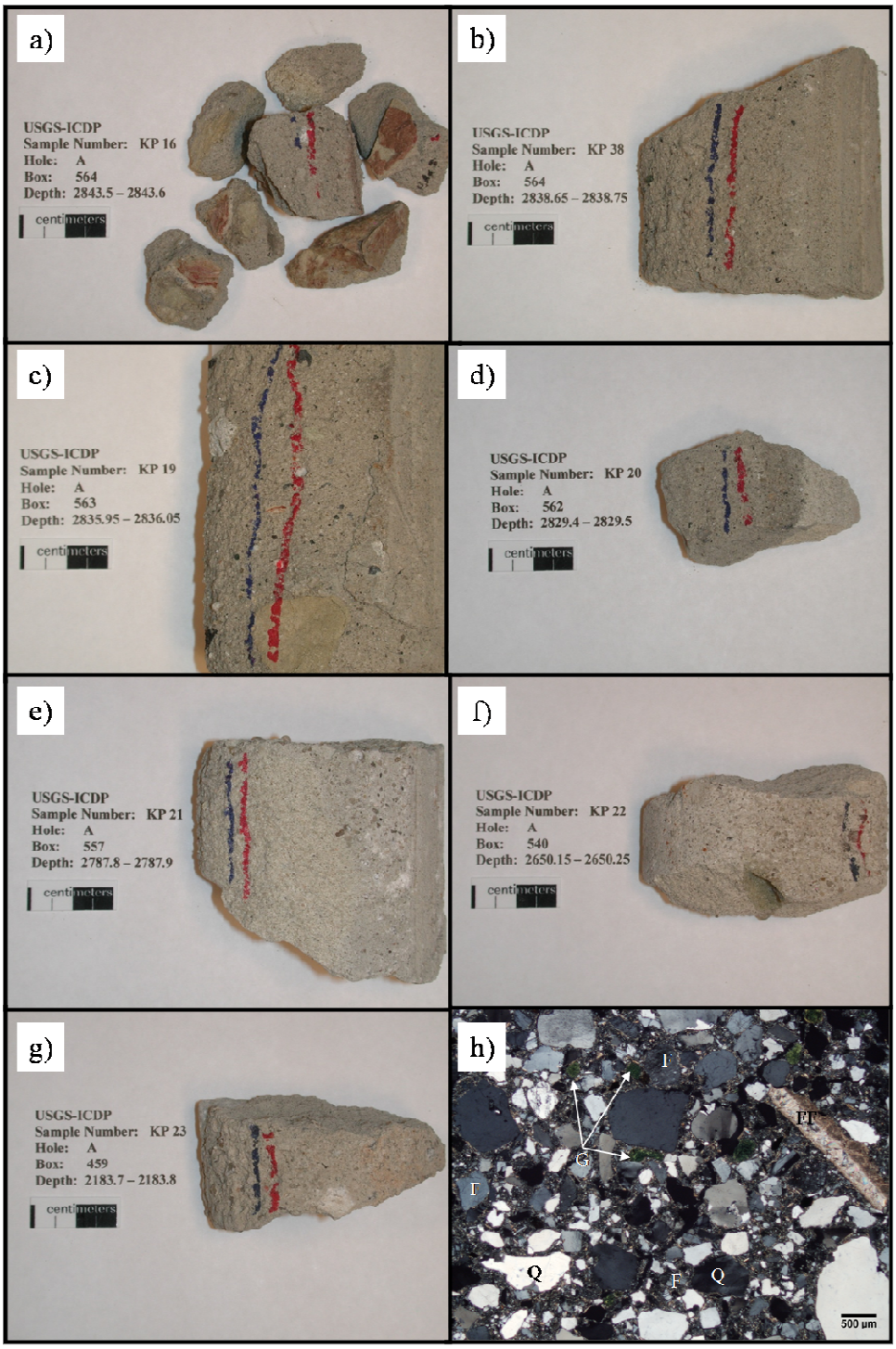

Fig. 18. Oriented core samples a) KP 16, b) KP 38, c) KP 19, d) KP 20, e) KP 21, f) KP 22, g) KP 23, and h) Photomicrograph of KP 16 (PPL); Q=quartz, F=feldspar, G=glauconite, FF=fossil fragment.

Modal Analysis

Samples KP 16, KP 38, KP 19, KP 20, KP 21, KP 22, and KP 23 (hand samples) are beige, clast-supported, slightly to moderately friable, clay- to pebble-sized, impactoclastic, sandy breccias with very angular to sub-rounded to rounded grain shapes (Fig. 18a-g). The minor value of cement (2-5%) present in these samples consists of carbonate for the deeper four samples (KP 16, KP 38, KP 19, and KP 20) and silica for KP 21, KP 22, and KP 23.

The thin section of KP 16 contains 30% each of quartz and feldspar, 20% clastic matrix, 8% glauconite, fossil fragments, and opaque minerals, 5% lithic fragments (quartzite and schist), and 5% muscovite, garnet, zoisite, tourmaline, and zircon (Fig. 18h). Sample KP 16 has floating point and line grain contacts. KP 16 a mottled, gray and beige appearance and also contains clasts of rust-colored soft, clayey material (Fig. 18a).

Sample KP 38 (thin section) has 33% quartz, 28% feldspar, 18% clastic matrix, 10% muscovite, zoisite, 8% glauconite, fossil fragments, and opaque minerals, and 2% lithic fragments (opaque fragment, quartzite, and schist). Sample KP 38 has a mottled, gray and beige appearance and floating point and line grain contacts.

Sample 19 (hand sample) is a beige, impactoclastic sandy breccia (Fig. 18c).

The thin section of KP 20 contains 33% quartz, 27% feldspar, 20% clastic matrix, 10% muscovite, garnet, zoisite, titanite, and garnet, 5% glauconite, fossil fragments, and opaque minerals, and 3% lithic fragments (opaque fragments and mudstone). Sample KP 20 has floating point, line, and concavo-convex grain contacts. KP 20 a mottled, gray and beige appearance (Fig. 18d).

Sample KP 21 (thin section) has 40% quartz, 35% feldspar, 10% clastic matrix, 5% muscovite, olivine, zoisite, garnet, and tourmaline, 3% opaque minerals, and 2% lithic fragments (quartzite). Sample KP 21 has floating and point grain contacts (Fig. 18e).

The thin section of KP 22 is extremely similar to KP 21. The main differences are that KP 22 has 45% quartz, 30% feldspar, 10% muscovite and garnet, and 8% clastic matrix. Sample KP 22 has floating, point, and line grain contacts (Fig. 18f).

Sample KP 23 (thin section) has approximately 35% quartz, 28% feldspar, 20% clastic matrix, 5% muscovite, garnet, and zoisite, 5% glauconite, fossil fragments, and opaque minerals, and 5% lithic fragments (schist, quartzite). Sample KP 23 has floating and point grain contacts (Fig, 18g).

Impact-related features

Features that may be related to the impact are not notably dramatic in this zone. Sample KP 16 contains 27 quartz grains with LITs and two with PFs. Sample KP 38 has

50 quartz grains with LITs, two grains with PFs, two toasted quartz grains, and a nearly opaque, amoeboid-shaped clast with subtle internal layering. Two small (<2 mm wide) opaque to isotropic bodies with undulating boundaries, 36 LITs in quartz, and two grains with PFs were observed in KP 20. At least three bent muscovite grains, 42 LITs in quartz, and three PFs in quartz are in sample KP 21, as well as one grain containing decorated PDFs. Sample KP 22 contains approximately three slightly toasted quartz grains, 64 grains with LITs, two with PFs, and one with PDFs. Sample KP 23 contains one zone of isotropic to opaque material, at least one toasted quartz grain, one fine-grained kink banded muscovite grain, 30 quartz grains with LITs, and three grains with PFs.

Discussion

The seven samples do not show evidence of having experienced extreme levels of shock, but such porous material can be an indistinct gauge of shock pressures (Grieve and Therriault 1995). Quantitative compositional analysis of the opaque to isotropic clasts in KP 38, KP 20, and KP 23 would have to be completed to determine if the clasts are melt-derived.

Assemblage 5: Upper zone

Assemblage 5 has an upper zone of matrix-supported, friable sedimentary-clast breccias from 618.2-443.9 m or 2028.22-1456.36 ft (Fig. 19). Subsection 1 contains KP 24 and KP 25 as they are both breccias with between 5 and 7% volume glauconite and <10% volume of rock fragments. Subsection 2 includes KP 26 and KP 27, which are described together because they are the shallowest examples of breccia that contain approximately 40% volume of rock fragments and are, at least in part, carbonate-cemented. Four samples are grouped in Subsection 3 due to their approximate 5 to 10% volume glauconite content and their locations in the extreme upper zone of the sedimentary breccia.

Subsection 1

The pre-impact classification of rocks in Assemblage 5, subsection 1, includes clastic sediments (quartz arenite and mudstone) that came from Lower Cretaceous non-marine deposits thin, Upper Cretaceous and Lower Paleogene marine deposits. The post-impact classification is a matrix-supported, slightly glauconitic, impactoclastic breccia, which formed as marine and non-marine sediments were mixed by impact modification processes.

Sample number: KP 24	Depth: 1982.50-1982.65 ft	(604.27-604.31 m)
Sample number: KP 25	Depth: 1965.40-1965.50 ft	(599.05-599.08 m)

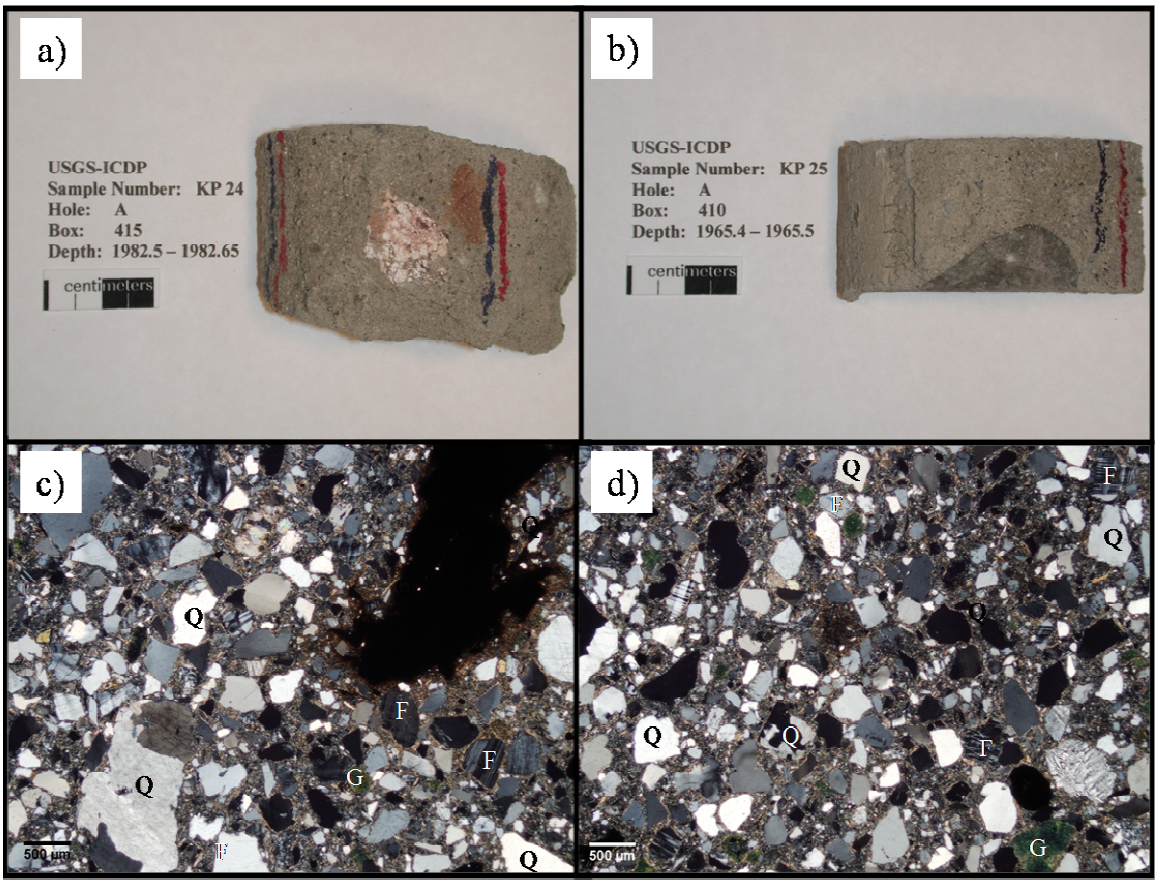

Fig. 19. Oriented core samples a) KP 24 and b) KP 25, and oriented representative photomicrographs c) KP 24 (XPL) and d) KP 25 (XPL); Q=quartz, F=feldspar.

Modal Analysis

Thin section analysis indicates that show the grain size of KP 24 and KP 25 is clay to pebble for these tan, matrix-supported, impactoclastic breccias (Fig. 19a and b). Approximately 50% of each sample contains equal amounts of quartz and feldspar, the clayey to silty matrix is 20% of the sample volume, 10% is glauconite, opaque minerals, and calcite, and 7-8% of each sample consists of lithic fragments. Grains are very angular to rounded, and types of grain contacts in these samples include floating, point, and line. Sample KP 24 consists of both metamorphic and sedimentary rock fragments, whereas KP 25 contains only sedimentary fragments. Approximately 10% of KP 24 is

muscovite, tourmaline, zircon, garnet, zoisite, olivine, and titanite, and only 5% of KP 25 contains muscovite and titanite. Fossils are very rare in each sample.

Impact-related features

Each sample contains sparse bent muscovite grains, from 3-4 quartz grains containing PFs, and between 30 to 40 quartz grains with LITs. Bent mica grains are may not be associated with the impact event. Opaque to partially isotropic bodies with undulatory boundaries are in both KP 24 and KP 25 (like in right half of Fig. 19c).

Discussion

Some of the opaque to partially isotropic zones in each sample appear 'banded', and they also commonly have a reddish rim around the clast boundaries. It is possible that these bodies are not melt particles, but they could be pyrite accumulations, pyrite-rich mudstone, and the 'banded' or layered clasts could reflect relict bedding. The reddish rims are likely oxidized areas around the clasts. Unconsolidated material could have been launched from the target and contorted to then settle at the core location.

Subsection 2

The pre-impact classification of rocks in Assemblage 5, subsection 2, includes clastic sediments (quartz arenite and mudstone) that came from Lower Cretaceous non-marine deposits thin, Upper Cretaceous and Lower Paleogene marine deposits. The post-impact classification is a matrix- to clast-supported, slightly glauconitic, rock fragment-rich, clay- to pebble-sized impactoclastic breccia, which formed as marine and non-marine sediments were mixed by impact modification processes (Fig. 20).

Sample number: KP 26 Depth: 1718.60-1718.70 ft (523.83-523.86 m)

Sample number: KP 27 Depth: 1503.20-1503.30 ft (457.77-457.80 m)

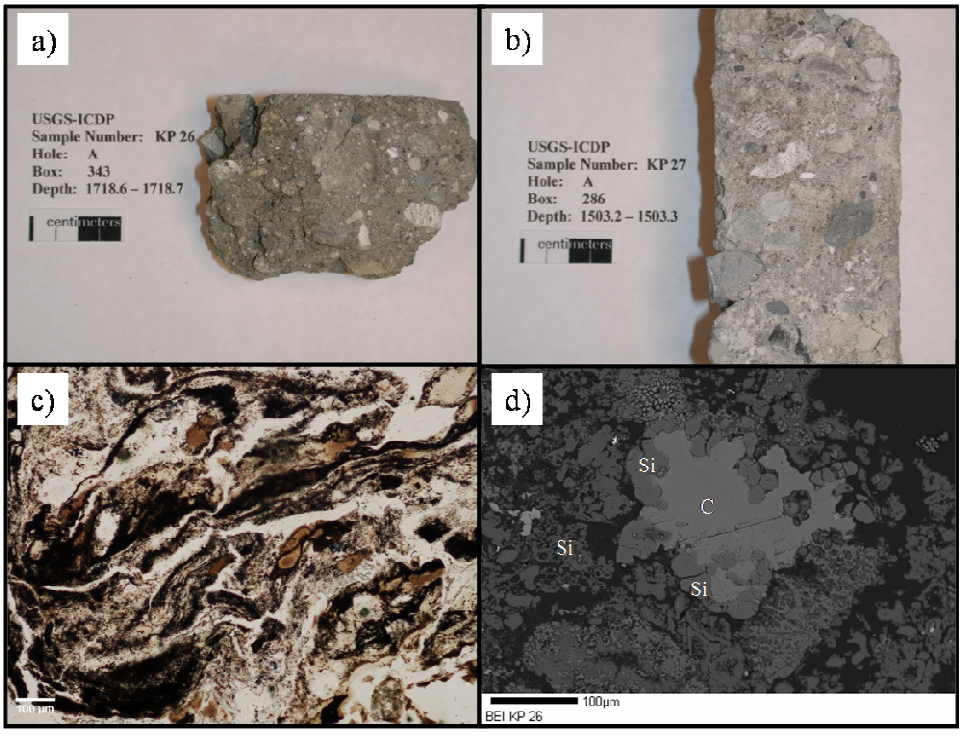

Fig. 20. Oriented core samples a) KP 26 and b) KP 27, c) Photomicrograph of KP 26 (arrows point to schlieren in melt clast; PPL), and d) Electron backscatter image of KP 26 (showing immiscibility texture between silica and calcite); Si=silica, C=calcite.

Modal Analysis

Samples KP 26 and KP 27 (thin sections) are both light gray, matrix- to clast-supported, friable, clay- to pebble-sized, impactoclastic breccias with weak carbonate cement, 17% quartz, and 20% clayey to silty matrix (Fig. 20a and b). Both samples also have grain shapes that are very angular to rounded with grain contact types including floating, point, and line. Of the two samples, only one fossil fragment was detected in KP 26. The dominant trait for each sample is the high percentage (approximately 40%) of metamorphic and sedimentary rock fragments. Sample KP 26 has 8% feldspars, 8% opaque minerals, glauconite, and fossils, 5% muscovite, olivine, zircon, epidote, and biotite, and 2% carbonate cement. An estimated 14% of KP 27 consists of feldspars, 5% opaque minerals and glauconite, 1% apatite, muscovite, zircon, and olivine, and 3% silica and carbonate cement.

Impact-related features

Samples KP 26 and KP 27 contain bent muscovite grains as well as microtwinned calcite. Both samples contain approximately 30 quartz grains with LITs and three to six quartz grains with PFs. There is a dramatic example of kink bands in muscovite in KP 26 as well as at least two zones of isotropic material with flow-banding (plucked areas look like they may have also contained similar material; Fig 20c). Sample KP 27 has zones of matrix consisting of silica and carbonate that appear ‘swirled’.

Discussion

Both samples are notable in that they contain a large percentage of rock fragments and sample KP 26 is the shallowest sample containing altered melt particles. Sparry calcite is present in an altered melt zone in KP 26 that displays an immiscibility texture with silica that could imply it recrystallized with the silica from melt (i.e., both minerals were molten at the same time; Fig 20d).

Subsection 3

The pre-impact classification of rocks in Assemblage 5, subsection 2, includes clastic sediments (quartz arenite, mudstone, and siltstone) that came from Lower Cretaceous non-marine deposits and thin, Upper Cretaceous and Lower Paleogene marine deposits. The post-impact classification is a matrix-supported, glauconitic, clay- to pebble-sized impactoclastic breccia, which formed as marine and non-marine sediments were mixed by impact modification processes (Fig. 21).

Sample number: KP 28	Depth: 1461.00-1461.10 ft	(445.31-445.37 m)
Sample number: KP 29	Depth: 1459.20-1459.30 ft	(444.76-444.79 m)
Sample number: KP 18	Depth: 1459.20-1459.30 ft	(444.76-444.79 m)
Sample number: KP 17	Depth: 1457.95-1458.05 ft	(444.38-444.41 m)

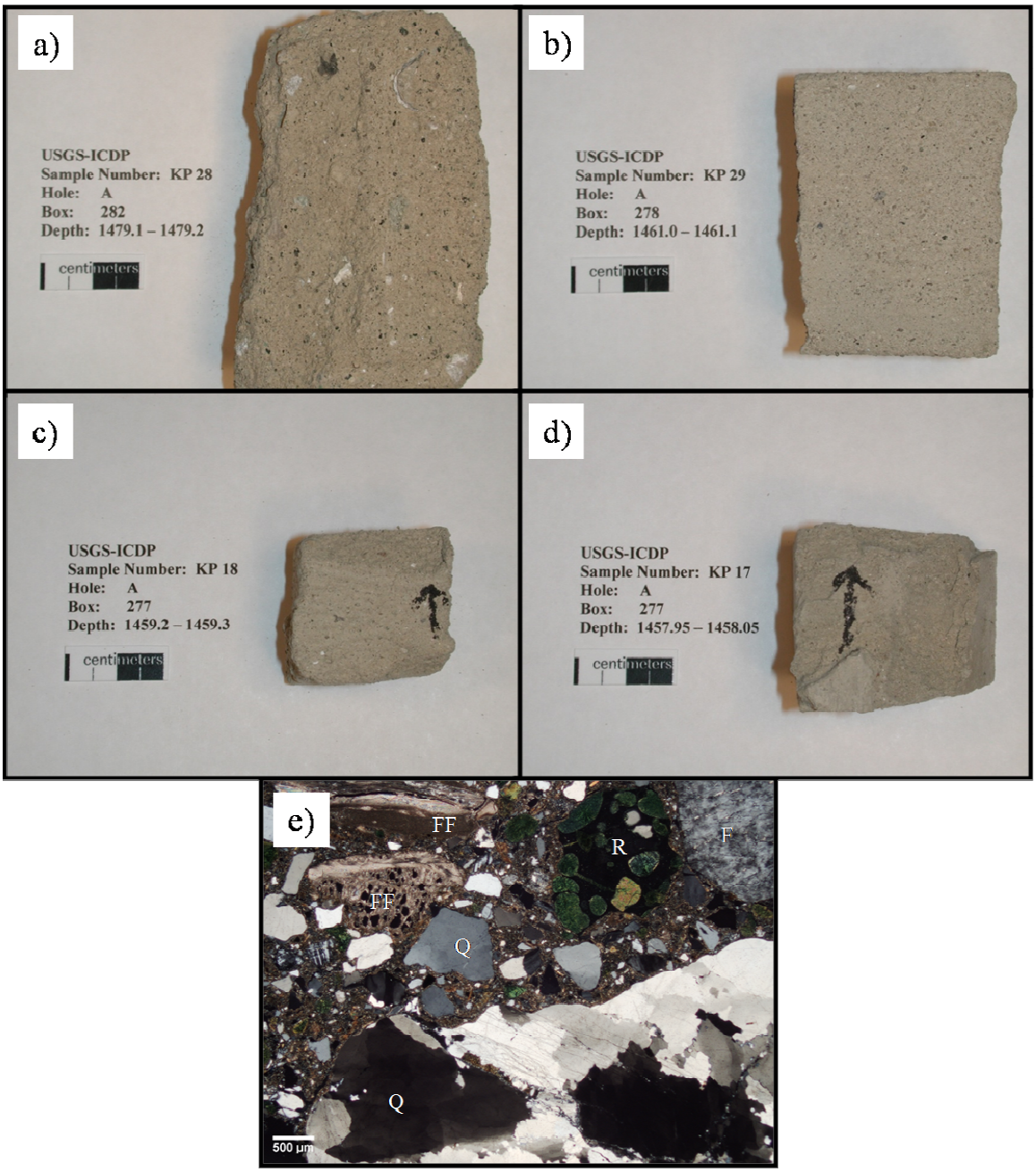

Fig. 21. Core samples a) KP 28, b) KP 29, c) KP 18 (oriented), d) KP 17 (oriented), and e) Photomicrograph of KP 28 (oriented; XPL); Q=quartz, F=feldspar, FF=fossil fragment, R=rip-up clast.

Modal Analysis

Grain size ranges from clay to pebble in greenish gray to beige-gray impactoclastic breccias KP 28, KP29, KP18, and KP 17 (thin sections) and the matrix is approximately 20% volume of the samples (Fig. 21a-d). Grain contacts are generally floating or point, rarely line. Constituent grains are matrix-supported and include rock fragments (schist, mudstone, siltstone, and rip-up clasts), glauconite, fossils, opaque minerals, muscovite, and anhedral quartz and feldspar. Fossils were not detected in KP 17. Samples are friable with a relatively weakly cemented, clayey matrix. Sample KP 28 is 19% quartz, 18% feldspar, 18% lithic fragments, 17% glauconite, opaque minerals, and fossils, 5% muscovite and zircon, and 3% is silica cement (Fig. 21a and e). Approximately 30% of KP 29 is quartz, 20% is feldspar, 15% contains lithic fragments, 10% is glauconite, opaque minerals, and fossils, 3% is silica cement, and 2% is muscovite (Fig. 21b). Sample KP 18 is 27% quartz, 21% feldspar, 15% glauconite, opaque minerals, and fossils, 10% lithic fragments, 2% silica cement, and 5% is muscovite and zircon (Fig. 21c). Sample KP 17 consists of 32% quartz, 22% feldspar, 15% glauconite and opaque minerals, 5% muscovite and zircon, 2% silica cement, and 1% lithic fragments (Fig. 21d).

Impact-related features

Sample KP 28 has 61 quartz grains with LITs, seven grains with PFs (in one grain they are very well-defined), and one toasted quartz grain. KP 29 contains an estimated 35 quartz grains with LITs, five grains with PFs, and two toasted quartz grains. Sample KP 18 has as many as 24 quartz grains with LITs, eight grains with PFs, and one quartz

grain with PDFs. Sample KP 17 contains slightly bent muscovite grains and approximately 10 quartz grains with LITs.

Discussion

The very poor sorting and presence of rip-up clasts are suggestive of a high-energy event. This glauconitic, sandy breccia is interpreted to represent material that was washed back into the crater (Poag et al. 2004; Glidewell et al. 2007; Glidewell et al. 2008). This material was disturbed, then moved to the core location, where only subtle shock features remain. Rare PDFs, PFs, and toasted quartz support that LITs in several grains may be annealed remnants of PDFs.

Post-Impact Section (near the base of Chicahominy Formation)

Sample KP30 signifies the resumed deposition following the impact event and it is entirely a post-impact deposit. This sample is a laminated, fossiliferous micrite/mudstone (Fig. 22).

Sample number: KP 30 Depth: 1456.13-1456.23 ft (443.83-443.87 m)

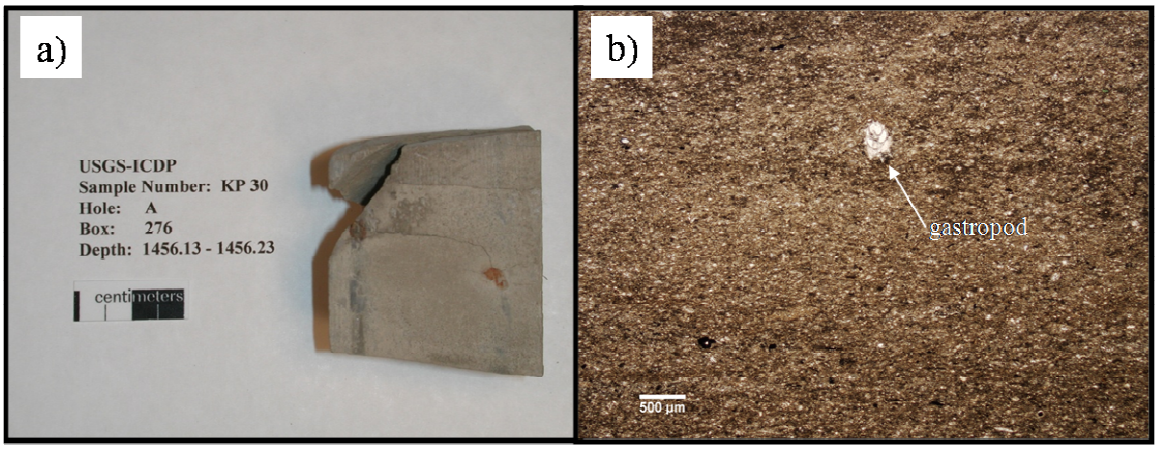

Fig. 22. Sample KP 30. a) Core sample (oriented) and b) Photomicrograph (oriented; PPL).

Modal Analysis

Sample KP 30 (thin section) is beige to tan, laminated, fossiliferous micrite and is the only sample above the impactite section considered in this study. This sample consists of 50% volume carbonate and clay/silt matrix with a grain size range from clay to medium sand (Fig. 22a and b). Fine-grained quartz, skeletal grains, and pyrite (individual grains and framboidal; C. E. Savrda, personal communication, 2007) are disseminated throughout the matrix and have floating grain contacts. Subtle laminations

are defined by elongate micritic bodies and pyrite accumulations (Fig. 22b). At the base of the oriented thin section, a pyrite body has a chaotic to dendritic pattern of upward progression in the sediment. On the macro-scale, the sample is beige to tan, but in thin section (PPL and XPL) the sample is lighter in the upper portion and grades down into darker material in the lower portion.

Impact-related features

Sample KP 30 is a post-impact sample and thus lacks impact effects.

Discussion

Laminated, fine-grained sediment signifies the post-impact return to a quiescent depositional environment. Brown color that gets darker 'down' the thin section likely indicates an increase in organic matter or disseminated pyrite. The branching pyrite body may be a biogenic structure that has been oriented more laterally from compaction.

VERTICAL DISTRIBUTION AND VARIATION OF SHOCK FEATURES

This section presents a review of the distribution of shock features throughout the span of the composite Eyreville core, as indicated by the fifty-two samples examined in this study. Several of these shock features are plotted on the Eyreville core log in Appendix C. Shock effects relevant to this research were introduced in Tables 1 and 2 and were quantified briefly in the sample descriptions above.

Residual shock effects found in rocks of the CBIS include microtwins, kink bands, linear inclusion trails (LITs), microfractures and microfaults, toasted quartz, planar fractures (PFs), planar deformation features (PDFs), ladder texture, mosaicism, and quenched silica glass or lechatelierite (Tables 1 and 2). In considering the wide range of shock effects, it is important to note the point made by Stöffler and Langenhorst (1994) that any change of the physical or chemical properties of a rock or mineral induced by shock waves is a shock effect. Stöffler and Langenhorst (1994) also point out that even though several of these features (e.g., non-planar fractures in quartz, coesite, or lechatelierite) also occur as a result of other geological processes, their occurrence in certain textural contexts and geologic settings necessarily implies impact origin. However, in some cases, it is impossible to tell if certain deformational microstructures, such as non-planar and planar fractures or deformation twins, are pre-impact or impact-

related features; this is an important consideration in that the target basement has been thoroughly reworked by Pan-African as well as Appalachian orogenic effects. Examples of mechanical deformation in mineral grains are shown in Fig. 23 and Fig. 24.

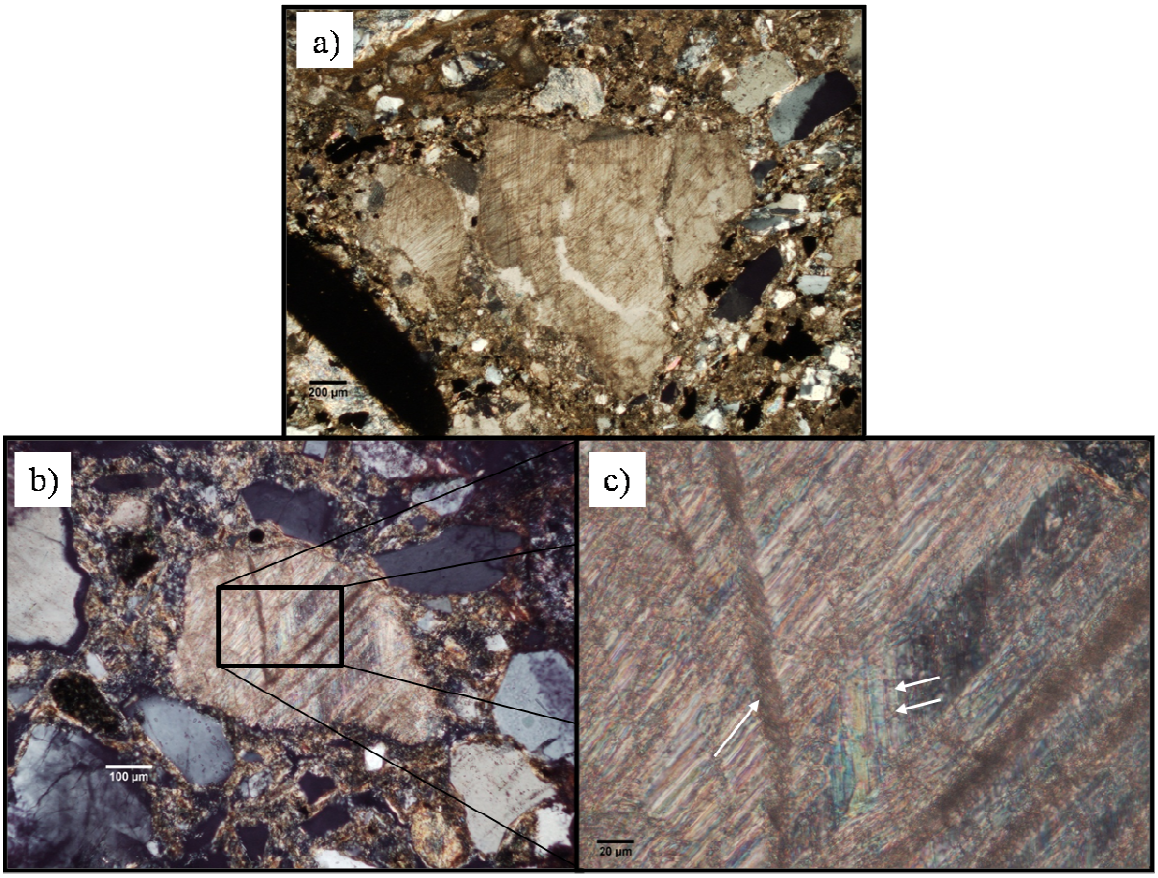

Fig. 23. Photomicrographs (XPL) of twins in calcite. a) KP 48 (5385.90-5386.00 ft or 1641.56-1641.59 m) and b), c) KP 26 (1718.60-1718.70 ft or 523.83-523.86 m).

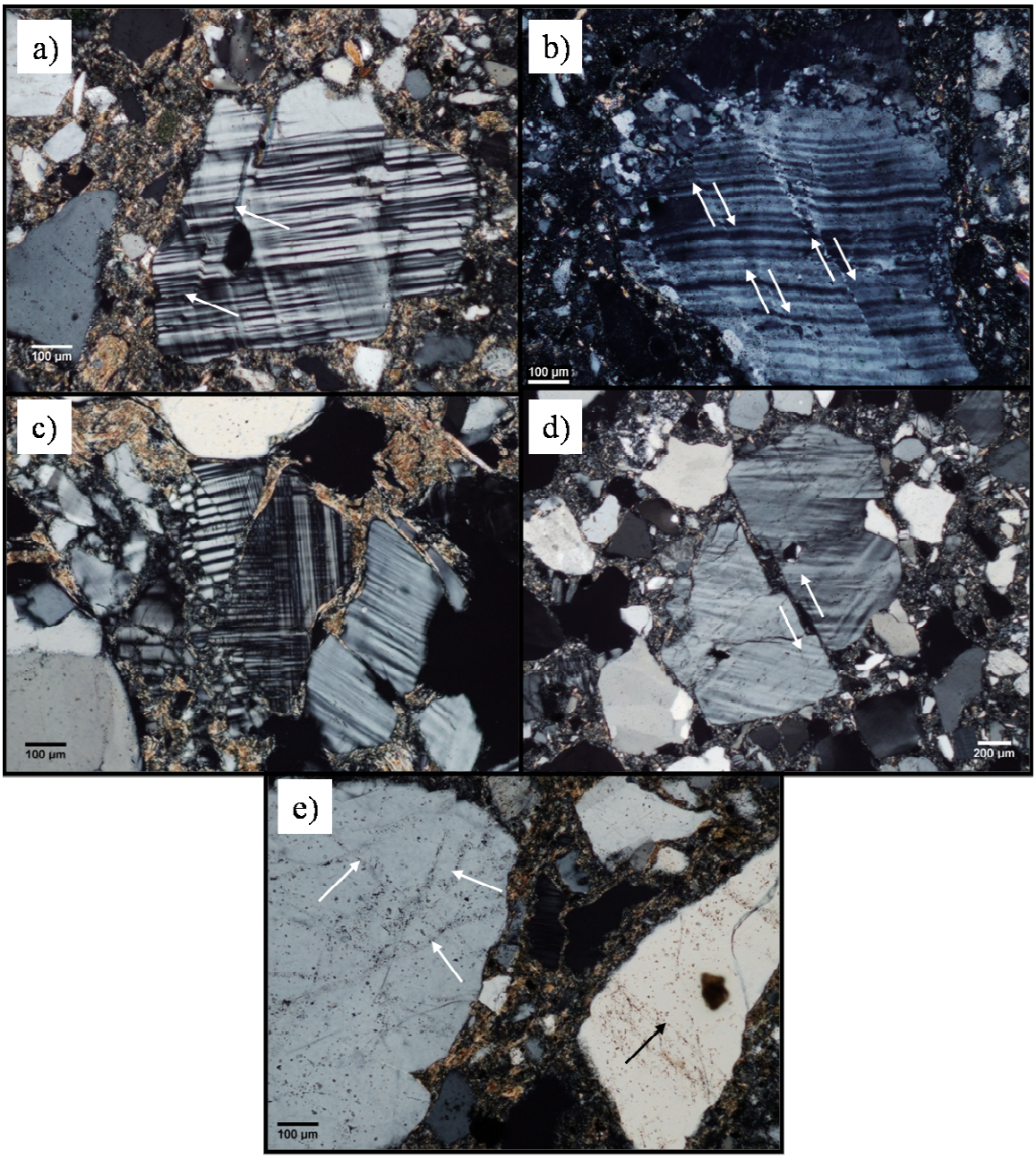

Fig. 24. Photomicrographs (XPL) of various deformation features. a) KP 29 (arrows point to kink bands in feldspar; 1459.20-1459.30 ft or 444.76-444.79 m), b) KP 7 (offset twin lamellae in feldspar; note recrystallized halo around grain; 4590.20-4590.30 ft or 399.09-1399.12 m), c) KP 15 (shattered feldspar grain; 3544.50-3544.60 ft or 1079.75-1079.78 m), d) KP 22 (faulted feldspar grain; 2650.15-2650.25 ft or 807.77-807.80 m), and e) KP 25 (arrows point to LITs in quartz; 1965.40-1965.50 ft or 599.05-599.08 m).

Microtwins, kink bands, and linear inclusion trails

Observed microstructures do not appear to have a distinct vertical trend or pattern but appear to be randomly distributed. Microtwins in calcite grains from the lower and upper portions of the core could be considered ambiguous shock indicators (Fig. 23a-c). Kink bands are common features of rocks deformed by normal tectonic processes, but they can also be caused or enhanced by shock deformation (Fig. 24a and f). Grains that are shattered and microfaulted could have been deformed by other processes as well, but their proximity to matching parts of the original grain suggests impact turbulence likely contributed to brittle failure (Fig. 24b-d). Also, linear inclusion trails (LITs) could represent annealed PDFs (Fig. 24e, Appendix C).

Toasted quartz and PFs

Toasted quartz grains also are indiscriminately scattered throughout the core section. Short and Gold (1996) first noted the distinct appearance of grainy brown to orange-brown quartz crystals from samples of the Manson impact structure, Iowa. Analyses later showed that this browning was due to sub-micron-scale fluid inclusions where rapid recrystallization obstructs significant diffusion of water and favors the formation of these inclusions (Whitehead et al. 2002). Toasted quartz typically contains PMs, so toasting is a characteristic feature of shocked rocks (Whitehead et al. 2002). The upper images of Fig. 25 (a and b) show pervasively toasted sample KP 42 and a distinctly

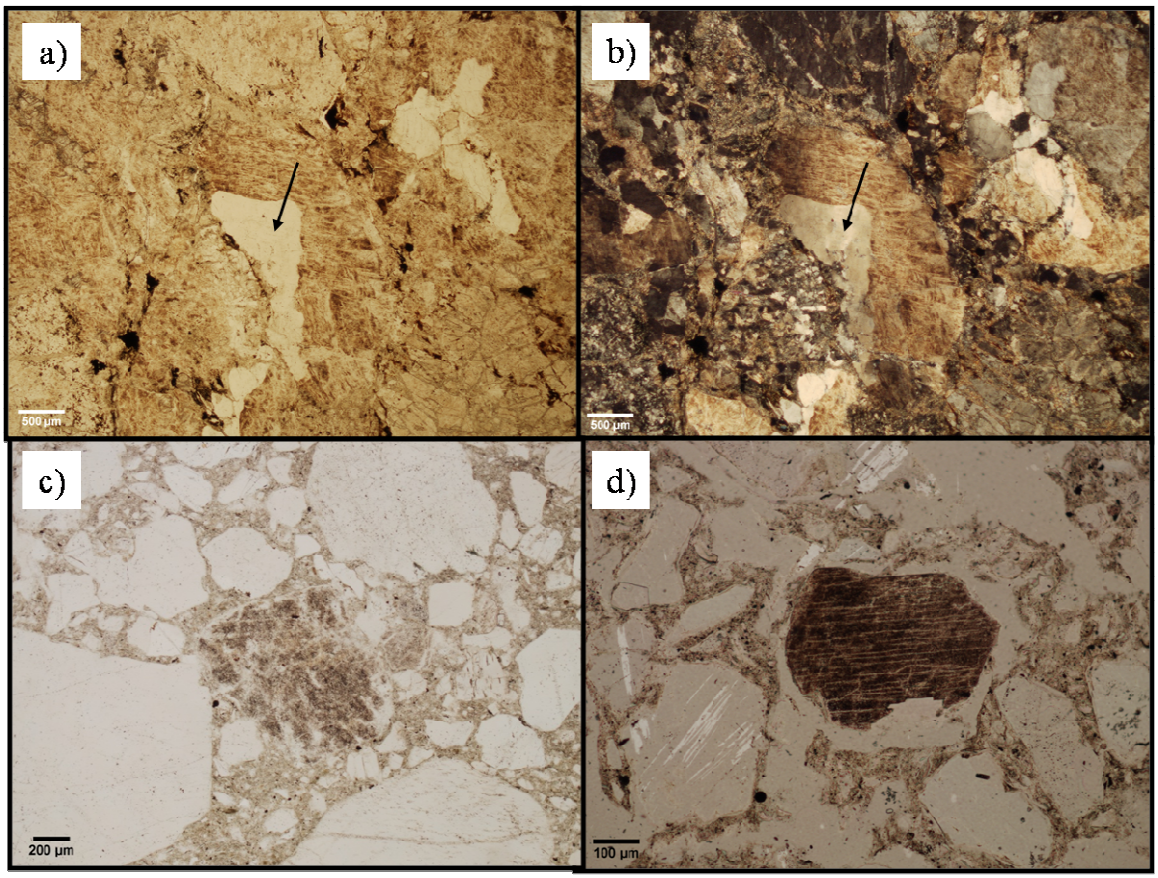

Fig. 25. Photomicrographs showing toasted quartz. a) KP 42 (4779.25-4779.40 ft or 1456.72-1456.76 m; arrow shows non-toasted sector, oriented; PPL), b) KP 42 (oriented; XPL), c) KP 22 (2650.15-2650.25 ft or 807.77-807.80 m; PPL), and d) KP 26 (1718.60-1718.70 ft or 523.83-523.86 m; PPL).

non-toasted sector in quartz just left of center. Sample KP 33 and KP 8 (lithic breccias) are shown in Fig. 25 (c and d, respectively).

Planar microstructures, ladder texture, and mosaicism

All of the shock effects listed above can be, and most are predominantly found in quartz. The total range of shock pressures by which unambiguous shock effects can be made in quartz is between five and more than 50 GPa (1 GPa = 10,000 bars; Stöffler and Langenhorst 1994). The most common method of assessing shock pressures from quartz is to measure the orientations of PFs or PDFs with respect to the grain's c-axis, which was employed in this study. Shock barometry for quartz through this technique has been developed through the work of numerous scientists, generally for crystalline rocks (e.g., Hörz 1968, Stöffler 1984). In other words, compilations of the past research associated with non-porous lithologies have resulted in the determination of specific orientations of planar microstructures (PMs) that are indicative of shock metamorphism and the orientations correlate to particular shock pressures (Table 3; French 1998). For example, certain measurements of the orientation of a planar feature to the optic axis of the grain are thought to indicate low shock pressures in crystalline rocks. Porous sediments, however, respond differently to shock waves with more heat generated as more energy is dissipated and absorbed by pore spaces and grain boundaries (French.1998). Shock temperatures in porous rocks can be an order of magnitude higher than those found in non-porous, crystalline rocks (Ahrens and Gregson 1964). Grieve et al. (1996) state that although the order of appearance of planar microstructure orientations in "nature and

Table 3. Typical crystallographic orientations of planar microstructures in shocked quartz (modified from Stöffler and Langenhorst 1994; French 1998).

Symbol	Miller Indexes	Polar Angle (angle between pole to plane and quartz c-axis)
c	* (0001)	0°
ω, ω'	* {10-13},{01-13}	23°
π, π'	* {10-12},{01-12}	32°
r, z	* {10-11},{01-11}	52°
m	{10-10}	90°
ξ	{11-22},{2-1-12}	48°
s	{11-21},{2-1-11}	66°
a	{11-20},{2-1-10}	90°
	* {22-41},{4-2-21}	77°
t	{40-41},{04-41}	79°
k	{51-60},{6-1-50}	90°
x	{51-61},{6-5-11}	82°
	{6-1-51},{15-61}	
—	{31-41},{4-3-11}	78°
	{4-1-31},{13-41}	
—	{21-31},{3-2-11}	74°
	{3-1-21},{12-31}	

*Prominent planes in characteristic shock fabrics according to experimental data and observation of various impact craters

experiment" may be comparable, there is no proof that absolute pressure estimates for natural events are equivalent. For this reason, pressure regimes that are associated with shock features are presented in a relative progression in Fig. 26.

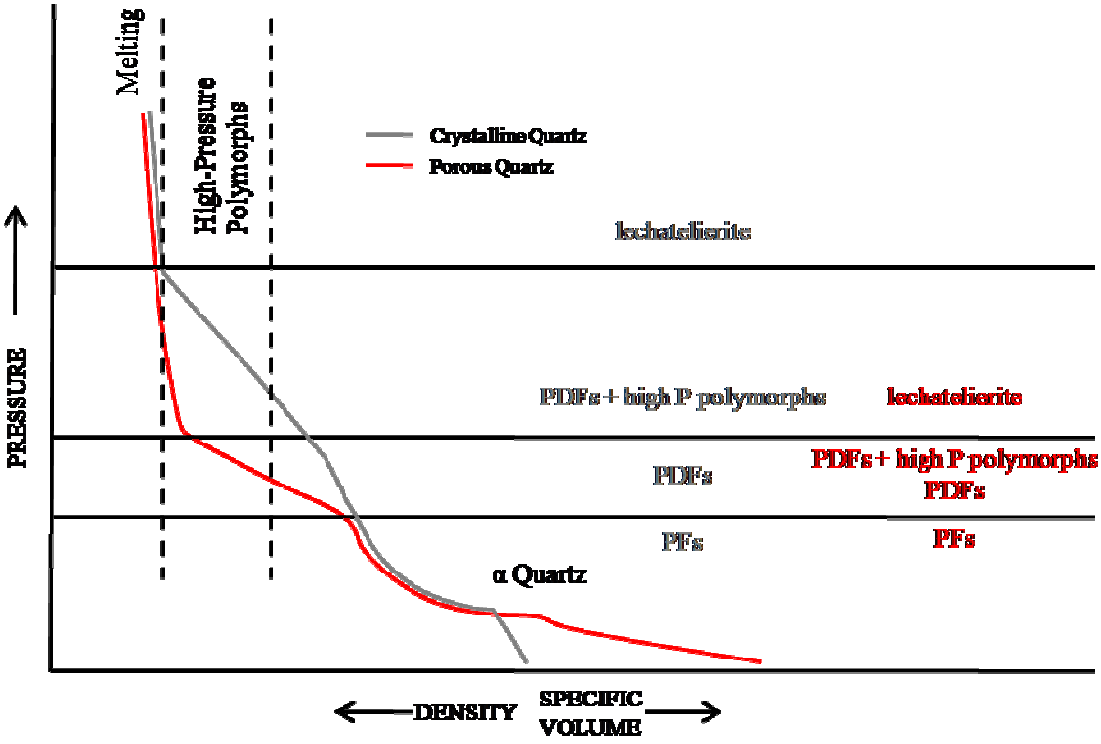

Fig. 26. Generalized pressure-density curve delineating relative pressure regimes of shock effects in crystalline and porous quartz (modified from Shipman et al. 1971 and Stöffler and Langenhorst 1994).

In order to assess variation of orientations of PMs with depth, 164 planes in 86 grains were measured. Results were matched with polar angles on Table 3, but 11.6% did not correspond and were not indexed. The plot on Fig. 27 shows variation throughout the uppermost (tan) zone that corresponds to the upper part of Assemblage 5, but in the green zone (middle and lower zones of sedimentary breccias, blocks, and boulders of Assemblage 5) ω or 23° polar angle is suppressed. There are no PDF-bearing samples

from the pink zone (granites in Assemblage 4; Fig. 27). Assemblage 3, denoted by the gray dashed line, the blue zone (Assemblage 2), and basal zone (Assemblages 1) all show similar varieties to the uppermost zone (tan; Fig. 27).

The dataset in Fig. 27 shows an agreement with the work of Grieve and Therriault (1995) and highlights a major difference of porous, sedimentary targets. The data may support the theory that strain is taken up closing voids and the pressure regime for ω was surpassed without PF or PDF formation (Grieve and Therriault 1995). It is also possible that PMs were destroyed by post-shock annealing. A plot of LITs and PDFs with depth is also shown on the core log provided in Appendix C.

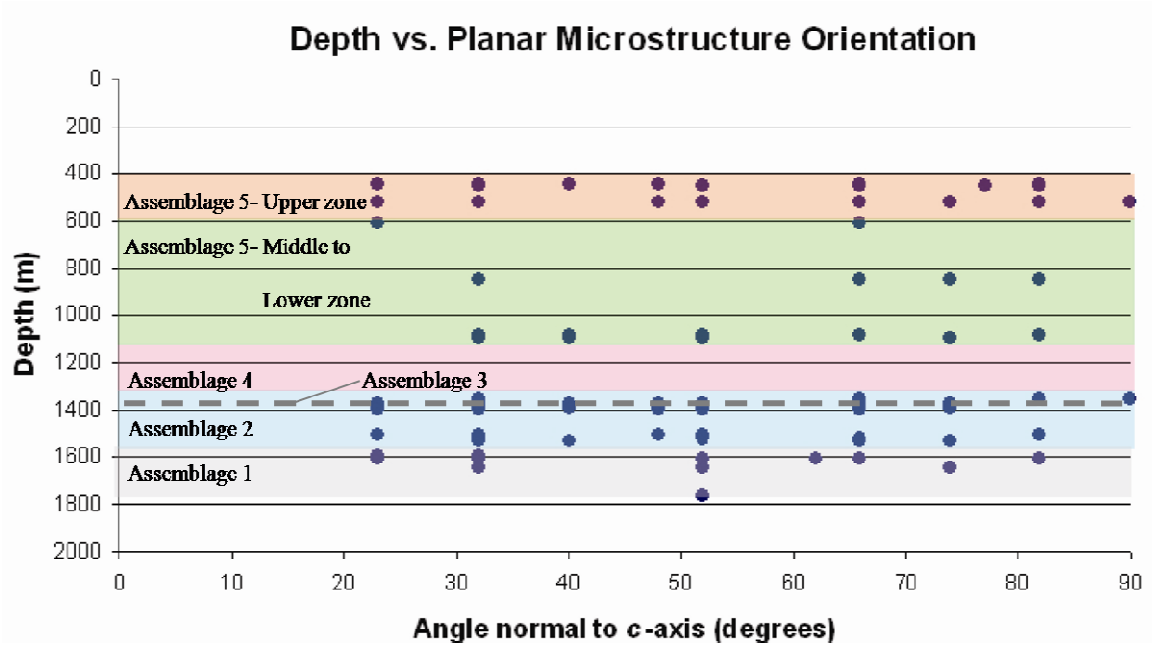

Fig. 27. Plot of depth versus quartz planar microstructure orientation in Eyreville samples.

The distribution of orientations comparable to values in Table 3 is shown in Fig. 28. Table 3 shows that polar angles greater than 32° (ω, r, z, s; Table 3) are most common among the cumulative measurements.

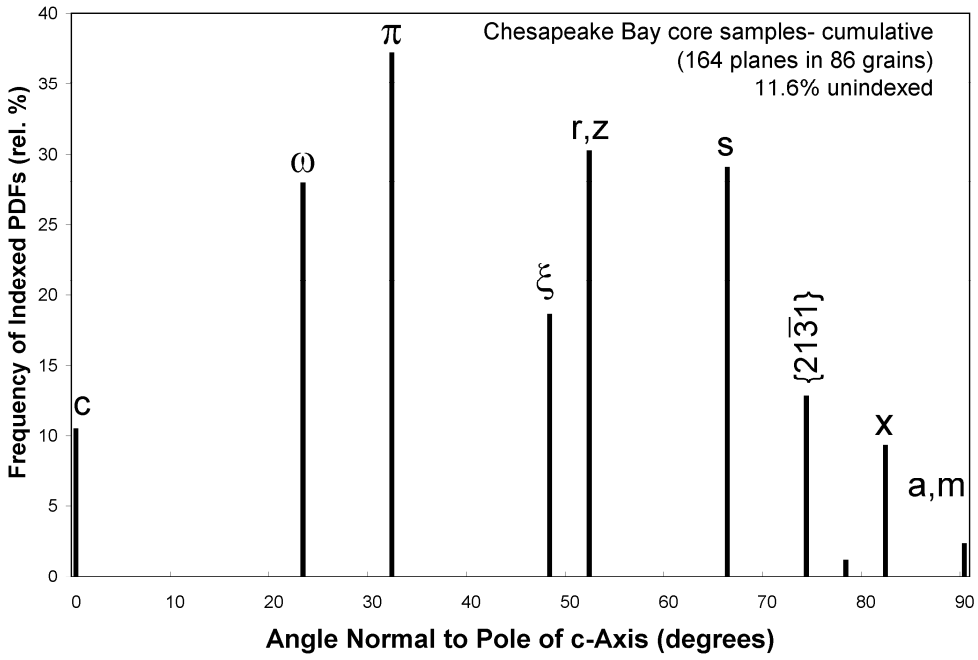

Fig. 28. Histogram showing distribution of orientations of planar microstructures in quartz for the Eyreville samples.

Examples of PMs are shown in Fig. 29. The deepest sample in this image set, KP 2, contains a biotite grain with three directions or sets of PMs (Fig. 29a). Samples KP 31 and KP 22 contain decorated PDFs (Fig. 29b-c). Sample KP 28 is just 7 m below the top of the impactite facies and contains a quartz grain with prominent PFs and associated PDFs. It is possible that this grain may have experienced shock pressures of at least 10 GPa (Koeberl et al. 1996). Ladder textures are present in feldspar and quartz in sample KP 45 from the middle section of suevites (Fig. 30a and b). The presence of PDFs in both minerals suggests the grains experienced a moderate shock regime, but the fact that the quartz grain contains 5 other sets of PDFs likely signifies higher shock pressures. Sample KP 45 contains ubiquitous PFs in quartz (Fig. 30b).

Mosaicism is a feature indicative of shock pressures slightly higher than that of PDFs (Fig. 26; Stöffler and Langenhorst 1994). This extinction pattern is distinct from typical tectonic strain-related undulatory extinction in quartz due to the smaller size of the extinguishing domains of the crystal (Stöffler and Langenhorst 1994). A grain of quartz from sample KP 4 displays mosaicism and also contains PFs throughout the grain (Fig. 31).

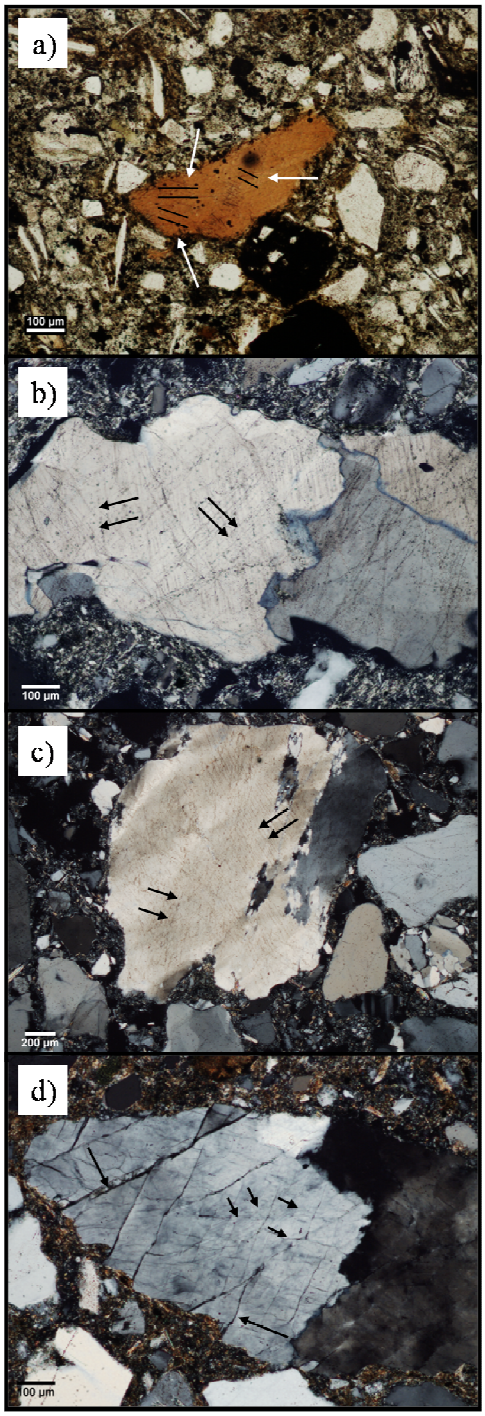

Fig. 29. Photomicrographs (XPL) showing PMs. a) KP 2 (5278.30-5278.40 ft or 1608.83-1608.86 m; arrows point to PMs in biotite, note zircon inclusion), b) KP 31 (4515.50-4515.60 ft or 1376.32-1376.35 m; arrows point to decorated PDFs in quartz; oriented), c) KP 22 (2650.15-2650.25 ft or 807.77-807.80 m; arrows point to decorated PDFs in quartz; oriented), and d) KP 28 (1461.00-1461.10 ft or 445.31-445.37 m; larger arrows indicate PFs, smaller arrows indicate PDFs in quartz.

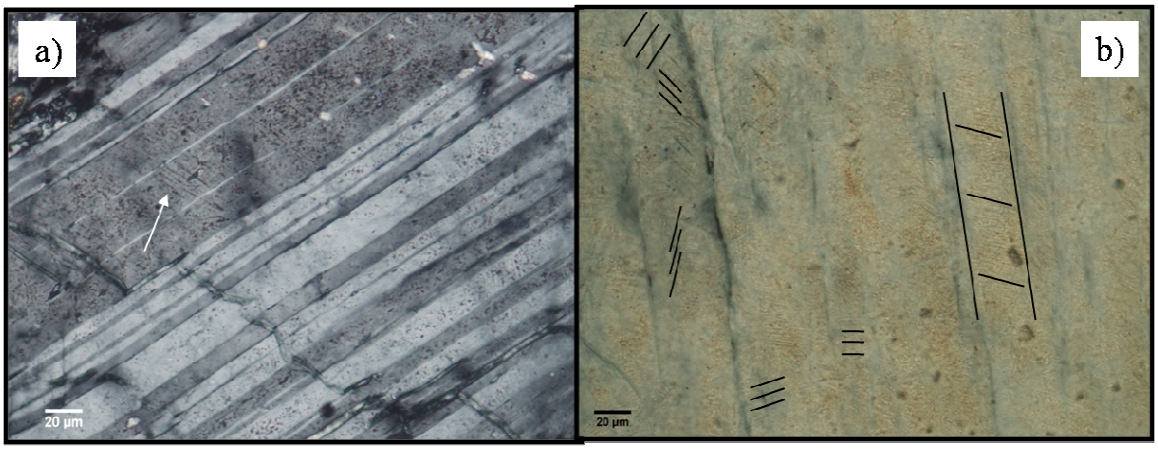

Fig. 30. Photomicrographs (XPL) showing ladder texture in feldspar and quartz in KP 45 (5013.30-5013.40 ft or 1528.05-1528.08 m). a) Arrows point to PDFs in feldspar in between twin lamellae in darker gray portion of grain and b) Ladder traced from PDFs between PFs in quartz; note 5 other sets of PDFs.

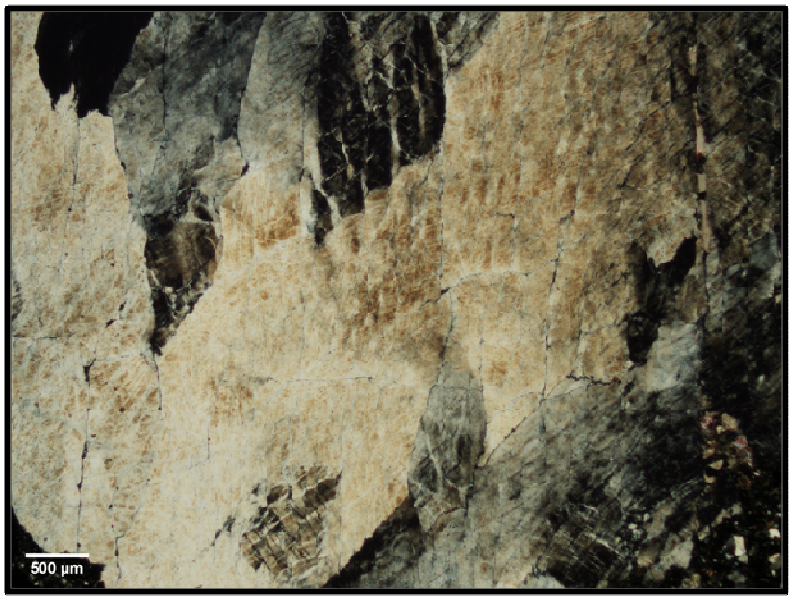

Fig. 31. Photomicrograph (XPL) of quartz in sample KP 4 (5082.05-5082.15 ft or 1549.01-1549.04 m) exhibiting mosaicism. PFs are ubiquitous in the grain.

Quenched silica glass (lechatelierite)

Temperatures above 1713° C (3115.4° F) and pressures greater than 35 GPa were reached, at least locally, in several zones of the upper suevite section (Stöffler and Langenhorst 1994). This zone contains what are interpreted to be recrystallized minerals, altered silica glass in various textures, as well as melt present as clasts and in the matrix (Appendix C). Samples that contain some altered melt particles include KP 26 from the Exmore resurge breccia in the top portion of the core, KP 8 contains a suevite fragment in the sub-granite sands of Assemblage 3, and KP 4 from the Assemblage 2that may have some altered melt in the matrix (Appendix C). In ascending order, samples KP 32, KP 39, KP 40, and KP 41 are classified as impact melt rocks. Possible recrystallized material from KP 39 is shown in Fig. 32a and b. The majority of the grain appears to have been recrystallized, but the isotropic material in the fracture shows the grain may have been partially melted and now contains some glassy material (Fig. 32a and b). This is a possibility especially because so much of the rest of the sample is melted. Several

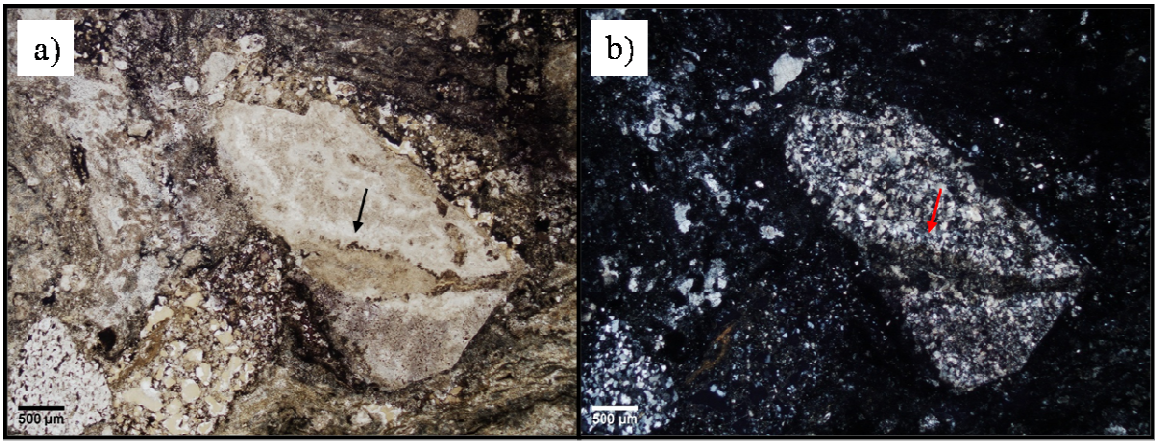

Fig. 32. Photomicrographs showing possible recrystallized and partially melted quartz grain in KP 39 (4611.90-4612.00 ft or 1405.71-1405.74 m). a) Slightly toasted, mottled quartz (PPL) and b) Arrow points to isotropic band that divides the grain (XPL).

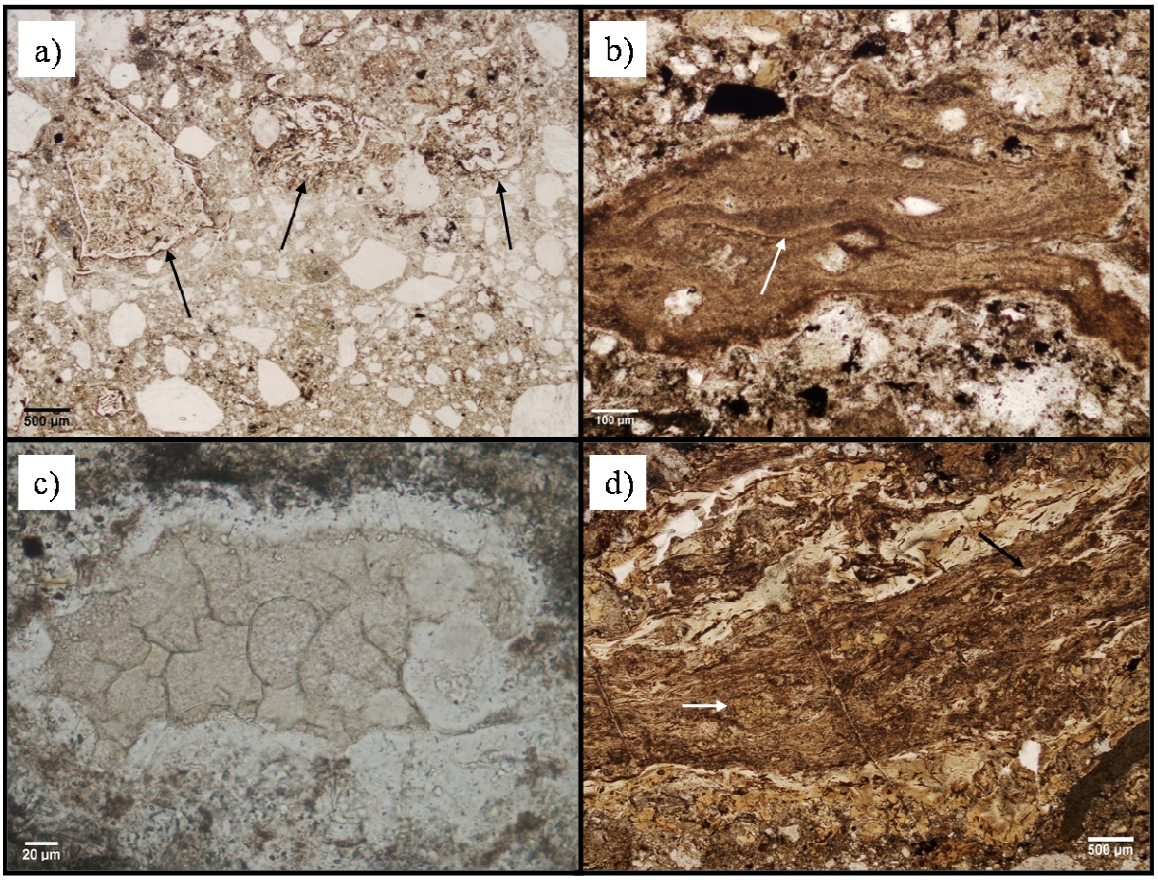

Fig. 33. Photomicrographs (PPL) of altered melt. a) KP 52 (4582.50-4582.60 ft or 1396.73-1396.76 m, arrows point to three melt clasts), b) KP 32 (4591.30-4591.45 ft or 1399.41-1399.46 m, arrow points to schlieren), c) KP 39 (4611.90-4612.00 ft or 1405.71-1405.74 m), and d) KP 40 (4632.85-4632.95 ft or 1412.03-1412.06 m; white arrow points to ballen, black arrow points to schlieren).

melt bodies are presented in Fig. 33. Small melt blebs are scattered in the matrix of KP 52 (Fig. 33a). Schlieren are prominent in samples KP 52 and KP 39 (Fig. 33b and d, respectively). Ballen texture is prevalent in sample KP 39 and is present in minor amounts in KP 40 (Fig. 33c and d, respectively).

DISCUSSION

In this discussion, the stratigraphic sections in ascending order (Assemblages 1 through 5) are assessed for evidence of shock from the impact event. However, note that Assemblage 4 is largely excluded due to lack of sample coverage. To the extent that the density of data allow, it is possible to estimate what zones of the core section were affected by impact-induced shock and to what relative extent they experienced it (i.e., Fig. 26). Shock pressure estimates are based on the work of Kieffer (1971). Peak shock pressures may have been higher locally for individual quartz grains than the final equilibration pressures due to target heterogeneities (Kieffer 1971).

Assemblage 1 contains several likely shock-related features. Quartz grains in KP 50 (5795.10-5795.25 ft or 1766.17-1766.21 m) of Assemblage 1 contain PMs (Fig. 34a) and what could be PDFs (Fig. 33a and b), albite has mechanical microtwins, and there are numerous examples of kink bands in mica (Fig. 34c). Kink-banded mica is a common metamorphic feature of unshocked rocks, but Koeberl et al. (1996) stated that they observed several intensely kink banded mica grains in moderately shocked granite from the Exmore core location within the Chesapeake Bay structure. All of these possible shock effects in such proximity to each other and their location in an impact crater lead to the parsimonious deduction that this sample experienced at least low levels

of shock (less than 8 GPa; Koeberl et al. 1996). The only other sample in Assemblage 1 that contains notable shock features is KP 49 (5464.30-5464.75 ft or 1665.43-1665.56 m; Fig. 7c). The intensely micro-faulted zones in the hand sample, which include some flow-banded areas around the micro-faults, appear to be a cataclastic rock that is partly mylonitized. Further study of the sample in thin section is a first step to determining if the elevated pressure-temperature features are from impact or other geologic processes. Samples in Assemblage 1 probably experienced shock pressures from less than 5.5 to 13 GPa (Kieffer 1971).

Assemblage 2 also contains notable shock features. Three samples from the lower and middle sections are shocked and all of the seven samples in the upper zone contain shock features. Sample KP 4 (5082.05-5082.15 ft or 1549.01-1549.04 m) includes quartz grains that are toasted, and also contains PMs. Sample KP 45 (5013.30-5013.40 ft or 1528.05-1528.08 m) has little, if any, melted material but it is essentially a highly shocked lithic breccia. Sample KP 44 (4937.00-4937.10 ft or 1504.80-1504.83 m) consists in part of interspersed altered melt particles with quartz containing common PMs. These features combined may indicate a moderate shock regime in the lower and middle sections for local zones where shocked constituent clasts or grains were affected by the shock wave. The upper section of Assemblage 2 unequivocally has the highest melt volume of all sections in the Eyreville core. Characteristic textures of altered melts and recrystallized grains are common in this zone indicating higher shock regimes. Sample number KP 52 (4582.50-4582.60 ft or 1396.73-1396.76 m) and KP 7 (4590.20-4590.30 ft or 1399.09-1399.12 m) are suevite and KP 32 (4591.30-4591.45 ft or

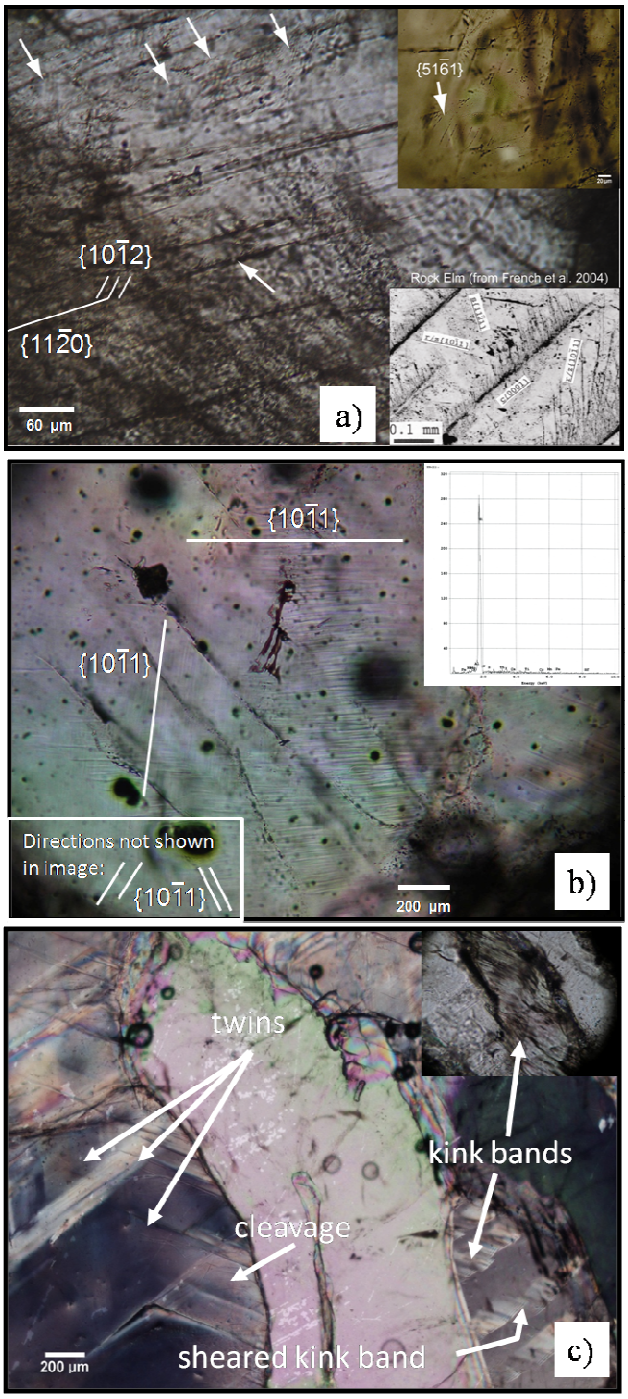

Fig. 34. Features offering possible evidence of low-level shock in KP 50. a) Upper arrows highlight PDFs jutting off of planar microstructures (lower arrow) like features noted at the Rock Elm structure (see inset; French et al. 2004); note high-angle PDF orientation illustrated in top right image, b) Sub-planar to planar lamellae in quartz grain (energy dispersive spectroscopy (EDS) spectra at top right indicate silica-rich composition), and c) Muscovite grains with prominent cleavage, twins, and kink bands. Note that thin section KP50 (images a-c) is slightly thicker than a standard thin section.

1399.41-1399.46 m), KP 39 (4611.90-4612.00 ft or 1405.71-1405.74 m), KP 40 (4632.85-4632.95 ft or 1412.03-1412.06 m), and KP 41 (4641.40-4641.50 ft or 1414.70-1414.73 m) all contain some altered melt in the matrix, so thus are considered impact melt rocks that experienced the highest temperatures and pressures. Sample KP 42 (4779.25-4779.40 ft or 1456.72-1456.76 m) is a highly shocked lithic breccia that may contain minor amounts of altered melt. Assemblage 2 likely experienced shock from 13 GPa for KP 42 and up to more than 35 GPa, in the cases of melt-dominated samples (Kieffer 1971).

In a rare discovery from a sample in Assemblage 2, spinels were found in altered melt within sample KP 41. Chemical analysis of these spinels showed anomalously high Ni and Cr levels. The ratio of Ni to Cr is similar to that of the composition of L- or LL-type chondritic meteorites. Therefore, these spinels could contain traces of an L- or LL-chondrite meteorite as deduced from the Ni-Cr ratio.

The greatest sample density is within Assemblage 3. The suevite clast in KP 8 (Subsection 1) near the base of the gravelly sand layer indicates that the suevitic component of sample KP 8 experienced high shock regimes between 13 and 30 GPa (Kieffer 1971). Quartz grains have evidence of shock deformation in Assemblage 3, Subsection 2, in samples Sample KP 33 (4559.70-4559.80 ft or 1389.80-1389.83 m), KP 9 (4508.00-4508.10 ft or 1373.97-1374.00 m), and KP 5 (4499.00-4499.10 ft or 1371.17-1371.20 m). Planar deformation features and mosaicism in these samples

present convincing evidence of low shock regimes from less than 5.5 to 13 GPa (Kieffer 1971).

In Assemblage 4, granites are altered and the effects of shock are not apparent. Sample KP 10 (4441.35-4441.45 ft or 1353.66-1353.69 m) and KP 12 (3595.50-3595.80 ft or 1095.89-1095.98 m) either never possessed such features or the traits have been erased by post-impact alteration. Shock features in Assemblage 4 may indicate the samples experienced a low shock regime of less than 5.5 GPa (Kieffer 1971).

Assemblage 5 consistently contains grains characteristic of low shock regimes (PFs and occasional PDFs) with the exception of KP 26 (1718.60-1718.70 ft or 523.83-523.86 m) in Subsection 2. Sample KP 26 contains, at these depths, the highest altered melt clast in the core section with regard to the entire sample set. The upper section (2028.22-1456.36 ft or 618.2-443.9 m) contains grains that display PDF orientation of a variety of polar angles (red zone in Fig. 27). The middle and lower zones (3594.95-2028.22 ft or 1095.74-618.2 m), however, are missing the 23° or ω orientation (green zone in Fig. 27). This is a tendency that has been noted at other sedimentary-target impact structures (Grieve and Therriault 1995). The altered melt body in KP 26 could have locally experienced shock pressures greater than 35 GPa, while PDF-bearing quartz grains in the remainder of Assemblage 5 probably experienced up to 13 GPa (Kieffer 1971).

Shock behavior in a heterogeneous impact target is not well understood. It is possible that samples containing only minor residual shock effects may have experienced moderate levels of shock, but traces of this have been erased by annealing. Scientists studying craters around the world have included this as a possibility for sedimentary or porous targets, as there is a scarcity of PDFs in quartz compared to their frequency in structures formed in crystalline targets.

CONCLUSIONS

The following are some general and specific conclusions that may be drawn from the study of samples from the Eyreville core interval through the Chesapeake Bay impact structure filling sequence.

1) The Eyreville core represents the most complete sequence of impact-structure filling materials yet reported from any marine impact structure. Even so, the core does not go deeply enough to penetrate all the impact-structure filling materials and impact affected lithologies associated with the structure.

2) Petrographic study of the 52 samples from the Eyreville core shows a range of impact-induced features, including kink-bands, mechanical microtwins, planar microstructures in quartz and feldspar (linear inclusion trails, planar fractures and planar deformation features), toasted quartz, mosaicism in quartz, recrystallized minerals, and quenched silica glass (present as altered microspherules, clasts, and matrix material). Research results regarding planar microstructures in quartz agree with previous reports of high-angle orientations being prevalent in sedimentary target lithologies. It is also possible that some planar features were simply not preserved.

3) Stratigraphic distribution of the these features indicates that direct evidence of high shock regimes are sparsely scattered throughout the upper half of the core, but shock features from the most extreme impact metamorphism are concentrated in the Upper section of Assemblage 2.

4) Petrographic analysis of Assemblage 1 documents that the basal section of the core experienced at least low levels of shock most likely less than 12 GPa.

5) Assemblage 2 contains the greatest melt volume of the section, thus it experienced high shock regimes from 13 GPa to more than 35 GPa locally. Data from an altered melt particle indicate that the impactor that created the structure may have been an L- or LL-chondrite meteorite.

6) Analysis of the samples from Assemblage 3 revealed that PDF orientations were very similar to those found in the upper zone of Assemblage 5. A suevite clast was found in a sandy breccia near the base of Assemblage 3 which was likely ripped from Assemblage 2. The shock levels were likely less than 5.5 to as much as 13 GPa. This interval has the greatest sample density.

7) Assemblage 4 has the lowest sample density. Petrographic analysis of the granite interval shows no dramatic effects or shock and one of the two samples is

extremely altered, which may obscure any impact effects. Pressures of less than 5.5 GPa may have affected these samples.

8) Petrographic investigation of the Assemblage 5 interval revealed characteristics of sediments that had experienced at least a low shock regime, that experienced pressured no greater than approximately 13 GPa. Planar deformation feature orientations with low polar angles were missing in the middle to lower zones. An altered melt clast was found in a sample from the upper zone, emphasizing the thorough mixing that occurs after impact events. Glauconite was not detectable in thin sections from samples below the middle zone.

REFERENCES

Ahrens T. J. and Gregson V. G., Jr. 1964. Shock compression of crustal rocks- Data for quartz, calcite, and plagioclase rocks. *Journal of Geophysical Research* 69:4839-4874.

Baldwin R. 1949. *The Face of the Moon*. Chicago: University of Chicago. 239 p.

Barringer D. M., Jr. 1931. The Barringer meteorite. *Science* 73:66-67.

Bradley D. C. 1982. Subsidence in late Paleozoic basins in the northern Appalachians. *Tectonics* 1:107-123.

Catchings R. D., Saulter D. E., Powars D. S., Goldman M. R., Dingler J. A., Gohn G. S., Schindler J. S., and Johnson G. H. 2001. High-resolution seismic reflection/refraction images near the outer margin of the Chesapeake Bay impact structure, York-James Peninsula, southeastern Virginia. U. S. Geological Survey Report OF 01-0407:18 p.

Cederstrom D. J. 1945. Geology and ground-water resources of the coastal plain in southeastern Virginia. *Virginia Geological Survey Bulletin* 63:384 p.

Cederstrom D. J. 1946. Genesis of ground waters in the coastal plain of Virginia. *Economic Geology and the Bulletin of the Society of Economic Geologists* 41:218-245.

Dietz R. S. 1947. Meteorite impact suggested by the orientation of shatter-cones at the Kentland, Indiana, disturbance. *Science* 105:42-43.

Dietz R. S. 1959. Shatter cones in cryptoexplosion structures (meteorite impact?). *Journal of Geology* 67:496-505.

Dietz R. S. 1960a. Meteorite impact suggested by shatter cones in rock. *Science* 131:1781-1784.

Dietz R. S. 1960b. Vredefort ring structure; an astrobleme (meteorite impact structure). *Geological Society of America Bulletin* 71:2093.

Dietz R. S. 1964. Sudbury structure as an astrobleme. *Journal of Geology* 72:412-434.

Edwards L. E. and Powars D. S. 2003. Impact damage to dinocysts from the late Eocene Chesapeake Bay event. *Palaios* 18:275-285.

Edwards L. E., Horton, Jr. J. W., and Gohn G. S. 2004. Proceedings *ICDP-USGS Workshop on Deep Drilling in the Central Crater of the Chesapeake Bay Impact Structure Virginia*, *USA*. USGS Open File Report 2004-1016:85 p.

Engelhardt W. v. and Bertsch W. 1969. Shock induced planar deformation structures in quartz from the Ries crater, Germany. *Contributions to Mineralogy and Petrology*. 20:203-234.

French B. M. 1967. Sudbury structure, Ontario; some petrographic evidence for origin by meteorite impact. *Science* 156:1094-1098.

French B. M. 1998. Traces of Catastrophe: A handbook of shock-metamorphic effects in terrestrial meteorite impact structures. Houston: Lunar and Planetary Institute 954:120 p.

French B. M., Cordua, W. S., and Plescia J. B. 2004. The Rock Elm meteorite impact structure, Wisconsin; geology and shock-metamorphic effects in quartz. *Geological Society of America Bulletin* 116:200-218.

French B. M. and Short N. M. (eds) 1968. Shock metamorphism of natural materials. Baltimore: Mono Book Corporation. 644 p.

Gates A. E., Simpson C., and Glover, III L. 1986. Appalachian carboniferous dextral strike slip faults: An example from Virginia. *Tectonics* 5:119-133.

Gates A. E., Speer J. A., and Pratt T. L. 1988. The Alleghanian southern Appalachian Piedmont: A transpressional model. *Tectonics* 7:1307-1324.

Glass B. P. 1989. North Amercian tektite debris and impact ejecta form DSDP Site 612. *Meteoritics and Planetary Science* 24:209-218.

Glidewell J., Harris R. S., King, Jr. D. T., and Petruny L.W. 2007. Observations and analysis of shock metamorphism, suevite melt bodies, microspherules, and Ni-Cr spinels in selected samples from the ICDP-USGS Chesapeake Bay impact structure Eyreville cores. *Geological Society of America Abstracts with Programs* 39(6):452.

Glidewell J., Harris R. S., King, Jr. D. T., and Petruny L.W. 2008. Stratigraphy, petrology, and shock petrography based on well logs and selected samples from the Eyreville drill core: Chesapeake Bay impact structure, Virginia (abstract #2438). 39th Lunar and Planetary Science Conference. CD-ROM.

Glover, III L. 1989. Tectonics of the Virginia Blue Ridge and Piedmont, In *Tectonics of the Virginia Blue Ridge and Piedmont: International Geological Congress 28th, Field Trip Guidebook T 363* edited by Glover, III L., Evans, N. H., Patterson J. G., and Brown W. C. Washington, D. C.: American Geophysical Union. pp. 1-29, 52-59.

Glover, III L., Sheridan R. E., Holbrook W. S., Ewing J., Talwani M., Hawman R. B., and Wang P. 1997. Paleozoic collisions, Mesozoic rifting, and structure of the Middle Atlantic states continental margin: An 'EDGE' Project report. *Geological Society of America Special Paper* 314:107-135.

Gohn G. S., Bruce T. S., Catchings R. D., Emry S. R., Johnson G. H., Levine J. S., McFarland E. R., Poag, C. W., and Powars D. S. 2001. Integrated geologic, hydrologic, and geophysical investigations of the Chesapeake Bay impact structure, Virginia, USA: a multi-agency program (abstract #1901). 32nd Lunar and Planetary Science Conference. CD-ROM.

Gohn G. S., Koeberl C., Miller K. G., Reimold W. U., Cockell C. S., Horton, Jr. J. W., Sanford W. E., and Voytek M. A. 2006. Chesapeake Bay Impact Structure Drilled. *Eos* 87:349,355.

Grieve R. A. F., Langenhorst F., and Stöffler D. 1996. Shock metamorphism in nature and experiment: II. Significance in geosciences. *Meteoritics and Planetary Science* 31:6-35.

Grieve R. A. F. and Pilkinton M. 1996. The signature of terrestrial impacts. *AGSO Journal of Australian Geology and Geophysics*. 16:399 p.

Halusa G. and NASA/GSFC/JPL MISR Science Team 2000. MISR Views Delaware Bay, Chesapeake Bay, and the Appalachian Mountains. November 2006. http://visibleearth.nasa.gov/view_rec.php?id=309.

Hibbard J. P., van Staal C. R., and Rankin D. W. 2007. A comparative analysis of pre-Silurian crustal building blocks of the northern and the southern Appalachian Orogen. *American Journal of Science* 307:23-45.

Hildebrand A. R., Penfield G. T., Kring D. A., Pilkington M., Carmargo-Zanoguera A., Jacobson S. P., and Boynton W. V. 1991. Chicxulub crater: A possible Cretaceous/Tertiary boundary impact crater on the Yucatán Peninsula Mexico. *Geology* 19:867–871.

Hobbs C. H. 2004. Geologic history of Chesapeake Bay, USA. *Quaternary Science Reviews* 23:641-661.

Horton, Jr. J. W., Powars D. S., and Gohn G. S. 2005a. Studies of the Chesapeake Bay impact structure- Introduction and discussion, In *Studies of the Chesapeake Bay impact structure-The USGS-NASA Langley corehole, Hampton, Virginia, and related coreholes and geophysical surveys*. edited by Horton, Jr,. J. W., Powars D. S., and Gohn G. S. *U.S. Geological Survey Professional Paper* 1688:A-K.

Horton, Jr. J. W., Aleinikoff J. N., Kunk M. J., Naesar C. W., and Naesar N. D. 2005b. Petrography, structure, age, and thermal history of granitic coastal plain basement in the Chesapeake Bay impact structure, USGS-NASA Langley core, Hampton, Virginia, In *Studies of the Chesapeake Bay impact structure-The USGS-NASA Langley corehole, Hampton, Virginia, and related coreholes and geophysical surveys*. edited by Horton, Jr,. J. W., Powars D. S., and Gohn G. S. *U.S. Geological Survey Professional Paper* 1688:A-K.

Horton, Jr. J. W., Gohn G. S., Gibson R. L., Reimold W. U., and Edwards L. E. 2007. Geologic column of the ICDP-USGS Eyreville-B core, Chesapeake Bay impact structure: Breccias, blocks, and crystalline rocks, 1095-1766 m depth. *Geological Society of America Abstracts with Programs* 39(6):314.

Hörz F. 1968. Statistical measurements of deformation structures and refractive indices in experimentally shock loaded quartz. In Shock metamorphism of natural materials. edited by French B. M. and Short N. M. Baltimore: Mono Book Corporation. pp. 243-253.

Hörz F. 1969. Structural and mineralogical evaluation of an experimentally produced impact crater in granite. *Contributions to Mineralogy and Petrology* 21:365-377.

Hörz F. 1970. Static and dynamic origin of kink bands in micas. *Journal of Geophysical Research* 75:965-977.

Johnson G. H., Kruse S. E., Vaughn A. W., Lucey J. K., Hobbs, III C. H., and Powars D. S. 1998. Postimpact deformation associated with the late Eocene Chesapeake Bay impact structure in southeastern Virginia. *Geology* 26:507-510.

Kieffer S. W. 1971. Shock metamorphism of the Coconino sandstone at Meteor Crater, Arizona. *Journal of Geophysical Research* 76:5449-5473.

King, Jr. D. T., Petruny L. W. 2003. Comparison of Wetumpka impact structure (Late Cretaceous, Alabama) with Chesapeake Bay crater (Eocene, Eastern U.S.), In *Deep Drilling in the Central Crater of the Chesapeake Bay Impact Structure, Virginia, USA: A Proposal to the International Continental Scientific Drilling Program*. edited by Gohn G. S. 2004:47 p.

King, Jr. D. T., Harris R. S., Petruny L.W., and Glidewell J. 2007. Chesapeake Bay and Wetumpka: Stratigraphy and processes in marine impact structures. *Geological Society of America Abstracts with Programs* 39(6):315.

Koeberl C. 1989. New estimates of area and mass for the North American tektite strewn field. Proceedings, 19th Lunar and Planetary Science Conference pp. 745-751.

Koeberl C., Poag C. W., Reimold W. U., and Brandt D. 1996. Impact origin of the Chesapeake Bay structure and the source of the North American tektites. *Science* 271:1263-1266.

Koeberl C. 1997. Impact cratering: the mineralogical and geochemical evidence. *Oklahoma Geological Survey Circular* 100:30–54.

Koeberl C. 2002. Mineralogical and geochemical aspects of impact craters. *Mineralogical Magazine* 66:745–768.

Mark K. 1987. *Meteorite craters*. Tucson: The University of Arizona Press. 288 pp.

Melosh H. J. 1989. *Impact cratering- a geologic process*. New York: Oxford University Press. 245 p.

Mixon R. B. 1985. Stratigraphic and geomorphic framework of Uppermost Cenozoic Deposits in the Southern Delmarva Peninsula, Virginia and Maryland. *U.S. Geological Survey Professional Paper* 1067-G:53 p.

Ormö J. and Lindström. M. 2000. When a cosmic impact strikes the sea bed. *Geological Magazine* 137:67-80.

Pati J. K. and Reimold W. U. 2007. Impact cratering- fundamental process in geosciences and planetary science. *Journal of Earth Systems Science* 116:81-98.

Pettijohn F. J., Potter P. E., and Siever R. 1987. *Sand and sandstone*, 2nd ed. New York: Springer-Verlag. 553 p.

Phillips W. R. 1971. *Mineral optics: Principles and techniques*. San Francisco: W. H. Freeman and Co. 172-197 p.

Poag C. W. 2002. Synimpact-postimpact transition inside Chesapeake Bay crater. *Geology* 30:995-998.

Poag C. W., Koeberl C., and Reimold W. U. 2004. *The Chesapeake Bay crater: Geology and geophysics of a Late Eocene submarine impact structure.* Berlin: Springer-Verlag. 522 p.

Poag C. W., Powars D. S., Poppe L. J., Mixon R. B., Edwards L. E., Folger D. W., and Bruce S. 1992. Deep Sea Drilling Project Site 612 bolide event: New evidence of a late Eocene impact-wave deposit and possible impact site, U.S. east coast. *Geology* 20:771-774.

Poag C. W., Powars D. S., Poppe L. J., Mixon R. B., Edwards L. E., Folger D. W., and Bruce S. 1993. Deep Sea Drilling Project Site 612 bolide event: New evidence of a late Eocene impact-wave deposit and possible impact site, U.S. east coast: Reply (modified). *Geology* 21:478-479.

Poag C. W., Watts A. B., Cousin M., Goldberg D., Hart M. B., Miller K. G., Mountain G. S., Nakamura Y., Palmer A., Schiffelbein P. A., Schreiber B. C., Tarafa M., Thein J. E., Valentine P. C., and Wilkens R. H. 1987. *Initial reports of the Deep Sea Drilling Project*. Washington, D. C.:U.S. Government Printing Office 95:1-817.

Powars D. S. 2000. The effects of the Chesapeake Bay impact crater on the geological framework and the correlation of hydrogeologic units of southeastern Virginia, south of the James River. *U.S. Geological Survey Professional Paper* 1622:53 p.

Powars D. S., and Bruce T. S. 1999. The effects of the Chesapeake Bay impact crater on the geological framework and correlation of hydrogeologic units of the lower York-James Peninsula, Virginia. *U.S. Geological Survey Professional Paper* 1612:82 p.

Powars D. S., Edwards L. E., and Gohn G. S. 2007. Geologic column of the ICDP-USGS Eyreville-A and -B cores, Chesapeake Bay impact structure: Sediment-clast breccias and sediment-blocks 1095.7-443.9 m. *Geological Society of America Abstracts with Programs* 39(6):314.

Powars D. S., Gohn G. S., Edwards L. E., Bruce T. S., Catchings R. D., Emry S. R., Johnson G. H., Levine J. S., Poag C. W., and Pierce H. A. 2001. Structure and composition of the southwestern margin of the buried Chesapeake Bay impact structure, Virginia. *Geological Society of America Abstracts with Programs* 33(6):203.

Powars D. S., Mixon R. B., and Bruce T. S. 1992. Uppermost Mesozoic and Cenozoic geologic cross section, outer Coastal Plain of Virginia. Proceedings, 1988 U.S. Geological Survey Workshop on the Geology and Geohydrology of the Atlantic Coastal Plain, edited by Gohn, G. S. *U.S. Geological Survey Circular* 1059. pp. 85-101.

Powars D. S., Mixon R. B., Edwards L. E., Andrews G. W., and Ward L. W. 1987. Evidence for Paleocene and lower Eocene pinch-outs on the north flank of the Norfolk Arch, Eastern Shore of Virginia. *Geological Society of America Abstracts with Programs* 19(2):124.

Powars D. S., Mixon R. B., Edwards L. E., Poag C. W., and Bruce T. S. 1990. Cross section of Cretaceous and Cenozoic strata, Norfolk Arch to Salisbury Basin, outer Coastal Plain of Virginia. *Geological Society of America Abstracts with Programs* 22(4):57.

Powars D. S., Poag C. W., and Bruce T. S. 1991. Uppermost Mesozoic and Cenozoic stratigraphic framework of the central and outer Coastal Plain of Virginia. *Geological Society of America Abstracts with Programs* 23(1):117.

Powers M. C. 1953. A new roundness scale for sedimentary particles. *Journal of Sedimentary Petrology* 23:117-119.

Ramsey K. W. 1992. Coastal response to Late Pliocene climate change: middle Atlantic coastal plain, Virginia and Delaware. Quaternary coasts of the United States: Marine and lacustrine systems. *SEPM (Society for Sedimentary Geology) Special Publication* 48:121-127.

Roddy D. J. 1966. An unusual dolomitic basal facies of the Chattanooga Shale in the Flynn Creek structure, Tennessee. *American Mineralogist* 51:270.

Sanford S. 1913. The underground water resources of the Coastal Plain of Virginia. *Virginia Geological Survey Bulletin* 5:361 p.

Sanford W. E. 2003. Heat flow and brine generation following the Chesapeake Bay bolide impact. *Journal of Geochemical Exploration* 78-79:243-247.

Self-Trail J. M. 2003. Shock-wave-induced fracturing of calcareous nannofossils from the Chesapeake Bay impact crater. *Geology* 31:697-700.

Schneider H. 1972. Shock-induced mechanical deformations in biotites from crystalline rocks of the Ries crater (Southern Germany). *Contributions to Mineralogy and Petrology* 37:75-85.

Sharpton V. L., Schuraytz B. C., Ming D. W., Jones J. H., Rosencrantz E., and Weidie A. E. 1991. Is the Chicxulub Structure in N. Yucatan a 200 km diameter impact crater at the K/T boundary? Analysis of drill core samples, geophysics, and regional geology. Proceedings, 22nd Lunar and Planetary Science Conference pp. 1223-1224.

Sheridan R. E., Musser D. L., Glover, III L., Talwani M., Ewing J. I., Holbrook W. S., Purdy G. M., Hawman R., and Smithson S. 1993. Deep seismic reflection data of EDGE U.S. mid-Atlantic continental-margin experiment: Implications for Appalachian sutures and Mesozoic rifting and magmatic underplating. *Geology* 21:563-567.

Sheridan R. E., Maguire T. J., Feigenson M. D., Patino L. C., and Volkert R. A. 1999. Grenville age of basement rocks in Cape May NJ well: new evidence for Laurentian crust in U.S. Atlantic Coastal Plain basement Chesapeake Terrane. *Journal of Geodynamics* 27:623-633.

Shipman F. H., Gregson V. G., and Jones A. 1971. A shock wave study of Coconino sandstone. *NASA Contractor Report* NASA-CR-1842:46 p.

Shoemaker E. M. 1963. *Impact mechanics at Meteor Crater, Arizona*; *Moon, Meteorites, and Comets*, edited by Middlehurst B. M. and Kuiper G. P. Chicago: University of Chicago. 301–336 p.

Shoemaker E. M. and Chao E. C. T. 1961. New evidence for the impact origin of the Ries Basin, Bavaria, Germany. *Journal of Geophysical Research* 66:3371-3378.

Shoemaker E. M., Gault D. E., Moore H. J., and Lugn. R. V. 1963. Hypervelocity impact of steel into Coconino Sandstone. *American Journal of Science* 261:668-682.

Sibol M. S., Snoke J. A., and Mathena E. C. 1996. Southeastern United States Seismic Network Bulletin no. 30. Blacksburg, Virginia: Seismological Observatory, Virginia Polytechnic Institute and State University. 62 p.

Sibol M. S., Bollinger G. A., and Chapman M. C. 1997. Catalog of southeastern United States seismicity compiled from various sources: Blacksburg, Virginia: Seismological Observatory, Virginia Polytechnic Institute and State University (electronic format).

Stöffler D. 1966. Zones of impact metamorphism in the crystalline rocks of the nordlinger Ries crater. *Contributions to Mineralogy and Petrology* 12:15-24.

Stöffler D. 1972. Deformation and transformation of rockforming minerals by natural and experimental shock processes. I. Behaviour of minerals under shock compression. *Fortschritte der Mineralogie*. 49:50–113.

Stöffler D. 1984. Glasses formed by hypervelocity impact. *Journal of Non-Crystalline Solids* 67:465-502.

Stöffler D. and Grieve R. A. F. 2003. Towards a unified nomenclature of metamorphism: 11. Impactites. A proposal on behalf of the IUGS Subcommission on the Systematics of Metamorphic Rocks. April 2003. http://www.bgs.ac.uk/scmr/docs/paper_12/scmr_paper_12_1.pdf.

Stöffler D. and Langenhorst F. 1994. Shock metamorphism of quartz in nature and experiment: I. Basic observation and theory. *Meteoritics and Planetary Science* 29:155-181.

Tennant D. 2001. *A Cosmic Tale of mystery, meteors, and one man's search for the truth: Part I*. Norfolk:Virginian-Pilot-Ledger Star, June 24.

Thein J. E. 1987. A tektite layer in upper Eocene sediments of the New Jersey continental slope (Site 612, Leg 95). In *Initial reports of the Deep Sea Drilling Project*. edited by Poag C. W., Watts A. B., Cousin M., Goldberg D., Hart M. B., Miller K. G., Mountain G. S., Nakamura Y., Palmer A., Schiffelbein P. A., Schreiber B. C., Tarafa M., Thein J. E., Valentine P. C., and Wilkens R. H. Washington, D. C.: U.S. Government Printing Office 95:1-817.

Udden J. A. 1898. Mechanical Composition of Wind Deposits. *Augustana Library Publication* 1:69 p.

U. S. Geological Survey (USGS). The national map seamless server. Accessed January 2008. http://seamless.usgs.gov.

Wegener A. 1921. *Die Entstehung der Mondkrater*. Braunschweig: Vieweg-Verlag. 48 p.

Wentworth C. K. 1922. A scale of grade and class terms for clastic sediments. *Journal of Geology* 30:377-392.

White R. S., Westbrook K., Fowler S. R., Spence G. D., Barton P. J., Joppen M., Morgan J., Bowen A. N., Prestcott C., and Bott M. H. 1987. Hatton Bank (northwest U. K.) continental margin structure. *Royal Astronomical Society Geophysical Journal* 89:265-272.

Whitehead J., Spray J. G., and Grieve R. A. F. 2002. Origin of "toasted" quartz in terrestrial impact structures. *Geology* 30:431-434.

APPENDIX A. Sample information

Table A lists information about each sample from the ICDP/USGS Eyreville A and B cores in the Auburn University collection. The samples are listed from the base of the stratigraphic section up in the same order as the descriptions in the Petrography section of this work.

Table A. Complete list of selected samples from ICDP/USGS Eyreville A and B cores.

Unique sample #	Hole	Box	Depth-sample top (ft)	Depth-sample bottom (ft)	Depth-sample top (m)	Depth-sample bottom (m)	Length-sample (ft)	Thin Section
KP 50	B	350	5795.1	5795.25	1766.17	1766.21	0.1	Yes
KP 51	B	320	5508.7	5508.8	1679.05	1679.08	0.1	Yes
KP 49	B	315	5464.3	5464.75	1665.43	1665.56	0.4	No
KP 48	B	307	5385.9	5386	1641.56	1641.59	0.1	Yes
KP 2	B	297	5278.3	5278.4	1608.83	1608.86	0.1	Yes
KP 1	B	296	5271.3	5271.4	1606.69	1606.72	0.1	Yes
KP 47	B	291	5221.4	5221.5	1591.48	1591.51	0.1	Yes
KP 3	B	284	5103.6	5103.7	1555.58	1555.61	0.1	Yes
KP 46	B	283	5089.7	5089.8	1551.34	1551.37	0.1	Yes
KP 4	B	282	5082.05	5082.15	1549.01	1549.04	0.1	Yes
KP 45	B	275	5013.3	5013.4	1528.05	1528.08	0.1	Yes
KP 6	B	221	4998.6	4998.7	1523.70	1523.73	0.1	Yes
KP 44	B	267	4937	4937.1	1504.80	1504.83	0.1	Yes
KP 43	B	259	4862.8	4862.9	1482.18	1482.21	0.1	Yes
KP 42	B	250	4779.25	4779.4	1456.72	1456.76	0.1	Yes
KP 41	B	236	4641.4	4641.5	1414.70	1414.73	0.1	Yes
KP 40	B	235	4632.85	4632.95	1412.03	1412.06	0.1	Yes
KP 39	B	233	4611.9	4612	1405.71	1405.74	0.1	Yes
KP 32	B	231	4591.3	4591.45	1399.41	1399.46	0.1	Yes
KP 7	B	231	4590.2	4590.3	1399.09	1399.12	0.1	Yes
KP 52	B	230	4582.5	4582.6	1396.73	1396.76	0.1	Yes
KP 8	B	228	4570.2	4570.4	1393.00	1393.06	0.2	Yes
KP 33	B	227	4559.7	4559.8	1389.80	1389.83	0.1	Yes
KP 31	B	222	4515.5	4515.6	1376.32	1376.35	0.1	Yes
KP 34	B	222	4512.23	4512.33	1375.33	1375.36	0.1	Yes

Table A. *Continued*. Complete list of selected samples from ICDP/USGS Eyreville A and B cores.

Unique sample #	Hole	Box	Depth-sample top (ft)	Depth-sample bottom (ft)	Depth-sample top (m)	Depth-sample bottom (m)	Length-sample (ft)	Thin Section
KP 9	B	222	4508	4508.1	1373.97	1374.00	0.1	Yes
KP 5	B	274	4499	4499.1	1371.17	1371.20	0.1	Yes
KP 10	B	214	4441.35	4441.45	1353.66	1353.69	0.1	Yes
KP 12	B	119	3595.5	3595.8	1095.89	1095.98	0.3	Yes
KP 11	B	119	3594.85	3594.95	1095.70	1095.73	0.1	Yes
KP 35	B	119	3593.75	3593.85	1095.37	1095.40	0.1	Yes
KP 36	B	116	3561.4	3561.5	1085.51	1085.55	0.1	Yes
KP 15	B	114	3544.5	3544.6	1079.75	1079.78	0.1	Yes
KP 13	B	99	3394.5	3394.6	1034.64	1034.67	0.1	Yes
KP 14	B	78	3172.7	3172.8	967.04	967.07	0.1	No
KP 37	A	567	2866	2866.1	873.50	873.53	0.1	Yes
KP 16	A	564	2843.5	2843.6	866.70	866.73	0.1	Yes
KP 38	A	564	2838.65	2838.75	865.22	865.25	0.1	Yes
KP 19	A	563	2835.95	2836.05	864.40	864.43	0.1	No
KP 20	A	562	2829.4	2829.5	862.37	862.40	0.1	Yes
KP 21	A	557	2787.8	2787.9	849.72	849.75	0.1	Yes
KP 22	A	540	2650.15	2650.25	807.77	807.80	0.1	Yes
KP 23	A	459	2183.7	2183.8	665.59	665.62	0.1	Yes
KP 24	A	415	1982.5	1982.65	604.27	604.31	0.2	Yes
KP 25	A	410	1965.4	1965.5	599.05	599.08	0.1	Yes
KP 26	A	343	1718.6	1718.7	523.83	523.86	0.1	Yes
KP 27	A	286	1503.2	1503.3	457.77	457.80	0.1	Yes
KP 28	A	282	1479.1	1479.2	450.83	450.86	0.1	Yes
KP 29	A	278	1461	1461.1	445.31	445.37	0.1	Yes
KP 18	A	277	1459.2	1459.3	444.76	444.79	0.1	Yes

Table A. *Continued*. Complete list of selected samples from ICDP/USGS Eyreville A and B cores.

Unique sample #	Hole	Box	Depth-sample top (ft)	Depth-sample bottom (ft)	Depth-sample top (m)	Depth-sample bottom (m)	Length-sample (ft)	Thin Section
KP 17	A	277	1457.95	1458.05	444.38	444.41	0.1	Yes
KP 30	A	276	1456.13	1456.23	443.83	443.87	0.1	Yes

APPENDIX B. Compilation of sample images

All imagery associated with each sample from the ICDP/USGS Eyreville A and B cores in the Auburn University collection has been compiled on DVD for Appendix B. The imagery includes core box photos (courtesy of David Powars, USGS- Reston), hand sample photos in various orientations, and, when feasible, photomicrographs as well as electron backscatter images from electron microprobe energy dispersive spectroscopy (EDS). Files are grouped into folders listed as sample names (for stratigraphic order of samples see Appendix A).

APPENDIX C. Composite Eyreville core log with samples

An oversized plot is provided in digital format on DVD of a composite core log for the ICDP/USGS Eyreville location. Sample numbers and stratigraphic sections and subsections are listed with depth on the plot. A natural gamma ray log provided by the USGS is also included. Possible to probable shock-related features are plotted as well to show their distribution with depth.

Chesapeake Bay impact structure

ICDP/USGS Eyreville A & B composite core log

DEPTH m ft

NATURAL GAMMA counts/sec 0 400

LITHOLOGY

PROBABLE ALTERED MELT (M), LITs (⁞⁞), & PDFs (///)

SAMPLE DEPTH

DESCRIPTION

1500 m
500 m
2000 m
2500 m
3000 m
1000 m
3500 m
4000 m
4500 m
1500 m
5000 m
5500 m

KP 30
KP 17
KP 18
KP 29
KP 28
KP 27
KP 26
KP 25
KP 24
KP 23
KP 22
KP 21
KP 20
KP 19
KP 38
KP 16
KP 37
KP 14
KP 13
KP 15
KP 36
KP 35
KP 11
KP 12
KP 10
KP 5
KP 9
KP 34
KP 31
KP 33
KP 8
KP 52
KP 7
KP 32
KP 39
KP 40
KP 41
KP 42
KP 43
KP 44
KP 6
KP 45
KP 4
KP 46
KP 3
KP 47
KP 1
KP 2
KP 48
KP 49
KP 51
KP 50

Post-impact- laminated micrite

Assemblage 5

Upper zone- matrix-supported, friable, sedimentary-clast breccia

443.9-515.9 m: Lower Cretaceous, crystalline basement, and rare Paleogene clasts

515.9-618.2 m: >50% oxidized clay-silt clasts and abundant crystalline basement clasts

Assemblage 5

Middle zone- clast-supported, sedimentary breccias and blocks

618.2-866.7 m: Lower Cretaceous sedimentary boulders/blocks as well as small-clast and massive sand zones, also highly-fractured paleosols

Assemblage 5

Lower zone- clast-supported, sedimentary blocks

866.7-1095.74 m: Lower Cretaceous sedimentary boulders/blocks as well as small-clast and massive sand zones

Assemblage 4

allochthonous block of granitic rocks overlain by gravelly sand derived from the Cretaceous Potomac Formation

Assemblage 3
mixed gravelly sand and lithic blocks

Assemblage 2

impact melt rock, suevite, and breccia

Upper section (1397.16-1474.05 m)- melt-rich suevite and impact melt rock with some cataclastic boulders

Middle section (1474.05-1551.19 m)- lithic-clast-rich suevite with blocks of cataclastic gneiss

Lower section (1551.19-1560.24 m)- graphite-rich breccia

Assemblage 1

schist and granite pegmatite (locally grades into coarse-grained granite)